Subcutaneous Fat: Thermogenesis and Metabolic Benefits

by

Margo P. Emont

A dissertation submitted in partial fulfillment
of the requirements for the degree of
Doctor of Philosophy
(Molecular and Integrative Physiology)
in The University of Michigan
2018

Doctoral Committee:

Assistant Professor Jun Wu, Chair
Professor Charles Burant
Professor Jiandie Lin
Professor Suzanne Moenter

Margo P. Emont
memont@umich.edu
ORCID iD: 0000-0001-9873-2784

DEDICATION

To my family—my mother who has supported me at every stage of my career, my brother who was always there to talk, and my father who was happy to see me begin my PhD and would have been happy to see me finish it.

ACKNOWLEDGMENTS

I would first like to thank my mentor, Jun Wu. I joined her lab because I could see the same love of and enthusiasm for science in her that I feel in myself. From Jun I learned how to think—not only in pursuing a project or critically analyzing a paper, but also in tenaciously applying for fellowships, managing a fledgling lab, and responding to reviewers. Jun's vision and drive are a force of nature and I was lucky to have that as an example during my PhD.

Secondly, I could not have completed this work without the collaboration and support from members of my and other labs. I would particularly like to thank Juan Jiang who was a joy to collaborate with on all of the projects we worked together on, as well the Wu lab, Heejin Jun, Dong-il Kim, Jiling Liao, and Xiaona Qiao, and our collaborator Jiankie Gong, for all of their help.

I would also like to thank my committee members, Charles Burant, Jiandie Lin, and Suzanne Moenter for their helpful critiques and support of my project and my growth as a scientist.

Finally, I would like to thank my friends and family. My mom provided encouragement and support at every step of the way and my brother was always there to talk about politics or reality television. My friends were always up for getting drinks and complaining about lab, or going hiking, or losing at pub trivia. I could not have done this without all of your support.

TABLE OF CONTENTS

DEDICATON ii

ACKNOWLEDGMENTS iii

LIST OF FIGURES vi

LIST OF TABLES viii

ABSTRACT ix

CHAPTER

I. Introduction: Transcriptional Control and Hormonal Response of Thermogenic Fat 1

Abstract 1

Introduction 1

Transcriptional Control of Thermogenic Fat 4

Secreted Molecules and Signaling in Thermogenic Fat 8

Human Thermogenic Fat 15

Concluding Remarks 16

References 21

II. Using a 3D Culture System to Differentiate Visceral Adipocytes *in vitro* 31

Abstract 31

Introduction 31

Materials and Methods 33

Results 39

Discussion 43

References 54

III. Cinnamaldehyde Induces Fat Cell-Autonomous Thermogenesis and Metabolic Reprogramming

Abstract 56

Introduction 56

Materials and Methods 57

Results 62

Discussion 65

References 84

IV. Development, Activation, and Therapeutic Potential of Thermogenic Adipocytes

Abstract 86

Introduction 86

Developmental Origins of Thermogenic Fat 88

Transcriptional Control of the Activation of Thermogenesis 89

Therapeutic Potential of Thermogenic Fat 92

Future Directions 96

References 100

LIST OF FIGURES

FIGURE

I.1 Transcriptional Regulation of the Thermogenic Program 18

I.2 The Regulation of Thermogenic Fat Cells by Secreted Factors 19

II.1 Schematic for the Isolation of Preadipocytes and Culture in Collagen Hydrogels. 45

II.2 Preadipocytes Isolated from Visceral Fat Depots Differentiate as Robustly as Those From Subcutaneous Depots in 3D but not 2D Culture. 46

II.3 Visceral Cells Differentiate as Robustly as Subcutaneous Cells in 3D Hydrogels and Contain Fewer and Larger Lipid Droplets 47

II.4 Preadipocytes Isolated from the Mesenteric Depot Differentiate Robustly in 3D Culture 48

II.5 Cells Grown in the Collagen Hydrogels Retain Depot Specific Gene Expression and Function 49

II.6 Adipocytes Differentiated in 3D Gels Maintain Normal Function in Response to Adrenergic Stimulation 50

II.7 Adipocytes Grown in 3D Gels Can Be Assayed for Oxygen Consumption 51

II.8 Adipocytes Grown in 3D Gels Are Acutely Regulated by Hormonal Stimulation 52

III.1 Acute CA Treatment Upregulates Thermogenic Gene Expression and Activates PKA Signaling in Murine Subcutaneous Fat Cells 68

III.2 CA Upregulates Thermogenic Gene Expression in Primary Inguinal Adipocytes of Multiple Inbred WT Mouse Strains 70

III.3 Gene Expression in CA-Stimulated Murine and Human Cells 71

III.4 Validation of TRPA1 Knockout Animals 72

III.5 Acute CA Treatment Increases Thermogenic Marker Expression and Activates PKA Signaling in Immortalized C3H-10T1/2 Cells, Indicating This is a Cell-Autonomous Adipocyte Response and not Due to the Presence of Other Non-Fat Cell Types That May Be Present in Primary Cultures 73

III.6 CA Activates a Thermogenic Response and Regulates Lipid Metabolic Gene Profiles in Human Subcutaneous Fat Cells 75

III.7. Acute CA Treatment Increases Thermogenic Marker Expression and Activates PKA Signaling in Human Subcutaneous Adipocytes from Multiple Donors 77

III.8 Chronic CA Treatment Upregulates Thermogenic Gene Expression in Murine and Human Subcutaneous Adipocytes 78

III.9 CA Upregulates Thermogenesis in Primary Brown Adipocytes 79

III.10 FGF21KO Cells Differentiate to a Similar Extent as WT Cells 80

IV.1 PRDM16 and PGC1α Interact with PPARγ to Activate the Thermogenic Program 98

LIST OF TABLES

TABLE

I.1 Thermogenic Fat in Humans Correlates with Physiological and Environmental Factors and Influences Metabolic Parameters 20

II.1 Primer Sequences for *qPCR* 53

III.1 Characteristics of Human Donors Used in this Study 81

III.2 Primer Sequences for Real-Time qPCR Analysis 82

IV.1 Recent Advances in Human Thermogenic Fat Study 99

ABSTRACT

Obesity and its associated metabolic diseases present a major public health problem around the world. The discovery that thermogenic fat is active in adult humans has sparked a renewal of interest in the study of its development and function and in the feasibility of using modulators of thermogenesis to work against obesity. In recent years there have been a number of exciting discoveries about the properties of thermogenic fat, and every new discovery demonstrates just how much we still don't understand about these cells. Research that gains further understanding through the development of tools or the identification of novel compounds that regulate thermogenic adipocytes may lead to novel therapeutics to target thermogenic fat and could have a profound impact on the efforts to harness the power of thermogenic fat to counteract obesity.

It has long been recognized that body fat distribution and regional adiposity play a major role in the control of metabolic homeostasis. However, the ability to study and compare the cell autonomous regulation and response of adipocytes from different fat depots has been hampered by the difficulty of inducing preadipocytes isolated from the visceral depot to differentiate into mature adipocytes in culture. In the first part of my thesis work, I present an easily created 3D culture system that can be used to differentiate preadipocytes from the visceral depot as robustly as those from the subcutaneous depot. The cells differentiated in these 3D collagen gels are mature adipocytes that retain depot-specific characteristics, as determined by imaging, gene expression, and functional assays. This 3D culture system therefore allows for study of the development and

function of adipocytes from both depots *in vitro*, and may ultimately lead to a greater understanding of site-specific functional differences of adipose tissues to metabolic dysregulation.

Cinnamaldehyde (CA) is a food compound that has previously been observed to be protective against obesity and hyperglycemia. In the second part of my thesis work, I report that CA activates a thermogenic response via PKA signaling in murine subcutaneous adipocytes and that chronic CA treatment induces metabolic reprogramming that is partially dependent on FGF21 and that may contribute to improving whole-body metabolic health. This phenomenon is fat cell-autonomous and well conserved in human adipose stem cells isolated from subcutaneous depots of multiple donors of different ethnicities and ages and with a variety of body mass indexes (BMI). Given the wide usage of cinnamon in the food industry, the notion that this popular food additive, instead of a drug, may activate thermogenesis, could ultimately lead to therapeutic strategies against obesity that are much better adhered to by participants.

The potential of the adipocyte in the understanding and treatment of human physiology in health and disease is clearly as of yet not fully realized. Here, I have provided a method to further study the differences between subcutaneous and visceral fat as well as investigated the pathways through which novel compounds can activate thermogenesis and metabolic reprogramming in murine and human subcutaneous adipocytes. A growing body of research has begun to show that the activation of human thermogenic fat can have a meaningful effect on human physiology, this tangible translational aspect of thermogenic adipocyte research gives promise to the idea that the tools developed here lay ground for further exciting discoveries that are yet to come.

CHAPTER I

Introduction: Transcriptional Control and Hormonal Response of Thermogenic Fat

Abstract

Obesity and its associated metabolic diseases present a major public health problem around the world. The discovery that thermogenic fat is active in adult humans has sparked a renewal of interest in the study of its development and function and in the feasibility of using modulators of thermogenesis to work against obesity. In recent years it has been shown that there are at least two distinct types of thermogenic fat cells; brown and beige fat. In this review we discuss the transcriptional mediators of thermogenesis and the signaling molecules that regulate thermogenic cells. We also review the effects of thermogenic fat activation on whole body metabolic parameters and evaluate the increasing evidence that activating thermogenesis in humans can be a viable method of ameliorating obesity. In these discussions we highlight targets that can potentially be stimulated or modified in anti-obesity treatments.

Introduction

Obesity is a major health problem in the United States and around the world. Over one third of adults in the United States [1] and 11% percent of adults worldwide are obese [2]. A number of conditions including heart disease, type 2 diabetes, and some cancers

This chapter has been published as: **Emont, M.P.**, Yu, H., and Wu, J. (2015). Transcriptional control and hormonal response of thermogenic fat. *J Endocrinol* 225, R35-R47

are more prevalent in obese individuals and worldwide approximately 3.4 million deaths each year are tied to obesity [2]. Obesity is characterized by an excessive amount of lipid accumulation in fat cells; as a result there has been a continual effort to find cellular processes and molecular targets in fat that can be manipulated in anti-obesity treatments.

Three types of fat cells have been identified to date [3]. White adipocytes are primarily used for energy storage; they contain a large lipid droplet and few cellular organelles. In contrast, brown adipocytes are primarily a site for adaptive thermogenesis which, unlike the obligatory thermogenesis that is a natural byproduct of metabolic processes, is activated in response to cold stimulation [4]. Brown adipocytes contain multiple small lipid droplets and a number of mitochondria, which express uncoupling protein 1 (UCP1), a major component of the thermogenic program and a specific marker of thermogenic adipocytes [5]. UCP1 is activated by long chain fatty acids and increases the conductance of the inner mitochondrial membrane, causing the mitochondria to produce heat at the expense of ATP production efficiency [6]. While overabundance of white fat is the defining characteristic of obesity and contributes to the development of metabolic disease, brown fat in fact works to counteract obesity by converting chemical energy into heat as opposed to storing it as lipid [3]. Brown fat is primarily found interscapularly in rodents and arises from $MYF5^+$ stem cells that can also differentiate into skeletal myocytes [7]. “Beige” or “brite” fat is a newly identified type of fat that is located in white adipose tissue and arises from $MYF5^-$ stem cells but has an inducible thermogenic program [8, 9]. We will refer to thermogenic cells in white fat depots as beige cells and to the process of the activation of thermogenic fat cells in white fat depots as “beiging” in this review. It is conceivable that other types of fat exist in addition to white, brown, and beige fat**.** Recent work

on marrow adipose tissue, for example, has begun to characterize the distinctive functions of these unique fat cells that are not seen in currently identified types of fat [10, 11].

Adaptive thermogenesis in fat is activated by cold exposure mainly through the signaling of catecholamines secreted by the sympathetic nervous system [5]. The sympathetic nervous system primarily signals through the α and β1-3 adrenergic receptors (AR), consequently in β-less mice, which lack all isoforms of the β adrenergic receptor, the brown fat depot is comprised of cells with large lipid droplets and blunted UCP1 expression [12]. The β ARs are G-protein coupled receptors that, upon stimulation, activate adenylyl cyclase and increase levels of intracellular cAMP. This leads to the phosphorylation of protein kinase A (PKA), which in turn activates the p38 MAP kinase (MAPK) pathway and induces cAMP response-element binding protein (CREB) mediated upregulation of UCP1 [5]. Studies have begun to show that therapeutics that act centrally can affect thermogenesis, for example a Glucagon-like peptide-1 (GLP1) receptor agonist works in the central nervous system to activate brown adipose tissue and may increase resting energy expenditure in humans [13]. β-adrenergic signaling may not be the only pathway for cold induced activation of thermogenic fat. Ye et al. showed that cultured, mature, adipocytes can upregulate thermogenesis in response to cold exposure, suggesting that there is also a cell autonomous cold sensing mechanism in fat cells [14]. This implies that there may be unexplored pathways that function in parallel with β AR signaling to activate cold induced thermogenesis.

This review focuses on the transcriptional control of thermogenic genes and the signaling beyond the sympathetic nervous system that regulates both brown and beige fat function. We also

discuss the effects that thermogenic fat activation may have on systemic metabolism in humans and highlight molecules that have begun to be tested as drug targets.

Transcriptional Control of Thermogenic Fat

The cascades mediated by a number of transcriptional factors and cofactors tightly control the adipogenic process. The unique mechanisms that regulate thermogenic fat are much less well understood. In the following section, we discuss the factors that contribute to the development of thermogenic cells and the activation of the thermogenic program (Figure I.1).

PPARγ

Peroxisome proliferator-activated receptor γ (PPARγ) is the master regulator of adipogenesis; ectopic expression of PPARγ stimulates the differentiation of fibroblasts into adipocytes [15]. PPARγ is a nuclear receptor that heterodimerizes with the retinoid x receptor (RXR) to induce transcription of genes related to the adipogenic program [16]. In addition to its central role in adipogenesis, PPARγ has been shown to be important in the regulation of thermogenesis. Chronic stimulation of adipocyte cultures with PPARγ agonists results in an induction of the thermogenic program [9, 17, 18]. Ongoing research is beginning to elucidate the molecular mechanisms by which PPARγ regulates thermogenesis. A mouse model with a point mutation in PPARγ was found to have normal development of adipose tissue but has defective thermogenesis [19] and more recently it was shown that SIRT1-dependent deacetylation of PPARγ plays a role in the upregulation of thermogenic genes [20]. It has also been proposed that stabilization of PRD1-BF1-RIZ1 homologous domain containing 16 (PRDM16) through the action of PPARγ agonists may contribute to the induction of thermogenesis [21]. These studies have begun to

provide mechanistic insight into our understanding of how PPARγ regulates the function of thermogenic fat.

PGC1α

The peroxisome proliferator-activated receptor γ coactivator 1 (PGC1) family of proteins are coactivators that are key inducers of mitochondrial biogenesis [22]. The first PGC1 protein to be identified is PGC1α, which was isolated in a yeast two-hybrid screen for PPARγ interacting proteins in brown fat [23]. Both PGC1α and a closely related family member, PGC1β, are regulators of the thermogenic program. Brown fat cells from PGC1α knockout animals have a decrease in cAMP induced thermogenesis and loss of both PGC1α and PGC1β in brown fat cells reduces basal levels of thermogenesis [24]. Additionally, while PGC1β knockout mice have a compensatory increase in PGC1α expression, there is a reduction of thermogenic gene expression in the brown fat of those animals [25]. Recently, interferon regulatory factor 4 (IRF4) has been shown to interact with PGC1α to mediate thermogenesis. In the model of IRF4 overexpression in UCP1 positive cells, thermogenesis is activated in brown fat of the transgenic animals compared to the controls. Additionally, a *Ucp1-CRE* driven IRF4 knockout results in cold intolerance and a reduction in thermogenic gene expression [26]. PGC1α has also been shown to induce the expression of Cell death-inducing DFFA-like effector (CIDEA), a regulator of UCP1 function. This interaction is inhibited through direct interaction of PGC1α with the corepressor receptor interacting protein 140 (RIP140) [27]. RIP140 had previously been reported to inhibit mitochondrial biogenesis and the expression of thermogenic genes such as UCP1 [28, 29]. PGC1α is also negatively regulated by retinoblastoma protein (Rb) and its closely related family member p107. Rb has been shown to suppress PPARγ signaling and promote osteogenic

differentiation and p107 knockout mice have increased expression of PGC1α and UCP1 in both brown and white fat depots [30, 31]. These studies show that various interacting proteins can regulate PGC1α function in mediating thermogenic gene expression.

PRDM16

PRDM16 is a zinc finger protein that is an important regulator of thermogenic fat. Ectopic expression of PRDM16 in cultured fibroblasts and *in vivo* results in thermogenic adipocyte differentiation [32]. It was subsequently found that PRDM16 expression in precursor cells determines cell fate, PRDM16 knockdown in primary brown fat precursor cells results in the differentiation of those cells into skeletal myotubes while overexpression of PRDM16 in skeletal muscle precursor cells results in brown adipocyte differentiation [7]. The mechanism by which PRDM16 determines precursor cell fate was later shown to be controlled in part by a transcription complex consisting of PRDM16 and CCAAT/enhancer binding protein β (C/EBPβ) [33]. Further *in vivo* models showed that fat specific PRDM16 overexpression results in improved metabolic function and less weight gain in high fat diet fed mice [34] and knocking out PRDM16 results in a loss of the thermogenic program in both brown and beige fat [35, 36]. Ongoing work is beginning to characterize the transcriptional complex that interacts with PRDM16 to promote thermogenesis [37].

EBF2

Early B-cell factor 2 (EBF2) is a helix-loop-helix transcription factor that regulates B lymphocytes and neuronal genes [38] and has been shown to regulate adipogenesis [39, 40]. More recently, EBF2 has also been shown to play a role in regulating the thermogenic program

in brown and beige adipocytes. A 2013 study used models of EBF2 knockout and overexpression to demonstrate that EBF2 helps to recruit PPARγ to the promoter regions of thermogenic target genes and, with PPARγ, activates the transcription of PRDM16. EBF2 knockout mice present defective brown fat development [41] and recent studies have indicated that EBF2 may also be involved in the regulation of beige fat function [42]. The identification of Brown fat long noncoding RNA 1 (Blnc1) has provided insight into the mechanisms of EBF2 action. Blnc1 was shown to be an important component of the EBF2 ribonucleoprotein complex [43]. Adipocytes that overexpress Blnc1 express thermogenic genes at a higher level than controls at both basal and stimulated states, underlining the role of the EBF2 transcription complex in regulating thermogenesis [43].

TLE3

Transducin-like enhancer of split 3 (TLE3) is a groucho family co-repressor that was identified as a modulator of adipogenesis in a high throughput cDNA screen [44]. It was found that PPARγ directly drives *Tle3* expression and that the TLE3 protein binds to PPARγ and uncharacteristically acts as a co-activator to promote differentiation [44]. Subsequent work has shown that TLE3 is actually a white fat selective protein; overexpression of TLE3 in fat leads to a decrease in thermogenic gene expression and a fat specific TLE3 knockout has an increase in the thermogenic response to cold exposure [45]. Co-expression experiments revealed that TLE3 and PRDM16 “compete” to bind to PPARγ and the resulting distinct transcription complexes determine the expression of either lipid storage “white fat specific” genes or thermogenic fat specific genes [45].

SMAD

Transforming growth factor β (TGFβ) signaling through SMAD proteins has been shown to negatively regulate adipogenesis [46]. A SMAD3 global knockout mouse is resistant to diet induced obesity and there is increased UCP1 expression in the adipose tissue of these animals compared to controls [47]. Similarly, treating wild type animals with exogenous TGFβ1 reduced thermogenic gene expression in fat [47]. Zinc finger protein 423, a transcriptional regulator of SMAD proteins, has been identified as playing a key role in preadipocyte fate commitment [48]. The therapeutic potential of targeting TGFβ signaling has been explored using a dominant negative activin receptor type IIB fusion protein that promotes thermogenesis through binding of TGFβ and inhibition of downstream signaling [49].

Secreted Molecules and Signaling in Thermogenic Fat

While sympathetic signaling is the most understood pathway for the activation of adaptive thermogenesis, new research has focused on identifying other secreted factors that can activate thermogenic fat, both to gain a greater understanding of the regulation of the thermogenic program and to identify potential targets for drug discovery (Figure I.2).

FGF family

Fibroblast growth factor (FGF) family members such as FGF1 and FGF15/19, have been implicated in contributing to the regulation of glucose homeostasis and the beiging of white fat [50, 51]. FGF21 is the family member most well studied in metabolism; it has been shown to regulate glucose homeostasis, lipid metabolism, insulin sensitivity, ketogenesis, and the prevention of cardiovascular disease [52-56]. FGF21 is mostly produced in and released from the

liver; however, thermogenic activation also increases FGF21 expression in subcutaneous and brown adipose tissue [57, 58]. Ongoing research is investigating the differential roles of liver- and adipose tissue-derived FGF21 in regulating energy homeostasis [59]. Systemic administration of FGF21 increases the expression of UCP1 [60] and genetic ablation of FGF21 impairs the ability of animals to adapt to cold exposure [58]. Though FGF21 is not expressed in the central nervous system, it can cross the blood-brain barrier to induce sympathetic nerve activity and thus centrally increase thermogenic gene expression and energy expenditure [61]. Recent studies have revealed that adiponectin at least partially mediates the effects of FGF21 on energy expenditure and insulin action [54, 62]. Due to the beneficial effects of FGF21 in metabolism, there has been considerable interest in the development of an FGF21 analog drug, the successful production of which could potentially provide new strategies to improve metabolic health in humans [63].

COX2 and Prostaglandins

Cyclooxygenase-2 (COX2) is an enzyme that synthesizes prostaglandins (PG) in response to stimuli such as inflammatory signaling [64]. In 2010, two independent studies reported the induction of COX2 in white fat depots upon cold-exposure or β-adrenergic stimulation [65, 66]. Pharmacological inhibition or genetic ablation of COX2 diminishes the cold or β-AR activation induced beiging of white adipose tissue [65, 66]. Overexpression of COX2 has been shown to increase UCP1 expression in adipose tissue, elevate energy expenditure, and reduce weight gain [65]. More recently, prostaglandin E2 (PGE_2) and the enzyme that synthesizes it, microsomal synthase-1 (mPGES-1), were shown to play a role in the development of beige fat [67].

Retinoic acid

Retinoic acid (RA), the active derivative form of vitamin A, is mainly synthesized intracellularly from retinaldehyde (Rald) by retinaldehyde dehydrogenases (RALDHs) [68]. Studies have suggested that RA, Rald and RALDHs all play functional roles in regulating thermogenic gene expression. It has long been recognized that RA induces UCP1 expression both in cultured brown adipocytes and in brown adipose tissue [69]. In mouse embryonic fibroblast-derived adipocytes, UCP1 expression is highly elevated upon all-trans RA stimulation in a p38 MAPK-dependent manner [70]. Rald has also been implicated in the induction of the thermogenic program; Plutzky and colleagues have shown that RALDH1 knockout mice have elevated levels of Rald and exhibit increased energy expenditure, improved insulin sensitivity, and resistance to diet-induced obesity [71]. Later studies demonstrated that the beneficial metabolic effects of Rald signaling likely act through a PGC1α mediated pathway [72].

Thyroid Hormone

Thyroid hormones are produced by the thyroid and bind to thyroid hormone receptors (TR) α1-2 and β1-2 to affect to growth and metabolism in target tissues throughout the body, including bone, liver, heart, and fat [73]. Thyroxine, or T_4 thyroid hormone, comprises the majority of thyroid output and deiodinases at peripheral tissues, such as the liver and kidney, remove the 5' iodine on T_4 to form the metabolically active form of thyroid hormone, triiodothyronine (T_3) [73]. T_3 is responsible for increasing the metabolic rate and it has been shown to work in concert with norepinephrine to induce transcription of UCP1 in the brown adipose tissue of rats *in vivo* [74]. Later studies showed that the treatment of primary fetal brown adipocytes from rats with T_3 increases *Ucp1* transcription and stabilizes *Ucp1* mRNA [75]. The ability of T_3 to induce

thermogenesis was shown to be dependent on the TR isoform that it signals through, the TRβ1 specific agonist GC-1 stimulates UCP1 expression but a TRα1 agonist does not [76, 77]. While thyroid hormone can directly activate the thermogenic program in fat cells, T_3 signaling in the hypothalamus through AMPK also works to activate the central nervous system to induce thermogenesis via β3 AR signaling [78].

Natriuretic Peptides

The natriuretic peptides (NPs) are a family of cardiac and vascular derived hormones that regulate sodium homeostasis in blood and urine. There are three main types of NPs; atrial natriuretic peptide (ANP), and B- and C-type natriuretic peptides (BNP and CNP) [79]. Additionally, there are two major classes of NP receptors; NP receptors A and B mediate an intracellular cyclic guanosine monophosphate-dependent signaling cascade, while the NP receptor C (NPRC) facilitates the removal of NPs from circulation [80]. The discovery that NP receptors are expressed in the adipose tissue of rats and humans opened an area of inquiry into the actions of NPs in fat [81, 82] and it was subsequently shown that ANP and BNP stimulate lipolysis in human adipocytes [83]. Recent work on NPRC global knockout mice shows that these animals have increased ANP, reduced fat depot size, and increased thermogenic gene expression [84]. Further studies implicated both ANP and BNP in the regulation of thermogenesis, ANP was shown to mediate the induction of thermogenic genes through the stimulation of a cGMP/p38 MAPK pathway and the constant delivery of BNP to mice resulted in increased energy expenditure and beiging of white adipose tissue [84].

Signaling from Immune Cells

One consequence of obesity is a change of the macrophage populations seen in adipose tissue from anti-inflammatory M2 macrophages to pro-inflammatory M1 macrophages [85]. This switch in macrophage populations may contribute to the decrease in thermogenesis because catecholamines produced by M2 macrophages can signal through the β ARs to induce thermogenesis [86, 87]. Recently, it has been shown that other cells associated with the type 2 immune response, specifically type 2 lymphoid cells, can also contribute to the beiging of fat [88, 89]. The development of chronic inflammation during obesity leads to upregulation of the non-canonical NF-κB target, IκB kinase ε (IKKε) [90]. The increase of IKKε results in catecholamine resistance in adipose tissue, which in turn suppresses the induction of UCP1 [91]. This is consistent with the observation that an IKKε global knockout mouse has less inflammation, increased energy expenditure, and upregulation of thermogenic gene expression in the visceral depot compared to wild type animals [90]. Treating high fat diet fed animals with a specific inhibitor of both IKKε and the related kinase TBK1 results in reduced lipid deposition in brown adipose tissue and an increase in thermogenic gene expression [92]. These studies provide a model in which the development of obesity leads not only to the loss of a thermogenic signal from type 2 inflammatory cells but also to the development of chronic inflammation and subsequent resistance to thermogenic signals.

Myokines (Irisin and METRNL)

Induction of PGC1α in skeletal muscle has systematic benefits including an increase in energy expenditure and prevention of age-related obesity [93, 94]. Elevated expression of the protein fibronectin type III domain containing 5 (FNDC5) was seen in a model of skeletal muscle specific overexpression of PGC1α. Irisin, the cleaved form of FNDC5, is a secreted hormone

released after exercise that stimulates the beiging of white fat [95, 96]. Recently, irisin was demonstrated to be not only a myokine but also an adipokine that can be secreted from white fat tissue under certain physiological and pathological conditions [97]. It has been shown that cold exposure increases levels of circulating irisin, suggesting that shivering may result in irisin release from muscle and therefore providing another potential physiological mechanism by which irisin stimulates beiging [98]. In addition to irisin, meteorin-like (METRNL) has also recently been implicated as playing a role in metabolism. METRNL is a hormone that is released from muscle after exercise and from adipose tissue upon cold exposure. Intravenous injections of an adenoviral METRNL construct or direct injection of recombinant protein into mice induces thermogenesis in fat, increases whole-body energy expenditure and improves glucose tolerance through eosinophil-dependent IL4/IL13 signaling [99]. The identification and characterization of irisin and METRNL provide a model in which myokines released during exercise influence metabolism. The extent to which myokine signaling contributes to the overall metabolic benefits of exercise and how these signals interact with other exercise regulated pathways await further study.

Bone morphogenetic proteins

Bone morphogenetic proteins (BMPs) are members of the TGFβ superfamily and are involved in multiple biological processes in adipose tissue including enhancing preadipocyte proliferation [100], inducing adipogenesis [101], influencing adipocyte lineage commitment [102], and regulating thermogenesis [103, 104]. BMP7 has been shown to promote brown adipogenesis through the induction of PRDM16 and PGC1α [104]. Another family member, BMP8b, functions in the central nervous system to increase sympathetic output and therefore increases

the response of thermogenic fat to cold exposure through p38 MAPK and CREB signaling [103]. A BMP8b global knockout mouse has reduced thermogenic gene expression in adipose tissue compared to controls [103].

Newly discovered factors

More recently, additional secreted factors important to thermogenic fat biology have been reported [105-109]. For want of space, we will briefly discuss only a few of them here.

It has been observed that cachexia, the wasting of adipose and skeletal muscle tissues seen in diseases such as cancer, is associated with the activation of brown fat [110]. A recent study found that the thermogenic program is activated in fat cells treated with conditioned medium from Lewis lung carcinoma (LLC) cells, a well-characterized model of cachexia [106]. Global gene expression analysis of LLC cells identified parathyroid-hormone-related protein (PTHrP) as regulating the activation of thermogenesis, likely through the cAMP/PKA pathway [106]. This discovery has begun to provide mechanistic insight into the etiology of the development of cachexia and further studies may suggest treatments that can prevent tissue wasting during disease.

Adenosine has recently been shown to increase lipolysis in primary human and mouse adipocytes [107]. Adenosine is released from brown fat upon sympathetic stimulation and can signal brown adipocytes to stimulate thermogenesis. The adenosine receptor A_{2A} is not highly expressed in white adipose tissue, however, pharmacological activation of A_{2A} and viral delivery of A_{2A} into the subcutaneous depot of mice both significantly increase beiging [107].

Neuregulin 4 (NRG4), a member of the epidermal growth factor (EGF) family, was recently discovered to be a secreted factor that is released from brown fat [109]. NRG4 binds to ERBB receptors in the liver and its activation inhibits the SREBP1c-lipogenic pathway through trans-repression of the liver X receptor by STAT5. *In vivo* gain and loss of function studies have shown that NRG4 helps to ameliorate diet-induced obesity and insulin resistance [109]. These studies suggest that factors released from brown fat can play a role in regulating energy expenditure and systemic metabolism.

Human Thermogenic Fat

While originally it was believed that the only brown fat in humans was found in newborns and was rapidly lost postnatally, analysis of ^{18}F-fluorodeoxyglucose positron-emission tomographic and computed tomographic (PET-CT) scans showed that there is active thermogenic fat in some adults [111]. Biopsies of "hot" areas indicated by PET-CT scans reveal that the fat tissue in the supraclavicular region, as well as in the neck and paraspinal regions, expresses UCP1 [112-115]. The identity of the thermogenic fat in adults remains uncertain. While the thermogenic fat found in babies has the characteristics of classical brown fat, gene expression analyses performed on adult thermogenic fat have shown the presence of genes that are thought to be beige specific [8, 116-118], suggesting that they might be beige fat. Other studies have suggested that human thermogenic fat tissue may be a mixture of brown and beige cells [119, 120].

Recent work has indicated that thermogenic fat may play an important, active, metabolic role in humans (Table I.1). Multiple studies have shown that the presence of thermogenic fat is negatively correlated with age and BMI [112, 114, 115, 121, 122]. There is an increase in the

amount of detectable thermogenic fat in patients who underwent significant weight loss after gastric bypass surgery, suggesting that the decrease in the amount of thermogenic fat seen during obesity can be reversed [123]. It has also been shown that environmental temperature modulates the amount of detectable thermogenic fat in adults [112, 113, 115]. Furthermore, acute cold exposure increases resting metabolic rate more in individuals that have visible thermogenic fat on PET-CT scans compared to individuals without detectable thermogenic fat [124-128], this is in line with reports that there is increased glucose and fatty acid uptake in supraclavicular fat depots in response to cold exposure [125, 129]. Most excitingly, it has recently been shown that the accumulation of thermogenic fat in response to cold exposure results in improvements in insulin sensitivity and glucose homeostasis [130, 131] as well as a decrease in body weight [128]. These studies indicate that human thermogenic fat is a viable target for anti-obesity and anti-diabetic treatments.

Concluding Remarks

In the long pursuit of better understanding and more effective therapeutics for metabolic disease, we have become aware that many of these disorders are polygenic and multifactorial, suggesting the ultimate solution demands a thorough knowledge of all cell types involved, and of both cell autonomous regulation and intercellular communication. Increasing appreciation has been directed towards the role of adipose tissue in this complicated network. For two decades, since the cloning of leptin [132] and the discovery that fat tissue can generate inflammatory cytokines in obesity [133], the endocrine function of adipose tissue has been studied in detail and is relatively well understood. It has only been in the last decade that researchers and clinicians in the metabolic field have begun to recognize the potential influence of thermogenic fat cells on

whole body metabolism. We have made great advances in our understanding of how these cells are regulated both transcriptionally and by circulating factors and our knowledge of how these cells contribute to human metabolism is growing. Ongoing research is continually uncovering new methods to target these cells and recent studies have begun to show that some therapeutics already in clinical use, like the mineralocorticoid receptor antagonist spirolactone and the GLP1 receptor agonist liraglutide, may also be able to stimulate thermogenic fat [13, 134]. With this knowledge we can hopefully soon develop treatments that target thermogenic fat to fight against obesity and associated conditions.

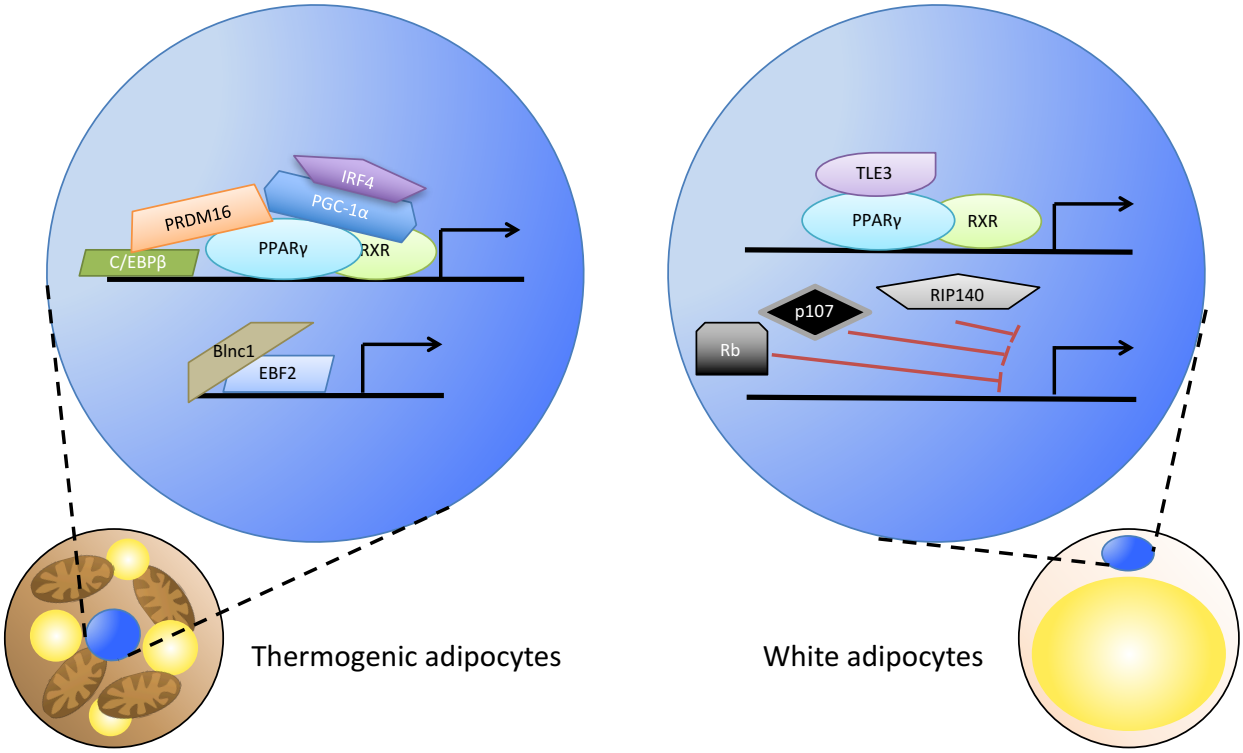

Figure I.1 Transcriptional Regulation of the Thermogenic Program
The PPARγ/RXR heterodimer plays a key role in regulating the development of all adipocytes. In thermogenic adipocytes (left) it also plays a major role in the regulation of the thermogenic program. A number of coactivators interact with PPARγ, including PGC1α which is regulated in part by IRF4, and PRDM16 which interacts with both PPARγ and C/EBPβ to drive thermogenesis. Other transcriptional regulators of thermogenesis include EBF2, which forms a ribonucleoprotein complex with Blinc1 to upregulate thermogenic genes. In white adipocytes (right) the PPARγ/RXR heterodimer instead interacts with TLE3, leading to the expression of white fat selective genes. Rb, p107, and RIP140 also work in white adipocytes to inhibit the transcription of thermogenic genes.

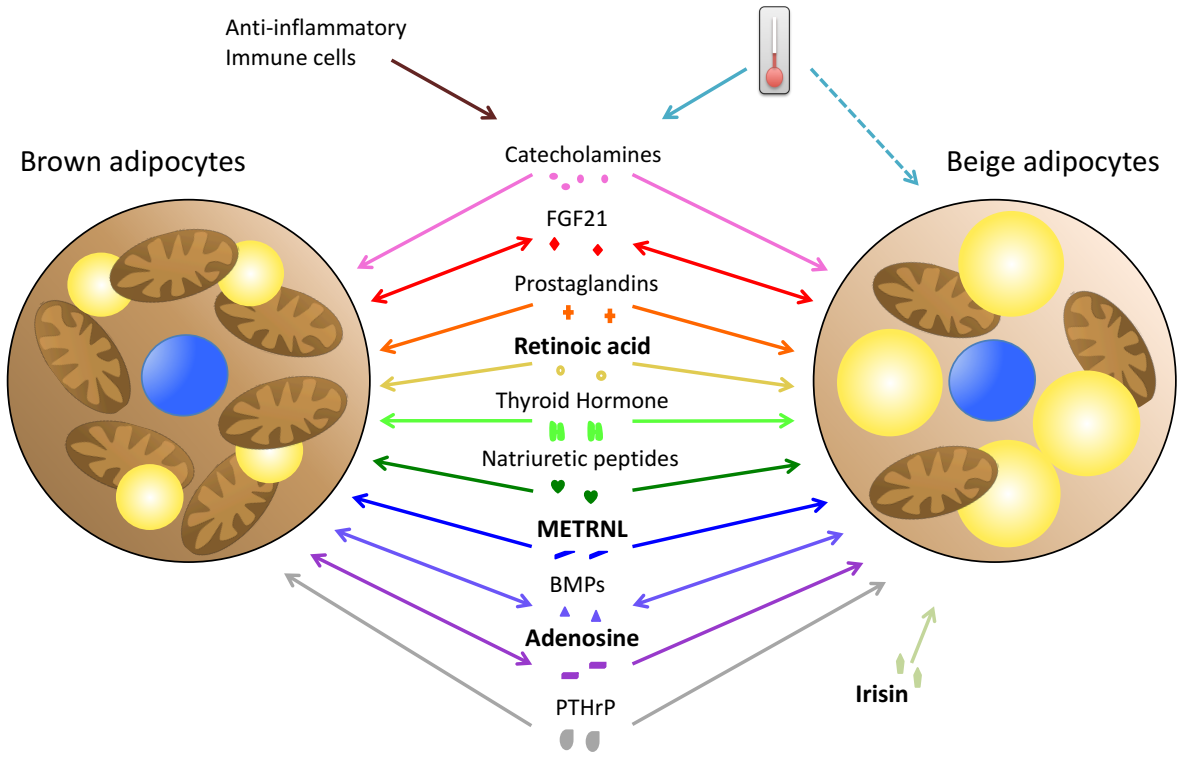

Figure I.2 The Regulation of Thermogenic Fat Cells by Secreted Factors
A number of secreted factors regulate the thermogenic program in brown and beige cells. Cold exposure induces production of catecholamines from the sympathetic nervous system (solid teal line) and may also activate beige fat through a cell autonomous mechanism (dashed teal line). Anti-inflammatory macrophages can also produce catecholamines. FGF21, PG, RA, NPs, thyroid hormone, METRNL, BMPs, adenosine, and PTHrP regulate thermogenesis in brown and beige cells. Additionally, the myokine irisin regulates thermogenesis in beige fat. FGF21, some BMPs, and adenosine have also been shown to be secreted by thermogenic adipocytes. To differentiate the factors that work in concert with central activation of thermogenesis and through beta-adrenergic signaling from those that work through independent pathways, these independent factors, RA, adenosine, Irisin, and METRNL, have been bolded.

	Thermogenic Fat	Sample Size (max)	Age (Range of means)	Sex	References
Age	Negatively correlated	4842	28-62	♀♂	[114, 115, 121, 122, 126, 135-138]
BMI	Negatively correlated	4842	24-62	♀♂	[112, 114, 115, 121-123, 128, 135-139]
Cold exposure & environmental temperature	Positively correlated	4842	23-62	♀♂	[112-115, 121, 124-126, 129, 135, 140, 141]
Respiratory Exchange Ratio & Nonshivering Thermogenesis	Increased by activation of thermogenic fat	27	23-40	♀♂	[112, 123, 124, 127, 129]
Glucose Homeostasis & Insulin Sensitivity	Improved by activation of thermogenic fat	12	21-45	♂	[130, 131]

Table I.1 Thermogenic Fat in Humans Correlates with Physiological and Environmental Factors and Influences Metabolic Parameters

References

1. Ogden, C.L., et al., *Prevalence of childhood and adult obesity in the United States, 2011-2012.* JAMA, 2014. **311**(8): p. 806-14.

2. WHO. *Fact Sheet on Obesity and Overweight*. 2014 08/2014 [cited 2014 11/4/2014]; Available from: http://www.who.int/mediacentre/factsheets/fs311/en/.

3. Rosen, E.D. and B.M. Spiegelman, *What we talk about when we talk about fat.* Cell, 2014. **156**(1-2): p. 20-44.

4. Himms-Hagen, J., *Role of thermogenesis in the regulation of energy balance in relation to obesity.* Can J Physiol Pharmacol, 1989. **67**(4): p. 394-401.

5. Cannon, B. and J. Nedergaard, *Brown adipose tissue: function and physiological significance.* Physiol Rev, 2004. **84**(1): p. 277-359.

6. Fedorenko, A., P.V. Lishko, and Y. Kirichok, *Mechanism of fatty-acid-dependent UCP1 uncoupling in brown fat mitochondria.* Cell, 2012. **151**(2): p. 400-13.

7. Seale, P., et al., *PRDM16 controls a brown fat/skeletal muscle switch.* Nature, 2008. **454**(7207): p. 961-7.

8. Wu, J., et al., *Beige adipocytes are a distinct type of thermogenic fat cell in mouse and human.* Cell, 2012. **150**(2): p. 366-76.

9. Petrovic, N., et al., *Chronic peroxisome proliferator-activated receptor gamma (PPARgamma) activation of epididymally derived white adipocyte cultures reveals a population of thermogenically competent, UCP1-containing adipocytes molecularly distinct from classic brown adipocytes.* J Biol Chem, 2010. **285**(10): p. 7153-64.

10. Scheller, E.L. and C.J. Rosen, *What's the matter with MAT? Marrow adipose tissue, metabolism, and skeletal health.* Ann N Y Acad Sci, 2014. **1311**: p. 14-30.

11. Cawthorn, W.P., et al., *Bone marrow adipose tissue is an endocrine organ that contributes to increased circulating adiponectin during caloric restriction.* Cell Metab, 2014. **20**(2): p. 368-75.

12. Bachman, E.S., et al., *betaAR signaling required for diet-induced thermogenesis and obesity resistance.* Science, 2002. **297**(5582): p. 843-5.

13. Beiroa, D., et al., *GLP-1 agonism stimulates brown adipose tissue thermogenesis and browning through hypothalamic AMPK.* Diabetes, 2014. **63**(10): p. 3346-58.

14. Ye, L., et al., *Fat cells directly sense temperature to activate thermogenesis.* Proc Natl Acad Sci U S A, 2013. **110**(30): p. 12480-5.

15. Tontonoz, P., E. Hu, and B.M. Spiegelman, *Stimulation of adipogenesis in fibroblasts by PPARγ2, a lipid-activated transcription factor.* Cell, 1994. **79**(7): p. 1147-1156.

16. Ahmadian, M., et al., *PPARgamma signaling and metabolism: the good, the bad and the future.* Nat Med, 2013. **19**(5): p. 557-66.

17. Fukui, Y., et al., *A new thiazolidinedione, NC-2100, which is a weak PPAR-gamma activator, exhibits potent antidiabetic effects and induces uncoupling protein 1 in white adipose tissue of KKAy obese mice.* Diabetes, 2000. **49**(5): p. 759-767.

18. Wilson-Fritch, L., et al., *Mitochondrial remodeling in adipose tissue associated with obesity and treatment with rosiglitazone.* J Clin Invest, 2004. **114**(9): p. 1281-9.

19. Gray, S.L., et al., *Decreased brown adipocyte recruitment and thermogenic capacity in mice with impaired peroxisome proliferator-activated receptor (P465L PPARgamma) function.* Endocrinology, 2006. **147**(12): p. 5708-14.

20. Qiang, L., et al., *Brown Remodeling of White Adipose Tissue by SirT1-Dependent Deacetylation of Pparγ.* Cell, 2012. **150**(3): p. 620-632.

21. Ohno, H., et al., *PPARgamma agonists induce a white-to-brown fat conversion through stabilization of PRDM16 protein.* Cell Metab, 2012. **15**(3): p. 395-404.

22. Puigserver, P., *Tissue-specific regulation of metabolic pathways through the transcriptional coactivator PGC1-alpha.* Int J Obes (Lond), 2005. **29 Suppl 1**: p. S5-9.

23. Puigserver, P., et al., *A Cold-Inducible Coactivator of Nuclear Receptors Linked to Adaptive Thermogenesis.* Cell, 1998. **92**(6): p. 829-839.

24. Uldry, M., et al., *Complementary action of the PGC-1 coactivators in mitochondrial biogenesis and brown fat differentiation.* Cell Metab, 2006. **3**(5): p. 333-41.

25. Lelliott, C.J., et al., *Ablation of PGC-1beta results in defective mitochondrial activity, thermogenesis, hepatic function, and cardiac performance.* PLoS Biol, 2006. **4**(11): p. e369.

26. Kong, X., et al., *IRF4 is a key thermogenic transcriptional partner of PGC-1alpha.* Cell, 2014. **158**(1): p. 69-83.

27. Hallberg, M., et al., *A functional interaction between RIP140 and PGC-1alpha regulates the expression of the lipid droplet protein CIDEA.* Mol Cell Biol, 2008. **28**(22): p. 6785-95.

28. Christian, M., et al., *RIP140-targeted repression of gene expression in adipocytes.* Mol Cell Biol, 2005. **25**(21): p. 9383-91.

29. Powelka, A.M., et al., *Suppression of oxidative metabolism and mitochondrial biogenesis by the transcriptional corepressor RIP140 in mouse adipocytes.* J Clin Invest, 2006. **116**(1): p. 125-36.

30. Scime, A., et al., *Rb and p107 regulate preadipocyte differentiation into white versus brown fat through repression of PGC-1alpha.* Cell Metab, 2005. **2**(5): p. 283-95.

31. Calo, E., et al., *Rb regulates fate choice and lineage commitment in vivo.* Nature, 2010. **466**(7310): p. 1110-4.

32. Seale, P., et al., *Transcriptional control of brown fat determination by PRDM16.* Cell Metab, 2007. **6**(1): p. 38-54.

33. Kajimura, S., et al., *Initiation of myoblast to brown fat switch by a PRDM16-C/EBP-beta transcriptional complex.* Nature, 2009. **460**(7259): p. 1154-8.

34. Seale, P., et al., *Prdm16 determines the thermogenic program of subcutaneous white adipose tissue in mice.* J Clin Invest, 2011. **121**(1): p. 96-105.

35. Harms, M.J., et al., *Prdm16 is required for the maintenance of brown adipocyte identity and function in adult mice.* Cell Metab, 2014. **19**(4): p. 593-604.

36. Cohen, P., et al., *Ablation of PRDM16 and beige adipose causes metabolic dysfunction and a subcutaneous to visceral fat switch.* Cell, 2014. **156**(1-2): p. 304-16.

37. Dempersmier, J., et al., *Cold-Inducible Zfp516 Activates UCP1 Transcription to Promote Browning of White Fat and Development of Brown Fat.* Mol Cell, 2015.

38. Hagman, J., et al., *Cloning and functional characterization of early B-cell factor, a regulator of lymphocyte-specific gene expression.* Genes & Development, 1993. **7**(5): p. 760-773.

39. Akerblad, P., et al., *Early B-Cell Factor (O/E-1) Is a Promoter of Adipogenesis and Involved in Control of Genes Important for Terminal Adipocyte Differentiation.* Molecular and Cellular Biology, 2002. **22**(22): p. 8015-8025.

40. Jimenez, M.A., et al., *Critical role for Ebf1 and Ebf2 in the adipogenic transcriptional cascade.* Mol Cell Biol, 2007. **27**(2): p. 743-57.

41. Rajakumari, S., et al., *EBF2 determines and maintains brown adipocyte identity.* Cell Metab, 2013. **17**(4): p. 562-74.

42. Wang, W., et al., *Ebf2 is a selective marker of brown and beige adipogenic precursor cells.* Proc Natl Acad Sci U S A, 2014. **111**(40): p. 14466-71.

43. Zhao, X.Y., et al., *A long noncoding RNA transcriptional regulatory circuit drives thermogenic adipocyte differentiation.* Mol Cell, 2014. **55**(3): p. 372-82.

44. Villanueva, C.J., et al., *TLE3 is a dual-function transcriptional coregulator of adipogenesis.* Cell Metab, 2011. **13**(4): p. 413-27.

45. Villanueva, C.J., et al., *Adipose subtype-selective recruitment of TLE3 or Prdm16 by PPARgamma specifies lipid storage versus thermogenic gene programs.* Cell Metab, 2013. **17**(3): p. 423-35.

46. Zamani, N. and C.W. Brown, *Emerging roles for the transforming growth factor-{beta} superfamily in regulating adiposity and energy expenditure.* Endocr Rev, 2011. **32**(3): p. 387-403.

47. Yadav, H., et al., *Protection from obesity and diabetes by blockade of TGF-beta/Smad3 signaling.* Cell Metab, 2011. **14**(1): p. 67-79.

48. Gupta, R.K., et al., *Transcriptional control of preadipocyte determination by Zfp423.* Nature, 2010. **464**(7288): p. 619-23.

49. Koncarevic, A., et al., *A novel therapeutic approach to treating obesity through modulation of TGFbeta signaling.* Endocrinology, 2012. **153**(7): p. 3133-46.

50. Fu, L., et al., *Fibroblast growth factor 19 increases metabolic rate and reverses dietary and leptin-deficient diabetes.* Endocrinology, 2004. **145**(6): p. 2594-603.

51. Jonker, J.W., et al., *A PPARgamma-FGF1 axis is required for adaptive adipose remodelling and metabolic homeostasis.* Nature, 2012. **485**(7398): p. 391-4.

52. Itoh, N., *FGF21 as a Hepatokine, Adipokine, and Myokine in Metabolism and Diseases.* Front Endocrinol (Lausanne), 2014. **5**: p. 107.

53. Kharitonenkov, A., et al., *FGF-21 as a novel metabolic regulator.* J Clin Invest, 2005. **115**(6): p. 1627-35.

54. Lin, Z., et al., *Adiponectin mediates the metabolic effects of FGF21 on glucose homeostasis and insulin sensitivity in mice.* Cell Metab, 2013. **17**(5): p. 779-89.

55. Patel, V., et al., *Novel insights into the cardio-protective effects of FGF21 in lean and obese rat hearts.* PLoS One, 2014. **9**(2): p. e87102.

56. Badman, M.K., et al., *Fibroblast growth factor 21-deficient mice demonstrate impaired adaptation to ketosis.* Endocrinology, 2009. **150**(11): p. 4931-40.

57. Hondares, E., et al., *Thermogenic activation induces FGF21 expression and release in brown adipose tissue.* J Biol Chem, 2011. **286**(15): p. 12983-90.

58. Fisher, F.M., et al., *FGF21 regulates PGC-1alpha and browning of white adipose tissues in adaptive thermogenesis.* Genes Dev, 2012. **26**(3): p. 271-81.

59. Markan, K.R., et al., *Circulating FGF21 is liver derived and enhances glucose uptake during refeeding and overfeeding.* Diabetes, 2014. **63**(12): p. 4057-63.

60. Coskun, T., et al., *Fibroblast growth factor 21 corrects obesity in mice.* Endocrinology, 2008. **149**(12): p. 6018-27.

61. Owen, B.M., et al., *FGF21 acts centrally to induce sympathetic nerve activity, energy expenditure, and weight loss.* Cell Metab, 2014. **20**(4): p. 670-7.

62. Holland, W.L., et al., *An FGF21-adiponectin-ceramide axis controls energy expenditure and insulin action in mice.* Cell Metab, 2013. **17**(5): p. 790-7.

63. Kharitonenkov, A. and A.C. Adams, *Inventing new medicines: The FGF21 story.* Mol Metab, 2014. **3**(3): p. 221-9.

64. Ricciotti, E. and G.A. FitzGerald, *Prostaglandins and inflammation.* Arterioscler Thromb Vasc Biol, 2011. **31**(5): p. 986-1000.

65. Vegiopoulos, A., et al., *Cyclooxygenase-2 controls energy homeostasis in mice by de novo recruitment of brown adipocytes.* Science, 2010. **328**(5982): p. 1158-61.

66. Madsen, L., et al., *UCP1 induction during recruitment of brown adipocytes in white adipose tissue is dependent on cyclooxygenase activity.* PLoS One, 2010. **5**(6): p. e11391.

67. Garcia-Alonso, V., et al., *Coordinate functional regulation between microsomal prostaglandin E synthase-1 (mPGES-1) and peroxisome proliferator-activated receptor gamma (PPARgamma) in the conversion of white-to-brown adipocytes.* J Biol Chem, 2013. **288**(39): p. 28230-42.

68. Niederreither, K. and P. Dolle, *Retinoic acid in development: towards an integrated view.* Nat Rev Genet, 2008. **9**(7): p. 541-53.

69. Puigserver, P., et al., *In vitro and in vivo induction of brown adipocyte uncoupling protein (thermogenin) by retinoic acid.* Biochem J, 1996. **317 (Pt 3)**: p. 827-33.

70. Mercader, J., A. Palou, and M.L. Bonet, *Induction of uncoupling protein-1 in mouse embryonic fibroblast-derived adipocytes by retinoic acid.* Obesity (Silver Spring), 2010. **18**(4): p. 655-62.

71. Ziouzenkova, O., et al., *Retinaldehyde represses adipogenesis and diet-induced obesity.* Nat Med, 2007. **13**(6): p. 695-702.

72. Kiefer, F.W., et al., *Retinaldehyde dehydrogenase 1 regulates a thermogenic program in white adipose tissue.* Nat Med, 2012. **18**(6): p. 918-25.

73. Yen, P.M., *Physiological and molecular basis of thyroid hormone action.* Physiol Rev, 2001. **81**(3): p. 1097-142.

74. Bianco, A.C., X. Sheng, and J.E. Silva, *Triiodothyronine Amplifies Norepinephrine Stimulation of Uncoupling Protien Gene Transcription by a Mechanism Not Requiring Protein Synthesis.* Journal of Biological Chemistry, 1988. **263**(34): p. 18168-18175.

75. Guerra, C., et al., *Triiodothyronine Induces the Transcription of the Uncoupling Protein Gene and Stabilizes Its mRNA in Fetal Rat Brown Adipocyte Primary Cultures.* Journal of Biological Chemistry, 1996. **271**(4): p. 2076-2081.

76. Ribeiro, M.O., et al., *Thyroid hormone--sympathetic interaction and adaptive thermogenesis are thyroid hormone receptor isoform--specific.* J Clin Invest, 2001. **108**(1): p. 97-105.

77. Martinez de Mena, R., T.S. Scanlan, and M.J. Obregon, *The T3 receptor beta1 isoform regulates UCP1 and D2 deiodinase in rat brown adipocytes.* Endocrinology, 2010. **151**(10): p. 5074-83.

78. Lopez, M., et al., *Hypothalamic AMPK and fatty acid metabolism mediate thyroid regulation of energy balance.* Nat Med, 2010. **16**(9): p. 1001-8.

79. Zois, N.E., et al., *Natriuretic peptides in cardiometabolic regulation and disease.* Nat Rev Cardiol, 2014. **11**(7): p. 403-12.

80. Anand-Srivastava, M.B., *Natriuretic peptide receptor-C signaling and regulation.* Peptides, 2005. **26**(6): p. 1044-59.

81. Sarzani, R., et al., *Expression of natriuretic peptide receptors in human adipose and other tissues.* J Endocrinol Invest, 1996. **19**(9): p. 581-5.

82. Sarzani, R., et al., *Comparative analysis of atrial natriuretic peptide receptor expression in rat tissues.* J Hypertens Suppl, 1993. **11**(5): p. S214-5.

83. Lafontan, M., et al., *Control of lipolysis by natriuretic peptides and cyclic GMP.* Trends Endocrinol Metab, 2008. **19**(4): p. 130-7.

84. Bordicchia, M., et al., *Cardiac natriuretic peptides act via p38 MAPK to induce the brown fat thermogenic program in mouse and human adipocytes.* J Clin Invest, 2012. **122**(3): p. 1022-36.

85. Lumeng, C.N. and A.R. Saltiel, *Inflammatory links between obesity and metabolic disease.* J Clin Invest, 2011. **121**(6): p. 2111-7.

86. Nguyen, K.D., et al., *Alternatively activated macrophages produce catecholamines to sustain adaptive thermogenesis.* Nature, 2011. **480**(7375): p. 104-8.

87. Qiu, Y., et al., *Eosinophils and type 2 cytokine signaling in macrophages orchestrate development of functional beige fat.* Cell, 2014. **157**(6): p. 1292-308.

88. Lee, M., et al., *Activated Type 2 Innate Lymphoid Cells Regulate Beige Fat Biogenesis.* Cell, 2014.

89. Brestoff, J.R., et al., *Group 2 innate lymphoid cells promote beiging of white adipose tissue and limit obesity.* Nature, 2014.

90. Chiang, S.H., et al., *The protein kinase IKKepsilon regulates energy balance in obese mice.* Cell, 2009. **138**(5): p. 961-75.

91. Mowers, J., et al., *Inflammation produces catecholamine resistance in obesity via activation of PDE3B by the protein kinases IKK{varepsilon} and TBK1.* Elife, 2013. **2**: p. e01119.

92. Reilly, S.M., et al., *An inhibitor of the protein kinases TBK1 and IKK-varepsilon improves obesity-related metabolic dysfunctions in mice.* Nat Med, 2013. **19**(3): p. 313-21.

93. Wenz, T., et al., *Increased muscle PGC-1alpha expression protects from sarcopenia and metabolic disease during aging.* Proc Natl Acad Sci U S A, 2009. **106**(48): p. 20405-10.

94. Puigserver, P. and B.M. Spiegelman, *Peroxisome proliferator-activated receptor-gamma coactivator 1 alpha (PGC-1 alpha): transcriptional coactivator and metabolic regulator.* Endocr Rev, 2003. **24**(1): p. 78-90.

95. Bostrom, P., et al., *A PGC1-alpha-dependent myokine that drives brown-fat-like development of white fat and thermogenesis.* Nature, 2012. **481**(7382): p. 463-8.

96. Huh, J.Y., et al., *FNDC5 and irisin in humans: I. Predictors of circulating concentrations in serum and plasma and II. mRNA expression and circulating concentrations in response to weight loss and exercise.* Metabolism, 2012. **61**(12): p. 1725-38.

97. Roca-Rivada, A., et al., *FNDC5/irisin is not only a myokine but also an adipokine.* PLoS One, 2013. **8**(4): p. e60563.

98. Lee, P., et al., *Irisin and FGF21 are cold-induced endocrine activators of brown fat function in humans.* Cell Metab, 2014. **19**(2): p. 302-9.

99. Rao, R.R., et al., *Meteorin-like is a hormone that regulates immune-adipose interactions to increase beige fat thermogenesis.* Cell, 2014. **157**(6): p. 1279-91.

100. Stewart, A., H. Guan, and K. Yang, *BMP-3 promotes mesenchymal stem cell proliferation through the TGF-beta/activin signaling pathway.* J Cell Physiol, 2010. **223**(3): p. 658-66.

101. Jin, W., et al., *Schnurri-2 controls BMP-dependent adipogenesis via interaction with Smad proteins.* Dev Cell, 2006. **10**(4): p. 461-71.

102. Huang, H., et al., *BMP signaling pathway is required for commitment of C3H10T1/2 pluripotent stem cells to the adipocyte lineage.* Proc Natl Acad Sci U S A, 2009. **106**(31): p. 12670-5.

103. Whittle, A.J., et al., *BMP8B increases brown adipose tissue thermogenesis through both central and peripheral actions.* Cell, 2012. **149**(4): p. 871-85.

104. Tseng, Y.H., et al., *New role of bone morphogenetic protein 7 in brown adipogenesis and energy expenditure.* Nature, 2008. **454**(7207): p. 1000-4.

105. Fang, S., et al., *Intestinal FXR agonism promotes adipose tissue browning and reduces obesity and insulin resistance.* Nat Med, 2015.

106. Kir, S., et al., *Tumour-derived PTH-related protein triggers adipose tissue browning and cancer cachexia.* Nature, 2014. **513**(7516): p. 100-4.

107. Gnad, T., et al., *Adenosine activates brown adipose tissue and recruits beige adipocytes via A receptors.* Nature, 2014.

108. Crane, J.D., et al., *Inhibiting peripheral serotonin synthesis reduces obesity and metabolic dysfunction by promoting brown adipose tissue thermogenesis.* Nat Med, 2014.

109. Wang, G.X., et al., *The brown fat-enriched secreted factor Nrg4 preserves metabolic homeostasis through attenuation of hepatic lipogenesis.* Nat Med, 2014.

110. Shellock, F.G., M.S. Riedinger, and M.C. Fishbein, *Brown adipose tissue in cancer patients: Possible cause of cancer-induced cachexia.* Journal of Cancer Research and Clinical Oncology, 1986. **111**(1): p. 82-85.

111. Nedergaard, J., T. Bengtsson, and B. Cannon, *Unexpected evidence for active brown adipose tissue in adult humans.* Am J Physiol Endocrinol Metab, 2007. **293**(2): p. E444-52.

112. van Marken Lichtenbelt, W.D., et al., *Cold-activated brown adipose tissue in healthy men.* N Engl J Med, 2009. **360**(15): p. 1500-8.

113. Virtanen, K.A., et al., *Functional brown adipose tissue in healthy adults.* N Engl J Med, 2009. **360**(15): p. 1518-25.

114. Cypess, A.M., et al., *Identification and importance of brown adipose tissue in adult humans.* N Engl J Med, 2009. **360**(15): p. 1509-17.

115. Saito, M., et al., *High incidence of metabolically active brown adipose tissue in healthy adult humans: effects of cold exposure and adiposity.* Diabetes, 2009. **58**(7): p. 1526-31.

116. Sharp, L.Z., et al., *Human BAT possesses molecular signatures that resemble beige/brite cells.* PLoS One, 2012. **7**(11): p. e49452.

117. Lee, P., et al., *Functional thermogenic beige adipogenesis is inducible in human neck fat.* Int J Obes (Lond), 2014. **38**(2): p. 170-6.

118. Lidell, M.E., et al., *Evidence for two types of brown adipose tissue in humans.* Nat Med, 2013. **19**(5): p. 631-4.

119. Cypess, A.M., et al., *Anatomical localization, gene expression profiling and functional characterization of adult human neck brown fat.* Nat Med, 2013. **19**(5): p. 635-9.

120. Jespersen, N.Z., et al., *A classical brown adipose tissue mRNA signature partly overlaps with brite in the supraclavicular region of adult humans.* Cell Metab, 2013. **17**(5): p. 798-805.

121. Ouellet, V., et al., *Outdoor temperature, age, sex, body mass index, and diabetic status determine the prevalence, mass, and glucose-uptake activity of 18F-FDG-detected BAT in humans.* J Clin Endocrinol Metab, 2011. **96**(1): p. 192-9.

122. Lee, P., et al., *A critical appraisal of the prevalence and metabolic significance of brown adipose tissue in adult humans.* Am J Physiol Endocrinol Metab, 2010. **299**(4): p. E601-6.

123. Vijgen, G.H., et al., *Increase in brown adipose tissue activity after weight loss in morbidly obese subjects.* J Clin Endocrinol Metab, 2012. **97**(7): p. E1229-33.

124. Yoneshiro, T., et al., *Brown adipose tissue, whole-body energy expenditure, and thermogenesis in healthy adult men.* Obesity (Silver Spring), 2011. **19**(1): p. 13-6.

125. Ouellet, V., et al., *Brown adipose tissue oxidative metabolism contributes to energy expenditure during acute cold exposure in humans.* J Clin Invest, 2012. **122**(2): p. 545-52.

126. Chen, K.Y., et al., *Brown fat activation mediates cold-induced thermogenesis in adult humans in response to a mild decrease in ambient temperature.* J Clin Endocrinol Metab, 2013. **98**(7): p. E1218-23.

127. van der Lans, A.A., et al., *Cold acclimation recruits human brown fat and increases nonshivering thermogenesis.* J Clin Invest, 2013. **123**(8): p. 3395-403.

128. Yoneshiro, T., et al., *Recruited brown adipose tissue as an antiobesity agent in humans.* J Clin Invest, 2013. **123**(8): p. 3404-8.

129. Orava, J., et al., *Different metabolic responses of human brown adipose tissue to activation by cold and insulin.* Cell Metab, 2011. **14**(2): p. 272-9.

130. Chondronikola, M., et al., *Brown adipose tissue improves whole-body glucose homeostasis and insulin sensitivity in humans.* Diabetes, 2014. **63**(12): p. 4089-99.

131. Lee, P., et al., *Temperature-acclimated brown adipose tissue modulates insulin sensitivity in humans.* Diabetes, 2014. **63**(11): p. 3686-98.

132. Zhang, Y., et al., *Positional cloning of the mouse obese gene and its human homologue.* Nature, 1994. **372**(6505): p. 425-32.

133. Hotamisligil, G., N. Shargill, and B. Spiegelman, *Adipose expression of tumor necrosis factor-alpha: direct role in obesity-linked insulin resistance.* Science, 1993. **259**(5091): p. 87-91.

134. Armani, A., et al., *Mineralocorticoid receptor antagonism induces browning of white adipose tissue through impairment of autophagy and prevents adipocyte dysfunction in high-fat-diet-fed mice.* FASEB J, 2014. **28**(8): p. 3745-57.

135. Au-Yong, I.T., et al., *Brown adipose tissue and seasonal variation in humans.* Diabetes, 2009. **58**(11): p. 2583-7.

136. Orava, J., et al., *Blunted metabolic responses to cold and insulin stimulation in brown adipose tissue of obese humans.* Obesity (Silver Spring), 2013. **21**(11): p. 2279-87.

137. Pfannenberg, C., et al., *Impact of age on the relationships of brown adipose tissue with sex and adiposity in humans.* Diabetes, 2010. **59**(7): p. 1789-93.

138. Yoneshiro, T., et al., *Age-related decrease in cold-activated brown adipose tissue and accumulation of body fat in healthy humans.* Obesity (Silver Spring), 2011. **19**(9): p. 1755-60.

139. Matsushita, M., et al., *Impact of brown adipose tissue on body fatness and glucose metabolism in healthy humans.* Int J Obes (Lond), 2014. **38**(6): p. 812-7.

140. Cypess, A.M., et al., *Cold but not sympathomimetics activates human brown adipose tissue in vivo.* Proc Natl Acad Sci U S A, 2012. **109**(25): p. 10001-5.

141. Vosselman, M.J., et al., *Systemic beta-adrenergic stimulation of thermogenesis is not accompanied by brown adipose tissue activity in humans.* Diabetes, 2012. **61**(12): p. 3106-13.

CHAPTER II

Using a 3D Culture System to Differentiate Visceral Adipocytes *in vitro*

Abstract

It has long been recognized that body fat distribution and regional adiposity play a major role in the control of metabolic homeostasis. However, the ability to study and compare the cell autonomous regulation and response of adipocytes from different fat depots has been hampered by the difficulty of inducing preadipocytes isolated from the visceral depot to differentiate into mature adipocytes in culture. Here, we present an easily created 3D culture system that can be used to differentiate preadipocytes from the visceral depot as robustly as those from the subcutaneous depot. The cells differentiated in these 3D collagen gels are mature adipocytes that retain depot-specific characteristics, as determined by imaging, gene expression, and functional assays. This 3D culture system therefore allows for study of the development and function of adipocytes from both depots *in vitro*, and may ultimately lead to a greater understanding of site-specific functional differences of adipose tissues to metabolic dysregulation.

Introduction

Obesity is a major public health problem, rates of which are rising yearly in children and adults around the world [1] and the development of obesity is directly linked to multiple diseases, such

This chapter has been published as: **Emont, M.P.,** Yu, H., Hong, X., Maganti, N., Stegemann, J.P., and Wu, J. (2015) Using a 3D Culture System to Differentiate Visceral Adipocytes *In Vitro. Endocrinology.* 156(12):4761-8.

as cardiovascular disease and type 2 diabetes [2, 3]. In addition to obesity itself, fat distribution is a major predictor of metabolic disease; individuals that hold most of their weight in above the waist, visceral, depots are at much greater risk of developing metabolic and heart disease than those that hold it below the waist in subcutaneous depots [4-6]. Because adipose tissue plays a crucial role in regulating glucose and lipid metabolism, understanding the unique innate characteristics of regional fat depots and inter-depot functional distinctions may provide mechanistic insights for the causality between central adiposity and the pathogenesis of metabolic disease.

Studies on the development and function of different fat depots in humans and rodent models have uncovered a number of differences between visceral and subcutaneous fat [7]. In response to energy surplus, more hyperplasia (increasing fat cell number) is observed in the subcutaneous depot whereas hypertrophic adaptation (increasing fat cell size) is more prominent in the visceral fat [8]. Obesity is often associated with chronic inflammation that in turn results in a loss of insulin sensitivity [3], inter-depot comparisons have revealed that visceral fat tissue exhibits more pro-inflammatory gene expression, suggesting differential contributions of the depots to the development of inflammation [9]. Regional adipose tissues also differ in response to central and hormonal regulation, for example, it has been shown that cold exposure causes much more profound “browning” in the subcutaneous white adipose tissue compared to visceral [10]. Depot-specific gene signatures, including some developmental transcription factors, have been identified using whole adipose tissue gene profiling approaches [9, 11], indicating that these functional differences may be linked to intrinsic differences between the adipocytes in the two depots.

To compare these two fat depots, most studies have taken the form of *in vivo* experiments of genetically modified animals and mechanisms of cell autonomous regulation were often elucidated through *in vitro* studies using primary adipocytes. While methods have been developed to directly culture mature adipocytes [12], the majority of *in vitro* studies use adipocytes converted from preadipocytes that were isolated from the stromal vascular fraction (SVF) [13, 14]. While this method has been used to successfully study subcutaneous fat, it is less effective for visceral fat; visceral cells differentiate poorly, only 30-40%, compared to the robust differentiation seen in subcutaneous cells [15]. As a result, many *in vitro* studies have been done on only subcutaneous fat, potentially missing visceral-specific regulatory mechanisms and differential physiological functions of these two depots.

Previous work has used three-dimensional (3D) culture in collagen matrices to study the interaction of adipocytes with the extracellular matrix and manipulate adipocytes for bioengineering applications [16-18]. In this study we designed and optimized a novel protocol to differentiate visceral adipocytes in a 3D collagen hydrogel system and demonstrate that visceral cells grown in these hydrogels differentiate as robustly as subcutaneous preadipocytes. We additionally show that these visceral adipocytes are functional fat cells that retain characteristics specific to the visceral depot. This user-friendly 3D culture protocol will enable *in vitro* studies of primary visceral preadipocytes, which may lead to new mechanistic insights into the development and function of visceral fat.

Materials and Methods

Animals

All animal experiments were carried out following protocols approved by the University Committee on Use and Care of Animals (UCUCA) at the University of Michigan and conducted in conformity with the Public Health Service Policy on Humane Care and Use of Laboratory Animals. Similar results were observed with mice of both genders. Individual experiments were performed on cells that were isolated from the subcutaneous and visceral tissues of the same animals and processed side by side.

SVF Isolation

Mice were sacrificed and fat tissue was dissected from the inguinal (subcutaneous), perigonadal (visceral), and mesenteric depots. Tissue was minced and digested in a solution containing Collagenase D (Roche 11088858001)/Dispase II (Roche 04942078001) + 10mM $CaCl_2$. After the tissue was fully digested, cells were suspended in wash media (DMEM/F12+GlutaMAX (Thermo Fisher 10565) supplemented with 10% FBS (Sigma F2442)), filtered through a 100-micron cell strainer, and centrifuged at 200-300 x *g* for 5 minutes. Same lots of the Collagenase, Dispase and FBS were used throughout this study. The supernatant was removed and the pellet was then disrupted, resuspended in wash media, and filtered through a 40-micron cell strainer. This suspension was similarly centrifuged, the supernatant was discarded, and the disrupted pellet was resuspended in growth media (DMEM/F12 + GlutaMAX supplemented with 15% FBS) and plated on 10 cm dishes that had been coated with collagen type 1 isolated from rat tail (Fisher CB-40236). Contaminating cell types (e.g. red blood cells, immune cells) were removed after one to two rounds of subculture. Adherent fibroblast-like preadipocytes were then trypsinized and counted using a hemocytometer before plating for differentiation on a collagen coated 12 well plate or seeding into a collagen hydrogel. For each experiment, the subcutaneous

and visceral cells were obtained from the same cohort of animals and were isolated and differentiated side by side.

Differentiation

To induce adipogenesis, cells were plated at a concentration of 300,000 cells per well of a collagen coated 12 well plate (2D) or seeded at a concentration of 300,000 cells per 500 μL gel into a collagen hydrogel (3D). Cells were stimulated in DMEM/F12 + GlutaMAX supplemented with 10% FBS, dexamethasone (5 μM, Sigma D4902), insulin (0.5 μg/mL, Sigma I5500), isobutylmethylxanthine (0.5 mM, Sigma I7018)), and rosiglitazone (1 μM, Cayman 71740). After two days of stimulation, cells were maintained in DMEM/F12 + GlutaMAX with 10% FBS and insulin (0.5 μg/mL). Analyses of mature adipocytes were performed 6-7 days after stimulation.

Seeding Cells in Collagen Hydrogels

Collagen was diluted prior to gel creation by adding 0.02 N acetic acid to high concentration rat tail collagen type I (Corning Fisher CB-354249) to a final concentration of 8 mg/mL. Preadipocytes were counted, pelleted, and resuspended in DMEM/F12 to a final concentration of 300,000 cells/50 μL (10X concentrated to the final seeding density). For each gel, 50 μL of this suspension was placed in a sterile eppendorf tube that contained 100 μL 5X DMEM/F12 (created using DMEM/F12 powder, Thermo Fisher 12500) and 50 μL FBS and the solution was mixed evenly by pipetting. 50 μL of 0.1 N NaOH was then added to this mixture, followed immediately by 250 μL 8 mg/mL acidic collagen solution. This step involves acute pH changes, which can be visually monitored with the pH indicator (phenol red) in the DMEM/F12 media. NaOH increases

the pH in the solution and causes the phenol red to turn a bright pink color, and the acidic collagen solution neutralizes the mixture and brings it back to an orange color. The cells were suspended evenly within the solution by pipetting and 500 μL of mixture was transferred to one well of a 24 well plate. The plates were placed in a 37°C incubator, and collagen within each well started to polymerize at the neutral pH. It takes approximately 10 minutes for gels to solidify, a change that can be assessed by development of a slightly cloudy appearance. Growth media was added to each well after polymerization was complete. Cells were differentiated in the gels using the standard differentiation procedure described above. For a schematic of cell isolation and gel creation, see Figure II.1.

Imaging

Oil Red O staining was performed as previously described [19]. For fluorescence, cells grown and differentiated in a gel (3D) or on a collagen coated glass bottom culture dish (2D) (MatTek) were fixed in 10% neutral-buffered formalin, washed twice with PBS, and incubated rocking at 4°C in the dark in PBS supplemented with 0.01 mg/mL BODIPY 493/503 (4,4-Difluoro-1,3,5,7,8-Pentamethyl-4-Bora-3a,4a-Diaza-*s*-Indacene, Life Technologies) and 1 μg/mL Propidium Iodide (Life Technologies). Samples were then washed twice with PBS and imaged using a confocal microscope. Gels were transferred to a glass bottom dish before imaging.

Gene Expression Analysis

To isolate RNA from 3D samples or adipose tissue, gels or fat tissues were homogenized in TRIzol reagent (Life Technologies) with a handheld homogenizer. RNA from cells grown in 2D was also isolated with TRIzol reagent and total RNA from 2D and 3D samples was isolated

according to the protocol provided by the manufacturer. Total RNA was reverse transcribed using M-MLV (Invitrogen) and analyzed using SYBR green (Fisher Scientific). All primer sequences are listed in Table II.1.

Image Quantitation

Fluorescent images were taken at 40x magnification as described in the manuscript. 50 images of visceral cells differentiated in 3D culture and 50 images of subcutaneous cells differentiated in 3D culture were blindly quantified by a co-author who counted the number of nuclei, the number of nuclei associated with lipid droplets, the number of lipid droplets per cell, and the diameter of the lipid droplets in each image. Lipid droplet diameter was determined using ImageJ.

ELISAs

Gels were incubated in 900 μL media supplemented with 1 μg/mL LPS for 4 hours. ELISAs were performed using R&D DuoSet® kits specific to mouse IL-6 or mouse TNF alpha according to the instructions provided by the manufacturer.

Western Blotting

Gels were serum starved for 4 hours and treated with or without 10 μM isoproterenol for 15 minutes. Samples were placed in 150 μL ice cold RIPA buffer supplemented with a cOmplete™ protease inhibitor cocktail tablet (Roche), homogenized using a handheld homogenizer, incubated, rocking, at 4°C for one hour, and centrifuged before being analyzed using SDS-PAGE.

Lipolysis

Gels were incubated with and without 10 μM isoproterenol (Sigma) at 37°C for one hour. The glycerol content of the supernatant was determined using free glycerol reagent (Sigma) according to the protocol provided by the manufacturer.

Cellular Respiration

Primary brown adipocytes were seeded into a collagen hydrogel and differentiated for 6 days as described in the manuscript. Gels were placed in PBS and minced with a razor blade before being transferred to the respiration system. Oxygen consumption was measured using a Strathkelvin Clark-type electrode as previously described [9].

GLUT4 Translocation

3T3-L1 cells stably expressing GFP tagged GLUT4 were a generous gift from Dr. Alan Saltiel's lab [20]. Cells were seeded into collagen hydrogels and differentiated for 7 days as described in the manuscript. Gels were washed twice in PBS and serum starved for 6 hours before treatment with or without 100 nM insulin. The intracellular distribution and translocation of GLUT4 were monitored and imaged with a confocal microscope.

Statistics

Data are expressed as mean ± standard error and significance was determined using a student's *t*-test. The reported "n" refers to the number of biological replicates of 2D wells or 3D gels tested in each experiment. $P \leq 0.05$ was considered significant, $P \leq 0.01$ is represented as "**", and $P \leq 0.001$ is represented as "***".

Results

Visceral Preadipocytes Differentiate as Robustly as Subcutaneous Preadipocytes in 3D Collagen Hydrogels

It has been previously reported that visceral preadipocytes do not differentiate to the same extent as subcutaneous cells in monolayer culture conditions [15, 21]. One possible reason for this is that they are intrinsically different than subcutaneous cells; visceral cells tend to form larger and fewer lipid droplets than subcutaneous cells *in vivo* [8] and thus may need more structural support and the ability to assume more natural shapes in order to differentiate into structurally fragile mature adipocytes with large lipid droplets. Collagen is a major structural protein in many tissues and has been used as a scaffolding biomaterial for a variety of cell culture and tissue engineering applications [22, 23]. We therefore tested collagen hydrogels to evaluate their utility in improving the differentiation of visceral preadipocytes. Various concentrations of collagen and different cell densities were tested and compared before we chose 4 mg/mL of collagen and 3 x 10^5 cells/500 μL gel as conditions that were ideal for promoting optimal visceral cell differentiation.

To test whether the collagen hydrogel system allows visceral preadipocytes to differentiate into mature fat cells to the same extent as subcutaneous preadipocytes, we grew and differentiated preadipocytes obtained from the SVF of subcutaneous and visceral depots side by side. The lack of lipid droplet accumulation in many visceral cells, as visualized by the absence of Oil Red O staining, demonstrated that these cells differentiated much more poorly than the subcutaneous cells in 2D cultures (II.2A, upper panels). Fluorescent imaging of 2D cultures stained with BODIPY (*boron-dipyrromethene*, a green fluorescent dye that is often used for staining lipids)

and Propidium Iodide (a red fluorescent dye that stains the nucleus) further showed a near complete differentiation in subcutaneous cells and poor differentiation of visceral cells (Figure II.2A, lower panels). When cultured in collagen hydrogels, the cells from both depots demonstrated robust differentiation (Figures II.2B, II.3A). Additionally, the visceral cells contain larger and fewer lipid droplets than the subcutaneous cells, consistent with morphology found *in vivo* and with previous reports of adipocytes grown in collagen gels [24-26] (Figure II.3B-D).

To evaluate adipogenesis at the molecular level, we tested the expression levels of mature adipocyte markers in subcutaneous and visceral fat cells in both 2D and 3D cultures. We found that *Adipoq, Fabp4* (also called *aP2*), and *Pparg* are significantly higher in subcutaneous 2D culture than in visceral 2D culture but are expressed at similar levels in 3D cultures (Figure II.2C). We also tested a number of genes involved in lipid and glucose metabolism *Atgl, Dgat1, Glut4, Hsl, Plin1* and *Scd1*. Expression of these genes was low in visceral 2D culture and greatly increased in both subcutaneous 2D and subcutaneous and visceral 3D cultures, showing that these cells have robust expression of metabolic genes that are necessary for mature adipocyte function (Figure II.2D). We also tested our 3D gel culture system with precursors isolated from mesenteric fat, another visceral depot. We found that, similar to those from the perigonadal depot, preadipocytes isolated from the mesenteric depot also undergo robust differentiation in the 3D culture system upon adipogenic stimulation (Figure II.4). Overall, these data suggest that our collagen 3D gels allow for vigorous differentiation of visceral preadipocytes *in vitro*.

Adipocytes Differentiated in the Collagen Hydrogels Retain Depot-Specific Characteristics

We next tested the expression levels of previously identified depot-specific gene signatures to investigate whether cells cultured in collagen gels maintain their original depot identity. We assayed *Shox2* and *Tbx15*, both of which are enriched in the subcutaneous depots of mice and humans [11, 27] as well as *Agt* and *Wt1,* which are enriched in the visceral depots of both mice [9, 24] and humans [27]. We first verified that these genes are enriched in their respective depots by assaying expression levels in tissue, then tested if they were similarly enriched in 2D and 3D culture. The inter-depot expression differences are more pronounced in 3D culture compared to 2D culture in all cases and depot specific enrichment of *Agt* is even reversed in 2D culture (Figure II.5A-B). These data suggest that tissue-specific gene expression patterns can be obscured in sub-physiological 2D culture conditions, and that the 3D culture system reliably replicates the magnitude of the differential gene expression and restores the dysregulated gene expression that sometimes occurs in 2D culture.

We next tested the expression of genes related to functional characteristics of both depots. Thermogenic genes have been shown to be expressed at higher levels in the subcutaneous depot [10] while the visceral depot has been shown to produce greater amounts of some cytokines [6]. We differentiated visceral and subcutaneous preadipocytes in gels and tested the expression levels of *Cidea, Cox7a1, Dio2, Ppargc1a,* and *Prdm16* which are genes associated with thermogenesis [9, 28], as well as *Ccl2* (also called *Mcp1*)*, Ccl5* (also called *Rantes*)*, Il6, Il10,* and *Tnfa* which are cytokines known to be secreted from fat [6]. Thermogenic gene expression was higher in the subcutaneous cells (Figure II.5C) while cytokine gene expression was higher in the visceral cells (Figure II.5D). Lipopolysaccharide (LPS) is an endotoxin found in the cell wall of gram-negative bacteria that produces a strong immune response in many tissues, including

adipose tissue. We treated cells from both depots cultured in 3D gels with LPS and observed clear inter-depot difference in both cytokine gene expression (Figure II.5E) and cytokine secretion, as measured by ELISA (Figure II.5F). Taken together, these data show that the collagen 3D culture system enables visceral and subcutaneous adipocytes to retain their depot-specific characteristics and can thus be used to study the intrinsic differences between adipocytes from the two depots.

Cells Differentiated in Collagen Hydrogels are Functional Adipocytes

Cells grown and differentiated in 3D culture were further tested to ensure that they retain the functionalities of mature adipocytes. It has been shown that upon cold exposure the adaptive thermogenic response is activated in white fat via adrenergic signaling [29]. We treated visceral and subcutaneous cells grown in 3D gels with isoproterenol, a pan β-adrenergic agonist, significantly increasing thermogenic gene expression in 3D cultures of both visceral and subcutaneous cells (Figure II.6A). Phosphorylation of p38 MAP Kinase (p38), a key regulator of β-adrenergic stimulated thermogenesis, was also increased in the isoproterenol treated samples (Figure II.6B). Hydrolysis of triglycerides to fatty acids and glycerol (lipolysis) is an important function of mature adipocytes and helps to maintain nutritional and energy homeostasis. We treated the gels with isoproterenol to mimic *in vivo* catecholamine stimulated lipolysis, and saw significantly increased glycerol content in the supernatant of stimulated visceral and subcutaneous gels (Figure II.6C), as well as an increase in the phosphorylation of hormone-sensitive lipase (HSL) (Figure II.6D), an important step in the initiation of lipolysis [30]. We were also able to measure oxygen consumption of adipocytes differentiated in 3D gels (Figure II.7) and assess their ability to respond to hormonal stimulation (Figure II.8). These results

suggest that cells grown in the hydrogels not only exhibit the morphological characteristics and gene expression profiles of mature adipocytes but also can fulfill their many functions.

Discussion

In an attempt to find a culture condition that would allow visceral preadipocytes to differentiate as robustly as subcutaneous preadipocytes *in vitro*, we optimized a collagen hydrogel system to determine the ideal growth and differentiation conditions for visceral cells. Compared to many commercially available 3D culture systems, our collagen gels are easy to create and do not require specialized equipment or technical skills. Culture and differentiation using this protocol does not demand more cells than what is normally used in the 2D culture system, and downstream functional analyses can be carried out using the same techniques commonly used on whole tissues or cells grown in 2D. Using this system we are able to differentiate visceral cells as robustly as subcutaneous cells grown in 2D and 3D culture, thus providing a system where cells from both depots can be studied side by side.

The reason why visceral cells do not differentiate as well as subcutaneous cells in 2D culture is not yet well understood. In this study we compared the differentiation potential of preadipocytes from these two depots in 2D and 3D cultures. The fact that the adipogenic potential of visceral cells can be restored in our collagen gel system suggest that the compromised adipogenesis seen in 2D is at least in part caused by some intrinsic properties of these precursors that can be ameliorated by the enhanced structural support of the 3D culture or other external factors. In visceral cells differentiated in gels, we observed robust expression of genes associated with metabolism as well as previously identified depot markers and functional markers, including

cytokines. This reliable replication of *in vivo* depot-specific characteristics underlines the utility of the 3D hydrogel system in studying the intrinsic differences of adipocytes from different depots.

In summary, we show that 3D collagen hydrogels are a valuable system for culturing and differentiating visceral adipocytes. These gels are easy to create, can be used for a variety of molecular and functional studies, and do not require specialized equipment beyond those used for 2D cell culture. With this system we can study the cell autonomous regulation of visceral and subcutaneous adipocytes side by side and gain a better understanding of their individual contributions to the pathogenesis of metabolic disease.

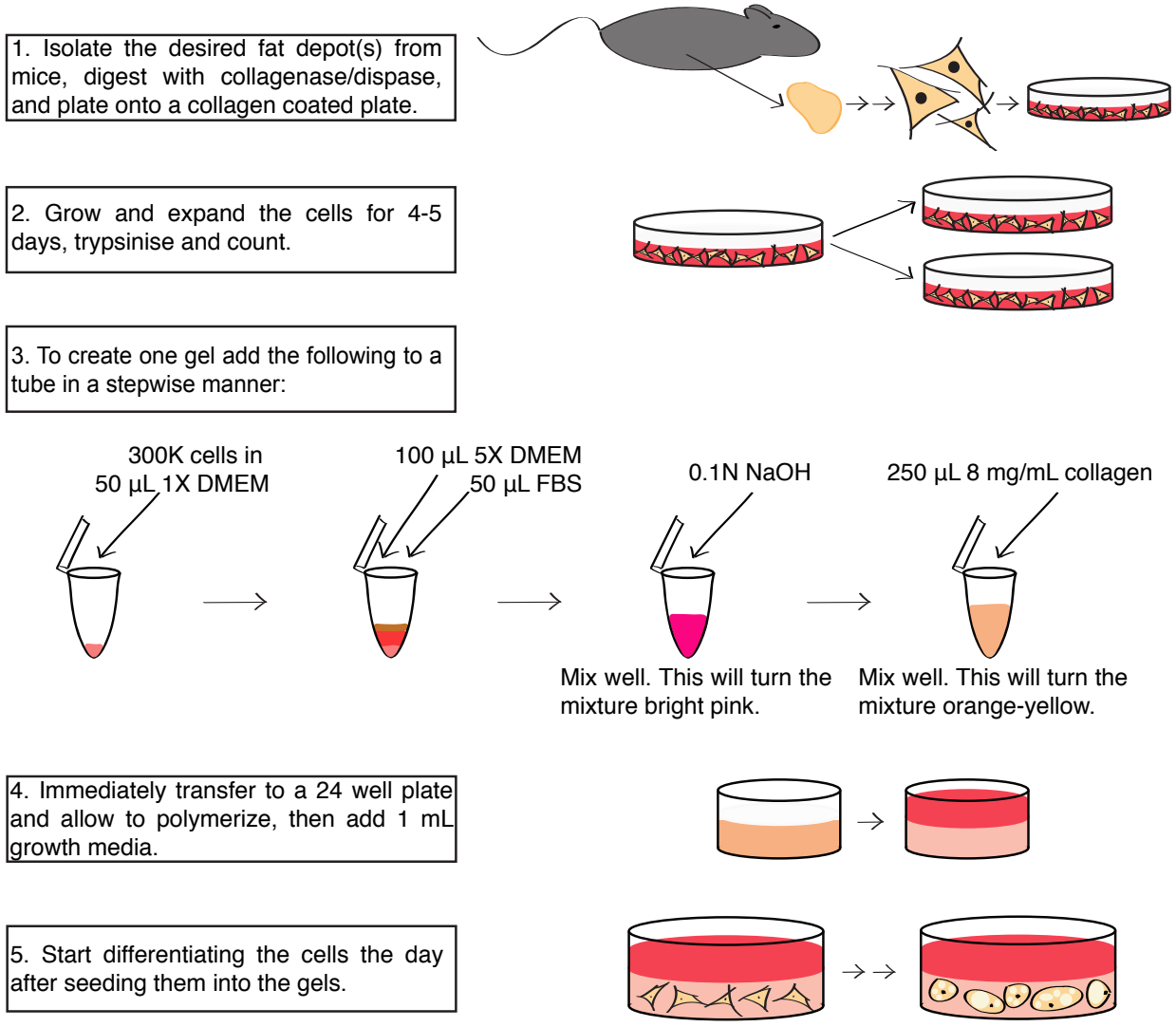

Figure II.1 Schematic for the Isolation of Preadipocytes and Culture in Collagen Hydrogels

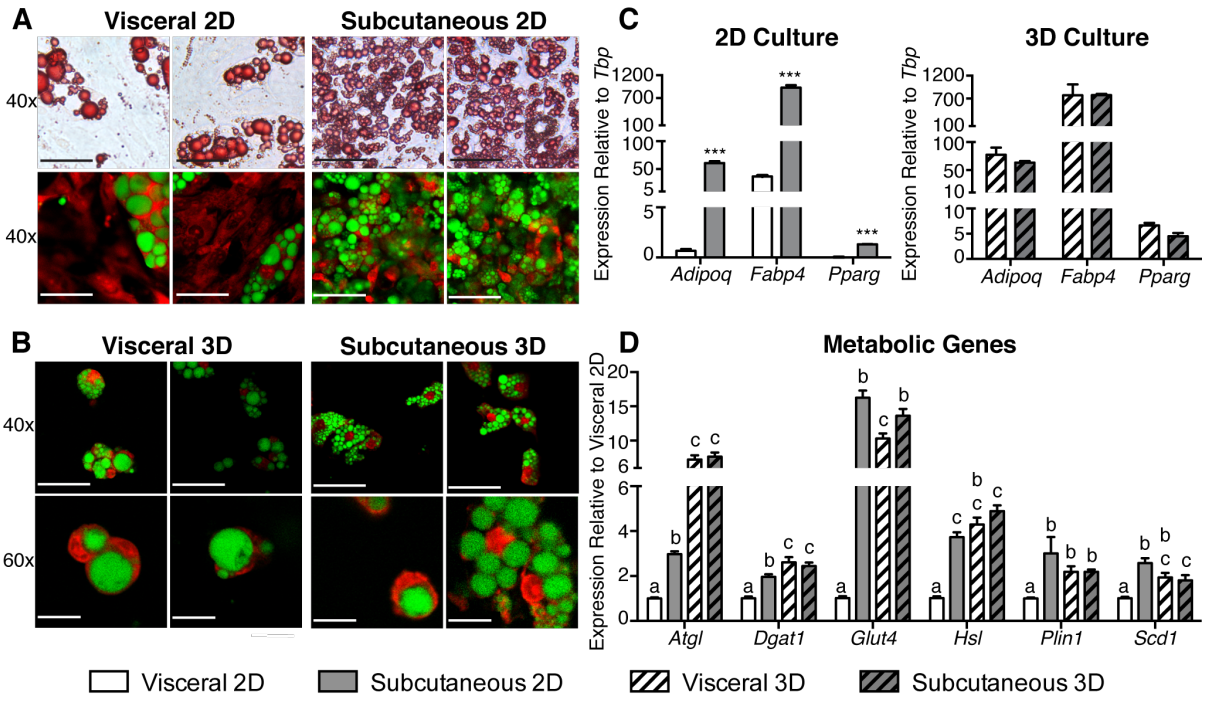

Figure II.2 Preadipocytes Isolated from Visceral Fat Depots Differentiate as Robustly as those from Subcutaneous Depots in 3D but not 2D Culture.

A. Representative morphologies of visceral and subcutaneous fat cells grown and differentiated in 2D culture, seen at 40x magnification. Upper panels, Oil Red O staining; lower panels, BODIPY (lipid, green)/Propidium Iodide (nucleus, red) staining **B.** Representative images of BODIPY/Propidium Iodide staining of visceral and subcutaneous cells grown in 3D culture at 40x and 60x magnifications. Scale bars for 40x images are 50 μm and scale bars for 60x images are 20 μm. **C.** Expression of mature adipocyte markers *Adipoq*, *Fabp4*, and *Pparg* were assessed using RT-qPCR in cultures of visceral and subcutaneous adipocytes differentiated on 2D plates or in 3D gels. Values are mean ± SEM (n=3), ***, $P \leq 0.001$. **D.** Expression levels of genes involved in glucose and lipid metabolism (*Atgl*, *Dgat1*, *Glut4*, *Hsl, Plin1*, and *Scd1*) were measured using RT-qPCR in cultures of visceral and subcutaneous adipocytes differentiated in 2D or 3D. Values are mean ± SEM (n=6), different letters indicate a statistically significant difference ($P \leq 0.05$).

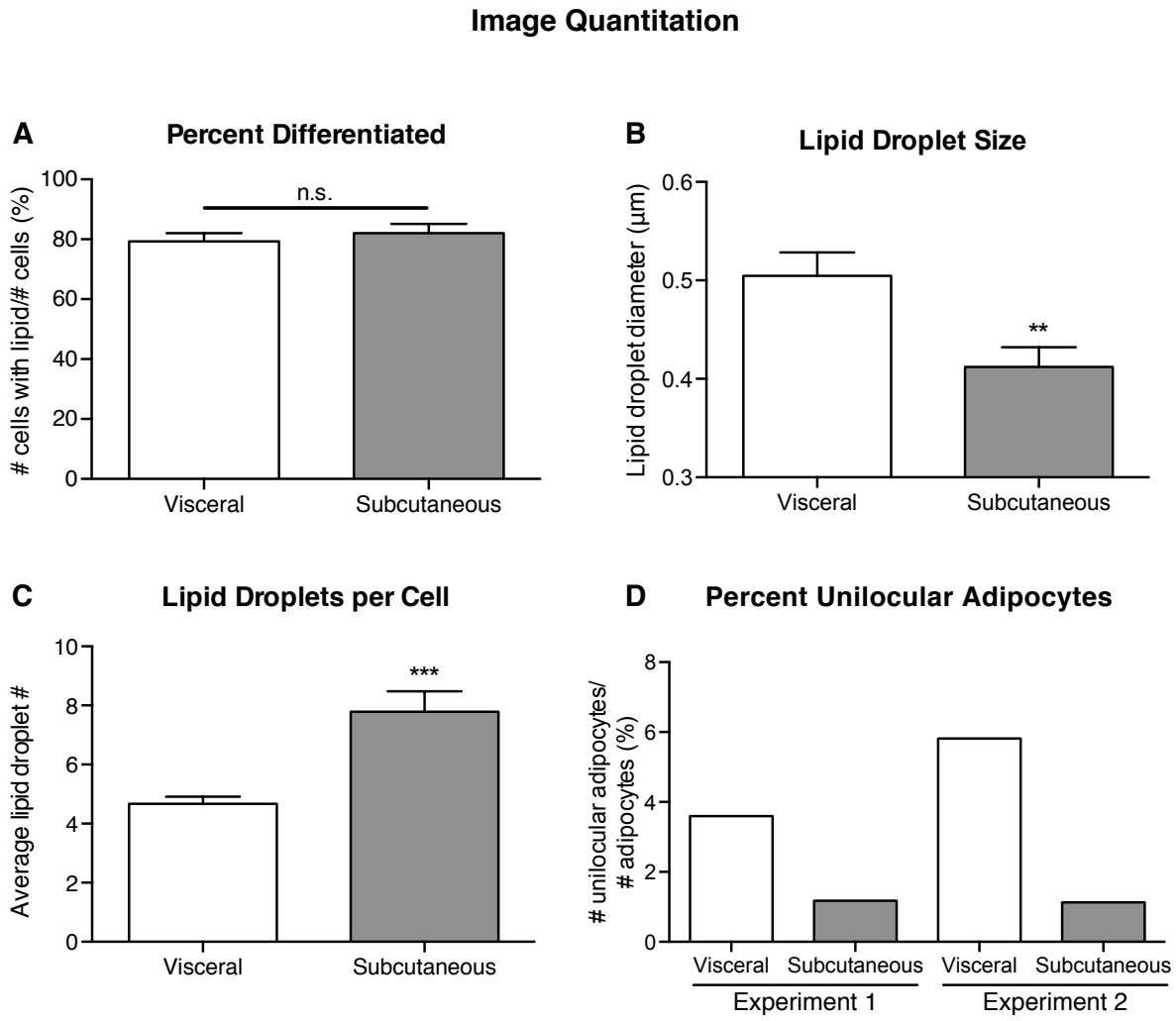

Figure II.3 Visceral Cells Differentiate as Robustly as Subcutaneous Cells in 3D Hydrogels and Contain Fewer and Larger Lipid Droplets

A. Quantifications of the percentage of total counted cells that contain lipid droplets in images of 3D cultures of visceral or subcutaneous cells. **B.** Measuring the diameter of lipid droplets in visceral and subcutaneous adipocytes differentiated in 3D culture shows that visceral cells contain larger lipid droplets than subcutaneous cells on average. **C.** Quantifying the number of lipid droplets in mature adipocytes from visceral or subcutaneous 3D culture reveals that, on average, visceral cells contain fewer lipid droplets than subcutaneous cells. **D.** Analysis of the percentage of mature adipocytes that are unilocular across the total number of adipocytes counted in two separate experiments shows that visceral 3D cultures contain a greater percentage of unilocular adipocytes. Over 200 cells were counted for each depot and lipid droplet diameters were measured on 50 blindly chosen cells from each depot, values are mean ± SEM, n.s., $P > .05$, **, $P \leq 0.01$, ***, $P \leq 0.001$.

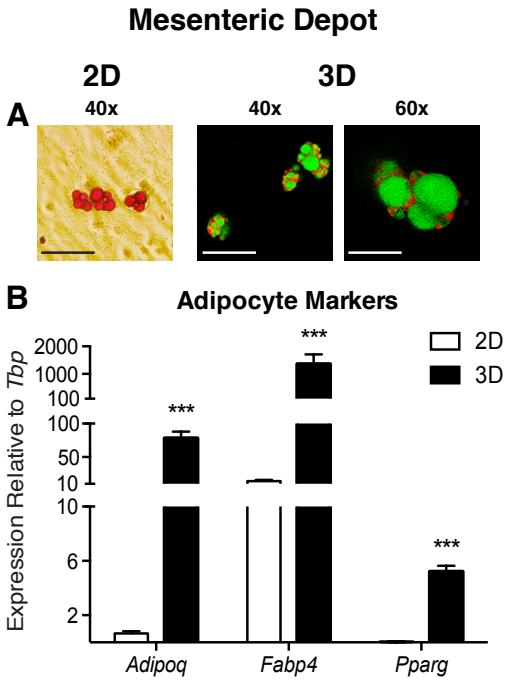

Figure II.4 Preadipocytes Isolated from the Mesenteric Depot Differentiate Robustly in 3D Culture

A. Oil Red O staining of mesenteric adipocytes differentiated in 2D culture and BODIPY (lipid, green)/Propidium Iodide (nucleus, red) staining of mesenteric adipocytes differentiated in 3D culture show improved differentiation of mesenteric cells in 3D culture. Scale bars for 40x images are 50 μm and scale bars for 60x images are 20 μm. **B.** Expression of mature adipocyte markers *Adipoq*, *Fabp4*, and *Pparg* were assessed using RT-qPCR in cultures of mesenteric adipocytes differentiated on 2D plates or in 3D gels to confirm that mesenteric cells grown in 3D hydrogels undergo much more complete differentiation. Values are mean ± SEM (n=6), ***, $P \leq 0.001$.

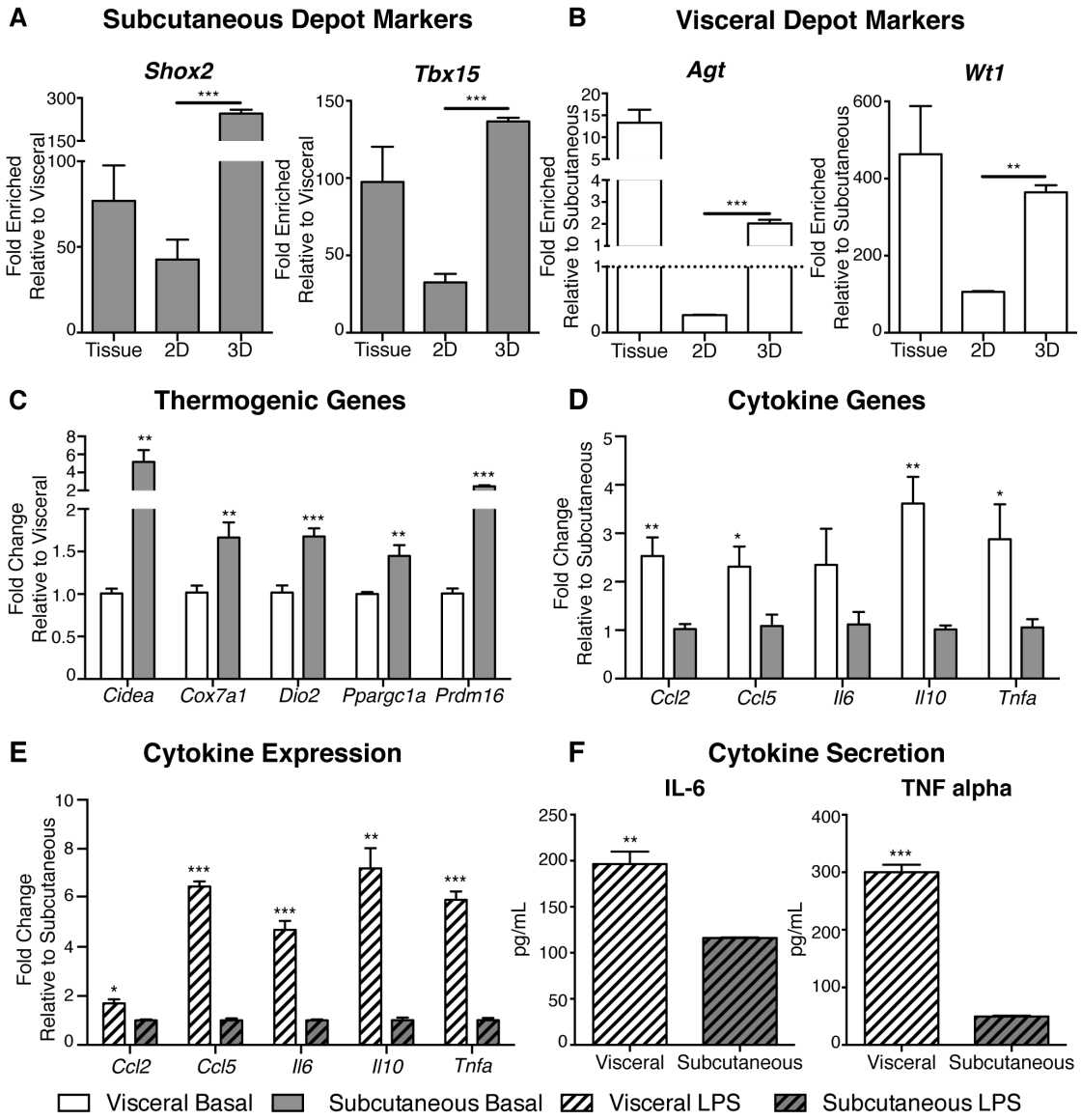

Figure II.5 Cells Grown in the Collagen Hydrogels Retain Depot Specific Gene Expression and Function

A-B. Expression of genes preferentially expressed in either subcutaneous (*Shox2* and *Tbx15*) or visceral (*Agt* and *Wt1*) adipose depots were assayed using RT-qPCR with RNA extracted from subcutaneous/visceral adipose tissue or subcutaneous/visceral cells differentiated in 2D or 3D culture. Relative enrichment of depot-specific expression is shown as mean ± SEM (n=3), **, $P \leq 0.01$; and ***, $P \leq 0.001$. **C.** Expression of thermogenic genes (*Cidea*, *Cox7a1, Dio2*, *Ppargc1a*, and *Prdm16*) was measured in 3D cultures of differentiated visceral and subcutaneous cells by RT-qPCR. **D-E.** Expression of cytokine genes (*Ccl2*, *Ccl5*, *Il6*, *Il10*, and *Tnfa*) was measured in basal (**D**) or LPS stimulated (**E**, 1 μg/mL LPS for 4 hours) subcutaneous or visceral cells differentiated in 3D gels. Values are mean ± SEM (n=5), *, $P \leq 0.05$, **, $P \leq 0.01$, ***, $P \leq 0.001$. **F.** Secretion of IL-6 and TNF alpha by visceral or subcutaneous cells grown in 3D gels was measured in the supernatant of gels stimulated with 1 μg/mL LPS for 4 hours. Values are mean ± SEM (n=3), **, $P \leq 0.01$, ***, $P \leq 0.001$.

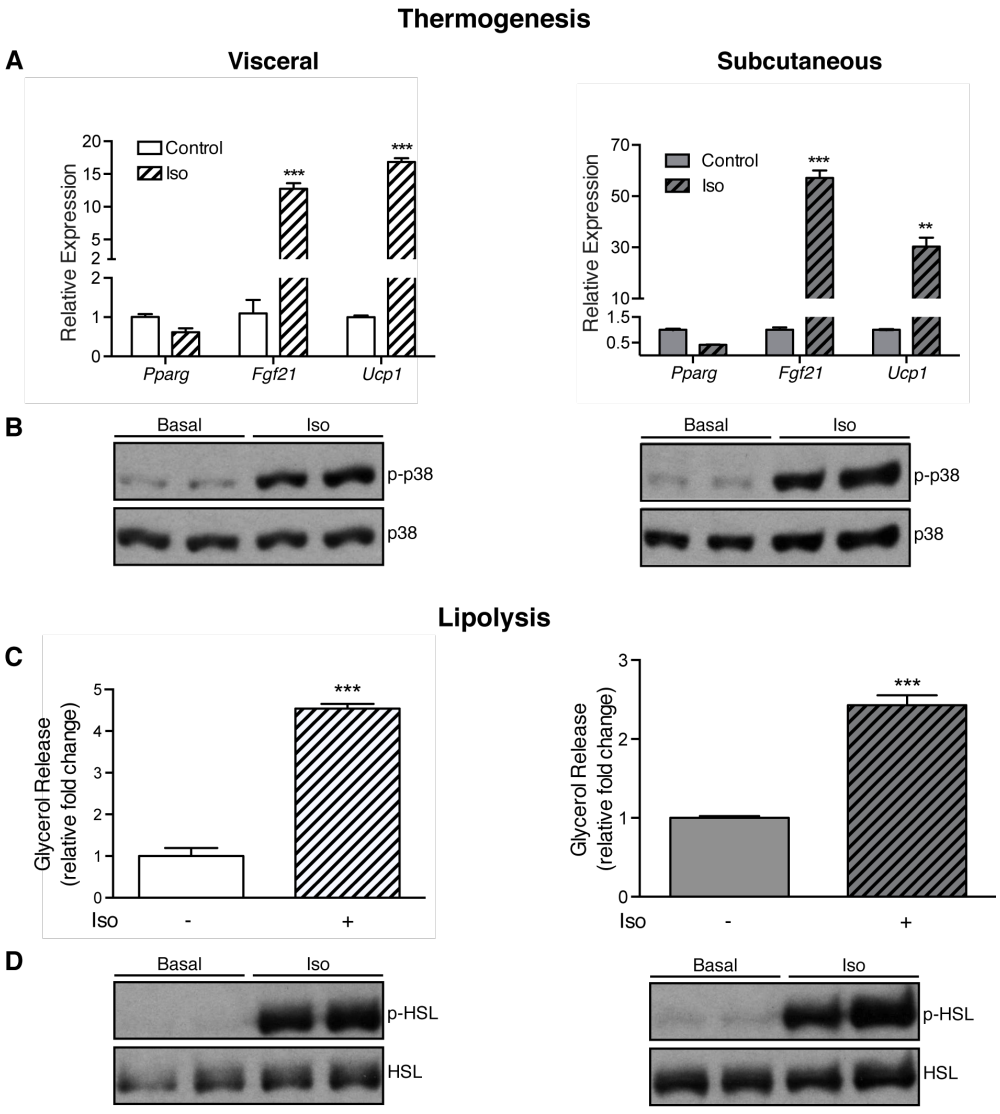

Figure II.6 Adipocytes Differentiated in 3D Gels Maintain Normal Function in Response to Adrenergic Stimulation

A. Differentiated visceral and subcutaneous cells grown in 3D gels were treated with or without isoproterenol (10 μM for 4 hours), then evaluated for gene expression levels of *Pparg*, *Fgf21* and *Ucp1* using RT-qPCR. Values are mean ± SEM (n=3), **, $P \leq 0.01$; and ***, $P \leq 0.001$. **B.** Differentiated visceral and subcutaneous cells grown in gels were treated with or without isoproterenol (10 μM for 15 minutes), then western blotted to determine levels of phospho- and total p38. **C.** Differentiated visceral and subcutaneous cells grown in 3D gels were incubated with or without isoproterenol (10 μM for 1 hour), supernatant was then assayed for glycerol content as a readout for lipolysis. Values are mean ± SEM (n=3), ***, $P \leq 0.001$. **D.** Differentiated visceral and subcutaneous cells grown in gels were treated with or without isoproterenol (10 μM for 15 minutes), then western blotted to assay levels of phospho-HSL (S563) or total HSL.

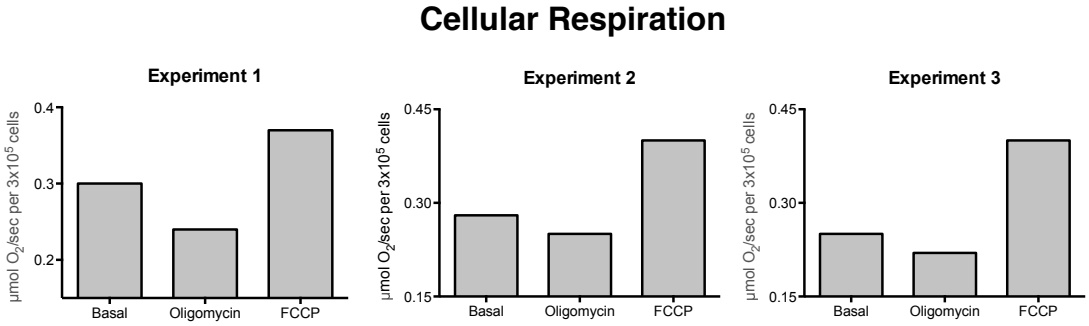

Figure II.7 Adipocytes Grown in 3D Gels Can Be Assayed for Oxygen Consumption
Brown adipocytes were also able to be grown and differentiated in 3D gels, similar to subcutaneous and visceral cells. Oxygen consumption measurements with 3D gels were demonstrated in these cells due to their higher mitochondrial content. Gels containing differentiated brown adipocytes were minced with a razor blade and oxygen consumption was measured. The results of three separate experiments are shown. For each experiment, oligomycin (Sigma) was added to measure uncoupled respiration, then FCCP (Sigma) was added to measure the maximal respiration.

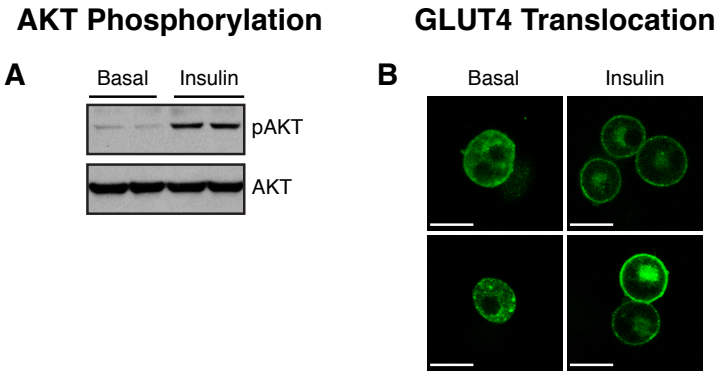

Figure II.8 Adipocytes Grown in 3D Gels Are Acutely Regulated by Hormonal Stimulation **A.** Cells grown in 3D gels undergo AKT phosphorylation in response to insulin stimulation. Visceral cells differentiated in 3D gels were serum starved for 4 hours, then treated with 10 nM insulin for 10 minutes. To determine the amount of AKT phosphorylation in the gels, levels of phospho-AKT (S473) or total AKT were measured by western blot. **B.** The glucose transporter GLUT4 translocates to the plasma membrane in response to stimulation within the adipocytes cultured in 3D gels. 3T3-L1 cells stably expressing GFP tagged GLUT4 were serum starved for 6 hours, then treated with 100 nM insulin for 30 minutes before being imaged with a confocal microscope. Two representative images of basal and insulin treated cells are shown. In untreated cells, GLUT4 is sequestered in vesicles in the cytoplasm, visualized by the diffuse GFP signal in the cells with insulin treatment (basal). Upon insulin stimulation, GLUT4 is translocated to the plasma membrane, resulting in the sharp ring of GFP seen on the borders of the cells. Scale bars are 20 μm.

Genes	Full Name	Forward	Reverse
Adipoq	Adiponectin	5'-GCACTGGCAAGTTCTACTGCAA-3'	5'-GTAGGTGAAGAGAACGGCCTTGT-3'
Agt	Angiotensinogen	5'-TCTCCTTTACCACAACAAGAGCA-3'	5'-CTTCTCATTCACAGGGGAGGT-3'
Ccl2 (Mcp1)	Chemokine (C-C motif) ligand 2	5'-TTAAAAACCTGGATCGGAACCAA	5'-GCATTAGCTTCAGATTTACGGGT-3'
Ccl5 (Rantes)	Chemokine (C-C motif) ligand 5	5'-GCTGCTTTGCCTACCTCTCC-3'	5'-TCGAGTGACAAACACGACTGC-3'
Cidea	Cell death activator CIDE-A	5'-TGCTCTTCTGTATCGCCCAGT-3'	5'-GCCGTGTTAAGGAATCTGCTG-3'
Cox7a1	Cytochrome c oxidase polypeptide 7A1	5'-GCTCTGGTCCGGTCTTTTAGC-3'	5'-GTACTGGGAGGTCATTGTCGG-3'
Dgat1	Diacylglycerol O-acyltransferase 1	5'-TCCGTCCAGGGTGGTAGTG-3'	5'-TGAACAAAGAATCTTGCAGACGA-3'
Dio2	Deiodinase, iodothyronine, type II	5'-CATCTTCCTCCTAGATGCCTA-3'	5'-CTGATTCAGGATTGGAGACGTG-3'
Fabp4 (aP2)	Fatty acid binding protein 4	5'-ACACCGAGATTTCCTTCAAACTG-3'	5'-CCATCTAGGGTTATGATGCTCTTC-3'
Fgf21	Fibroblast growth factor 21	5'-GTGTCAAAGCCTCTAGGTTTCTT-3'	5'-GGTACACATTGTAACCGTCCTC-3'
Il6	Interleukin 6	5'-TAGTCCTTCCTACCCCAATTTCC-3'	5'-TTGGTCCTTAGCCACTCCTTC-3'
Il10	Interleukin 10	5'-GCTCTTACTGACTGGCATGAG-3'	5'-CGCAGCTCTAGGAGCATGTG-3'
Lipe (Hsl)	Lipase, hormone-sensitive	5'-TGAGATGCCACTCACCTCTG-3'	5'-GCCTAGTGCCTTCTGGTCTG-3'
Plin1	Perilipin 1	5'-GGGACCTGTGAGTGCTTCC-3'	5'-GTATTGAAGAGCCGGGATCTTTT-3'
Pnpla2 (Atgl)	Patatin-like phospholipase domain containing 2	5'-AACACCAGCATCCAGTTCAA-3'	5'-GGTTCAGTAGGCCATTCCTC-3'
Pparg	Peroxisome proliferator-activated receptor gamma	5'-GCATGGTGCCTTCGCTGA-3'	5'-TGGCATCTCTGTGTCAACCATG-3'
Ppargc1a	Peroxisome proliferator-activated receptor gamma, coactivator 1 alpha	5'-AGCCGTGACCACTGACAACGAG-3'	5'-GCTGCATGGTTCTGAGTGCTAAG-3'
Prdm16	PR domain containing 16	5'-CCACCAGCGAGGACTTCAC-3'	5'-GGAGGACTCTCGTAGCTCGAA-3'
Scd1	Stearoyl-CoA desaturase-1	5'-TTCTTGCGATACACTCTGGTGC-3'	5'-CGGGATTGAATGTTCTTGTCGT-3'
Shox2	Short stature homeobox 2	5'- TGGAACAACTCAACGAGCTGGAGA-3'	5'-TTCAAACTGGCTAGCGGCTCCTAT-3'
Slc2a4 (Glut4)	Solute carrier family 2 (facilitated glucose transporter), member 4	5'-GTGACTGGAACACTGGTCCTA-3'	5'-CCAGCCACGTTGCATTGTAG-3'
Tbp	TATA box binding protein	5'-GAAGCTGCGGTACAATTCCAG-3'	5'-CCCCTTGTACCCTTCACCAAT-3'
Tbx15	T-Box 15	5'-TGTTCGCACACTGACCTTTG-3'	5'-CCAGTGCTGGAGGTGGTT-3'
Tnf (Tnfa)	Tumor necrosis factor alpha	5'-CCCTCACACTCAGATCATCTTCT-3'	5'-GCTACGACGTGGGCTACAG-3'
Ucp1	Uncoupling protein 1	5'-ACTGCCACACCTCCAGTCATT-3'	5'-CTTTGCCTCACTCAGGATTGG-3'
Wt1	Wilms tumor 1 homolog	5'-GAGAGCCAGCCTACCATCC-3'	5'-GGGTCCTCGTGTTTGAAGGAA-3'

Table II.1 Primer Sequences for *qPCR*

References

1. Hruby, A. and F.B. Hu, *The Epidemiology of Obesity: A Big Picture.* Pharmacoeconomics, 2014.

2. Gustafson, B. and U. Smith, *Regulation of white adipogenesis and its relation to ectopic fat accumulation and cardiovascular risk.* Atherosclerosis, 2015. **241**(1): p. 27-35.

3. Guilherme, A., et al., *Adipocyte dysfunctions linking obesity to insulin resistance and type 2 diabetes.* Nat Rev Mol Cell Biol, 2008. **9**(5): p. 367-77.

4. Shah, R.V., et al., *Visceral Adiposity and the Risk of Metabolic Syndrome Across Body Mass Index: The MESA Study.* JACC Cardiovasc Imaging, 2014. **7**(12): p. 1221-35.

5. Karpe, F. and K.E. Pinnick, *Biology of upper-body and lower-body adipose tissue--link to whole-body phenotypes.* Nat Rev Endocrinol, 2015. **11**(2): p. 90-100.

6. Tchkonia, T., et al., *Mechanisms and metabolic implications of regional differences among fat depots.* Cell Metab, 2013. **17**(5): p. 644-56.

7. Wajchenberg, B.L., *Subcutaneous and visceral adipose tissue: their relation to the metabolic syndrome.* Endocr Rev, 2000. **21**(6): p. 697-738.

8. Tchoukalova, Y.D., et al., *Regional differences in cellular mechanisms of adipose tissue gain with overfeeding.* Proc Natl Acad Sci U S A, 2010. **107**(42): p. 18226-31.

9. Cohen, P., et al., *Ablation of PRDM16 and beige adipose causes metabolic dysfunction and a subcutaneous to visceral fat switch.* Cell, 2014. **156**(1-2): p. 304-16.

10. Guerra, C., et al., *Emergence of brown adipocytes in white fat in mice is under genetic control. Effects on body weight and adiposity.* J Clin Invest, 1998. **102**(2): p. 412-20.

11. Gesta, S., et al., *Evidence for a role of developmental genes in the origin of obesity and body fat distribution.* Proc Natl Acad Sci U S A, 2006. **103**(17): p. 6676-81.

12. Sugihara, H., et al., *Primary cultures of unilocular fat cells: characteristics of growth in vitro and changes in differentiation properties.* Differentiation, 1986. **31**(1): p. 42-9.

13. Lafontan, M., *Historical perspectives in fat cell biology: the fat cell as a model for the investigation of hormonal and metabolic pathways.* Am J Physiol Cell Physiol, 2012. **302**(2): p. C327-59.

14. Néchad, M., et al., *Development of brown fat cells in monolayer culture.* Experimental Cell Research, 1983. **149**(1): p. 105-118.

15. Macotela, Y., et al., *Intrinsic differences in adipocyte precursor cells from different white fat depots.* Diabetes, 2012. **61**(7): p. 1691-9.

16. Chun, T.H. and M. Inoue, *3-D adipocyte differentiation and peri-adipocyte collagen turnover.* Methods Enzymol, 2014. **538**: p. 15-34.

17. Vashi, A.V., et al., *Adipose tissue engineering based on the controlled release of fibroblast growth factor-2 in a collagen matrix.* Tissue Eng, 2006. **12**(11): p. 3035-43.

18. Davidenko, N., et al., *Collagen-hyaluronic acid scaffolds for adipose tissue engineering.* Acta Biomater, 2010. **6**(10): p. 3957-68.

19. Preece, A., *A Manual for Histologic Technicians*. 1972: Little Brown & Co.

20. Chen, X.W., et al., *Activation of RalA is required for insulin-stimulated Glut4 trafficking to the plasma membrane via the exocyst and the motor protein Myo1c.* Dev Cell, 2007. **13**(3): p. 391-404.

21. Tchkonia, T., et al., *Fat depot origin affects adipogenesis in primary cultured and cloned human preadipocytes.* Am J Physiol Regul Integr Comp Physiol, 2002. **282**(5): p. R1286-96.

22. Elsdale, T. and J. Bard, *Collagen substrata for studies on cell behavior.* J Cell Biol, 1972. **54**(3): p. 626-37.

23. Walters, B.D. and J.P. Stegemann, *Strategies for directing the structure and function of three-dimensional collagen biomaterials across length scales.* Acta Biomater, 2014. **10**(4): p. 1488-501.

24. Chau, Y.Y., et al., *Visceral and subcutaneous fat have different origins and evidence supports a mesothelial source.* Nat Cell Biol, 2014. **16**(4): p. 367-75.

25. Napolitano, L., *THE DIFFERENTIATION OF WHITE ADIPOSE CELLS: An Electron Microscope Study.* The Journal of Cell Biology, 1963. **18**(3): p. 663-679.

26. Sugihara, H., et al., *Unilocular fat cells in three-dimensional collagen gel matrix culture.* J Lipid Res, 1988. **29**(5): p. 691-7.

27. Wolfs, M.G., et al., *Co-expressed immune and metabolic genes in visceral and subcutaneous adipose tissue from severely obese individuals are associated with plasma HDL and glucose levels: a microarray study.* BMC Med Genomics, 2010. **3**: p. 34.

28. Loft, A., et al., *Browning of human adipocytes requires KLF11 and reprogramming of PPARgamma superenhancers.* Genes Dev, 2015. **29**(1): p. 7-22.

29. Rosen, E.D. and B.M. Spiegelman, *What we talk about when we talk about fat.* Cell, 2014. **156**(1-2): p. 20-44.

30. Wahrenberg, H., F. Lonnqvist, and P. Arner, *Mechanisms underlying regional differences in lipolysis in human adipose tissue.* J Clin Invest, 1989. **84**(2): p. 458-67.

CHAPTER III

Cinnamaldehyde Induces Fat Cell-Autonomous Thermogenesis and Metabolic Reprogramming

Abstract

Cinnamaldehyde (CA) is a food compound that has previously been observed to be protective against obesity and hyperglycemia. Here we report that CA activates a thermogenic response via PKA signaling in murine subcutaneous adipocytes and that chronic CA treatment induces metabolic reprogramming that may contribute to improving whole-body metabolic health. This phenomenon is fat cell-autonomous and well conserved in human adipose stem cells isolated from subcutaneous depots of multiple donors of different ethnicities and ages and with a variety of body mass indexes (BMI). Given the wide usage of cinnamon in the food industry, the notion that this popular food additive, instead of a drug, may activate thermogenesis, could ultimately lead to therapeutic strategies against obesity that are much better adhered to by participants.

Introduction

The global obesity epidemic calls for effective intervention and treatments. Adipocytes in the subcutaneous fat depots have been reported to provide metabolic benefits, including their

This chapter has been published as: Jiang, J.*, **Emont, M.P.***, Jun, H., Qiao, X., Liao, J., Kim, D., Wu, J. (2017) Cinnamaldehyde induces fat cell-autonomous thermogenesis and metabolic reprogramming. *Metabolism*. 77, 58-64 *Contributed equally.

capability to be recruited and activated by thermogenic stimuli and thereby potentially improve systemic energy homeostasis [1]. The classical pathway for the activation of thermogenesis in adipocytes is through the activation of PKA and downstream enzymes including p38 MAPK, which in turn leads to the induction of the transcription of key thermogenic genes [2].

Previous studies have shown that cinnamaldehyde (CA), an essential oil found in cinnamon, can reduce diet-induced weight gain and improve glucose homeostasis when given to mice as a supplement in food [3, 4]. Interestingly, cinnamon consumption has also been reported to correlate with lower levels of fasting blood glucose in human studies [5]. However, the molecular mechanisms behind these effects have not yet been elucidated. Here, we show that CA directly acts on subcutaneous adipocytes to activate thermogenesis and PKA signaling and that chronic CA treatment induces thermogenic and metabolic reprogramming in these cells. Importantly, the beneficial effects of CA treatment that we observe in murine adipocytes are conserved in human subcutaneous fat cells, suggesting that CA may potentially be used to counteract obesity and improve systemic metabolism in humans.

Materials and Methods

Reagents

Trans-Cinnamaldehyde (C80687), isoproterenol (16504), dexamethasone (D4902), insulin (I5500), 3-IsoButyl-1-MethylXanthine (IBMX, I7018), biotin (B4639), D-pantothenic acid hemacalcium salt (P5155), Oligomycin A (75351), and Carbonyl cyanide 4-(trifluoromethoxy)phenylhydrazone **(**FCCP, C2920) were purchased from Sigma Aldrich. Rosiglitazone (71740) and H-89 (10010556) were purchased from Cayman Chemicals (Ann

Arbor, MI, USA). SB203580 (5633) was purchased from Cell Signaling Technology (Danvers, MA, USA). Collagenase D (11088882001), collagenase B (11088831001), dispase II (04942078001), and protease inhibitor cocktail (11836153001) were purchased from Roche.

Animals

All animal experiments were approved by the University of Michigan Institutional Animal Care and Use Committee and conducted in conformity with the Public Health Service Policy for Care and Use of Laboratory Animals. Wild-type C57BL/6J animals were obtained from The Jackson Laboratories (JAX 000664, Bar Harbor, ME, USA) and wild-type 129SVE and BALB/c animals were obtained from Taconic (Hudson, NY, USA). TRPA1 and FGF21 knockout animals were generated by crossing *Trpa1* flox/flox (JAX 008650) or *Fgf21* flox/flox animals (JAX 022361) with EIIa cre animals (JAX 003724), respectively. All animals were group housed in forced ventilation racks with *ad libitum* access to food and maintained at a 12h light/dark cycle (6 AM to 6 PM). Mice of both genders were used for the experiments presented in this manuscript.

Primary Cell Isolation

Inguinal or brown fat depots were isolated from mice, minced, and digested in a collagenase D/dispase II solution (inguinal fat) or collagenase B/dispase II solution (brown fat) shaking at 37°C for 10-15 minutes. Cells were filtered through a 100 μm cell strainer and centrifuged at 300-500 x *g* for 5 minutes to separate the floating mature adipocytes from the pelleted stromal vascular fraction (SVF), which contains the fibroblast-like preadipocytes. The SVF was resuspended in media, filtered through a 40 μm cell strainer, and centrifuged again, after which the pellet was resuspended in DMEM/F12 + GlutaMAX supplemented with 15% FBS and

penicillin-streptomycin and plated on a collagen-coated 10 cm plate. After at least one round of subculture, which helps to remove contaminating cell types such as red blood cells and immune cells, the preadipocytes were plated on collagen-coated 12 well plates for differentiation.

Murine Adipocyte Differentiation

To induce differentiation, confluent cultures of primary cells were stimulated in DMEM/F12 + GlutaMAX supplemented with 10% FBS, penicillin-streptomycin, dexamethasone (5 μM), insulin (0.5 μg/mL), IBMX (0.5 mM), and rosiglitazone (1 μM). After 2 days of stimulation, cells were maintained in DMEM/F12 + GlutaMAX with 10% FBS, penicillin-streptomycin and insulin (0.5 μg/mL). Analyses of mature adipocytes were performed 6-7 days after stimulation. C3H-10T1/2 (ATCC CCL-226) cells were cultured similarly to primary cells with the exception that for the base medium DMEM was used instead of DMEM/F12 + GlutaMAX in all instances.

Human Cell Culture and Differentiation

Human adipose-derived stem cells (hASCs) were isolated from lipoaspirates from the subcutaneous adipose tissue of donors undergoing voluntary surgery (a generous gift from Dr. Jeffrey M. Gimble, Tulane University, New Orleans, Louisiana, USA). Donor demographics are included in Table III.1. All specimens were collected and handled under the protocols reviewed and approved by the Western Institutional Review Board (Puyallup, WA) and the University of Michigan Medical School Institutional Review Board (IRBMED). Cells were cultured in MesenPRO RS media (Invitrogen) and grown on collagen-coated 10 cm plates. To differentiate, cells were seeded onto 12 well collagen-coated plates and stimulated in DMEM/F12 + GlutaMAX supplemented with 10% FBS, penicillin-streptomycin, dexamethasone (5 μM),

insulin (0.5 μg/mL), IBMX (0.5 mM), rosiglitazone (5 μM), biotin (33 μM) and pantothenic acid (17 μM). After 3 days of stimulation, cells were maintained in DMEM/F12 + GlutaMAX containing 10% FBS, penicillin-streptomycin, insulin (0.5 μg/mL), dexamethasone (5 μM), biotin (33 μM) and pantothenic acid (17 μM) until they were fully differentiated (8-10 days).

RNA Isolation and RT-qPCR Analysis

RNA was extracted from cells and tissue using TRI Reagent (Sigma, Saint Louis, MO, USA) according to the manufacturer's instructions. RNA was reverse transcribed to cDNA using M-MLV (Invitrogen, Carlsbad, CA, USA) and qPCR was performed using SYBR Green (Applied Biosystems, Woolston Warrington, UK) on a 7900HT Fast Real-Time PCR system (Applied Biosystems). Fold change was determined using the ΔΔCt method with samples normalized to the reference gene *36B4 (RPLP0)*. A list of qPCR primers used in this study is included in Table III.2.

Western Blot Analysis

Cells were lysed with RIPA buffer supplemented with protease inhibitor cocktail (Roche, Basel, Switzerland) and phosphatase inhibitors. Protein extracts were run on 10% SDS-PAGE gels and transferred to nitrocellulose membranes. Blots were exposed using ECL (Amersham, Pittsburgh, PA, USA). For antibody information, see the supplemental materials and methods. Cells were lysed with RIPA buffer (50 mM Tris-HCl, pH 7.5, 1% Triton X-100, 1% sodium deoxycholate, 0.1% SDS, 150 mM NaCl, 1 mM phenylmethylsulfonyl fluoride) supplemented with protease inhibitor cocktail (Roche) and phosphatase inhibitors (10 mM NaF, 60 mM β-glycerolphosphate, pH 7.5, 2 mM sodium orthovanadate, 10 mM sodium pyrophosphate). Protein extracts were run

on 10% SDS-PAGE gels and transferred to nitrocellulose membranes. The primary antibodies against p-PKA substrates (9621L), p-p38 MAPK (Thr180/Tyr182) (9215S), p38 MAPK (9212S), p-HSL Ser660 (4126L), HSL (4107S), HSP90 (4874S), α-Tubulin (2144), and β-Actin (8457S) were obtained from Cell Signaling Technology. The primary antibodies against p-PLIN1 Ser522/Ser517 (human S522 is equivalent to mouse S517) (4856) and total PLIN1 (4854) were obtained from Vala Sciences. Horseradish peroxidase (HRP)-conjugated anti-rabbit secondary antibody was obtained from Cell Signaling Technology and HRP-conjugated anti-mouse secondary antibody was obtained from Sigma. Blots were exposed using ECL (Amersham).

Immunocytochemistry

Primary cells were seeded onto collagen-coated coverslips and differentiated as described above. Differentiated cells were fixed in 10% formalin at room temperature for 10 minutes, washed 3 times in PBS, blocked in 10% donkey serum, and incubated overnight in 10% donkey serum and p-PLIN1 Ser517 antibody (Vala Sciences) before being washed and incubated in anti-rabbit Alexa 594 antibody (Abcam) and BODIPY (Invitrogen). Cells were washed and mounted on slides using Prolong Gold (Invitrogen) and imaged using an Olympus FV300 confocal laser-scanning microscope (Melville, NY, USA).

Respiration

Fully differentiated brown adipocytes treated with or without 100 μM CA for 24 h were suspended in respiration buffer (2.5 mM glucose, 5 mM pyruvate, 2.5 mM malate, 120 mM NaCl, 4.5 mM KCl, 0.7 mM Na_2HPO_4, 1.5 mM NaH_2PO_4, 0.5 mM $MgCl_2$, pH 7.4). Cellular oxygen consumption in the respiration buffer was recorded for 1 min during the basal, uncoupled, or

maximal stages using a Clark electrode (Strathkelvin Instruments). 4 mg/ml oligomycin and 1.5-2 μM FCCP were acutely added to the respiration chamber to measure the uncoupled and maximal respiration, respectively.

Oil Red O Staining

Cells were washed with PBS, then fixed in 10% formalin for 30 minutes. After fixation, cells were washed with dH_2O, dehydrated in 60% isopropanol for 10 minutes, then incubated in Oil Red O working solution (3 parts 3 mg/mL Oil Red O in 100% isopropanol + 2 parts dH_2O) for 10 minutes. After incubation, cells were washed with dH_2O and imaged using a Leica DM IRB inverted microscope and a Diagnostic Instruments Spot camera. Pictures of whole wells stained with Oil Red O were obtained using an Epson Expression 1680 scanner.

Statistical Analysis

Statistical analysis was performed using GraphPad Prism 6. Data are expressed as mean ± SEM. Statistical significance was determined using an unpaired two-tailed Student's t-test for two-group comparisons (*$p < 0.05$, **$p < 0.01$, ***$p < 0.001$). A one-way analysis of variance (ANOVA) was applied for multiple group comparisons involving one independent variable. The data presented is representative of 2-4 independent experiments.

Results

CA activates thermogenesis through PKA signaling in mouse subcutaneous fat cells

While the beneficial effects of CA on systemic metabolism have recently been observed [3, 4, 6], the underlying molecular basis of these effects remains largely unknown. To explore the

possibility that CA influences whole body metabolism through direct action on adipocytes, we treated fully differentiated adipocytes isolated from the murine inguinal subcutaneous fat depot with CA. Subcutaneous fat plays a unique role in maintaining energy homeostasis, demonstrating profound "browning" upon cold exposure and mediating protective metabolic functions during obesity [7]. Acute CA treatments induce expression of thermogenic markers including *Fgf21* and *Ucp1* without altering expression of general adipogenic markers such as *Pparg* and *Adipoq* in these primary subcutaneous adipocytes (Figures III.1A, III.2, and III.3A). The induction of thermogenesis in response to acute stimuli, such as treatment with β-adrenergic agonist isoproterenol (Iso), is mainly mediated through the activation of PKA and subsequent phosphorylation of p38 MAPK [2]. Indeed, we observed a robust phosphorylation of PKA substrates and p38 MAPK by CA at a comparable level to Iso in inguinal adipocytes (Figure III.1B). In addition to p38, PKA dependent phosphorylation of hormone-sensitive lipase (HSL) and lipid droplet-associated protein perilipin 1 (PLIN1) are also activated by CA in inguinal adipocytes (Figure III.1B and C). CA has been reported to be an agonist for transient receptor potential cation channel, member A1 (TRPA1) [4]. Emerging evidence suggests that signaling through the transient receptor potential (TRP) channels may cell-autonomously mediate adipocyte function [8, 9]. Interestingly, this CA-induced thermogenic response is TRPA1-independent since a similar response was observed in TRPA1KO inguinal adipocytes (Figures III.1D and E, III.4).

Phosphorylation of PKA substrates, p38 MAPK, HSL and PLIN1 by CA treatment were significantly blocked by PKA inhibitor H-89 in primary inguinal adipocytes (Figure III.1F). Consistently, the induction of *Fgf21* and *Ucp1* by CA in inguinal adipocytes was substantially

suppressed by H-89 and partially reduced by p38 MAPK inhibitor SB203580 (Figure III.1G and H), suggesting that CA-stimulated thermogenesis is dependent on PKA/p38 MAPK signaling. These results were confirmed in immortalized C3H-10T1/2 cells, indicating that the observed response to CA in primary inguinal fat is adipocyte cell-autonomous (Figure III.5). Taken together, these data revealed that CA directly stimulates a thermogenic response and PKA activation in murine subcutaneous fat cells.

CA activates thermogenesis and promotes metabolic reprogramming in human subcutaneous fat cells

It has been reported that in addition to the supraclavicular area, thermogenic adipocytes also exist in human subcutaneous fat depots [7, 10]. We observed a clear activation of the thermogenic response and PKA signaling in differentiated hASCs isolated from subcutaneous fat depots (Figures III.6A-F, III.3B). This phenomenon is consistently observed across multiple human donors of different ethnicities and ages and with varied BMI (Table III.1, Figure III.7). Previous studies have shown that long-term CA supplementation in food can protect mice from diet-induced obesity and hyperglycemia [3, 6]. *In vitro*, upon chronic treatment with CA, *Fgf21* and *Ucp1* were significantly upregulated in both murine inguinal adipocytes and human subcutaneous fat cultures (Figures III.8, III.6J, L, and M). Thermogenic genes (*Cidea, Cycs, Tfam)* and genes encoding key enzymes in the citric acid cycle (*Idh3a, Cs*) were upregulated after chronic exposure to CA. Cumulative evidence supports that many aspects of lipid metabolism can be altered in response to cold exposure or β-adrenergic agonist treatment [11, 12]. We observed that chronic CA treatment upregulates the expression of lipolytic genes (*Hsl, Atgl),* key regulators in fatty acid oxidation (*Cpt1b, Ppara*), lipogenic genes (*Gyk, Dgat1*), and

Pdk4, an enzyme that enhances lipid metabolism and has recently been reported to be responsible for major metabolic adaptations during white-to-beige conversion of human adipocytes (Figure III.6J, L, and M) [13]. Increased oxidative metabolism in mitochondria is known to be accompanied by increased reactive oxygen species (ROS) production. Chronic CA treatment also upregulated the expression of ROS-detoxifying enzymes including *Sod1* and *Sod2*, which may protect activated thermogenic adipocytes from oxidative damage (Figure III.6J, L, and M). Murine brown adipocytes additionally showed a thermogenic response to both acute and chronic CA treatment, including an increase in oxygen consumption in cells treated with chronic CA (Figure III.9).

Acute CA treatment led to considerable induction of *Fgf21,* an important metabolic regulator which can be secreted by adipocytes and function in an autocrine or paracrine manner to induce thermogenesis and affect metabolic pathways [14]. In wild type (WT) inguinal adipocytes, CA treatment induced a clear elevation of *Egr1* and *cFos*, known FGF21 target genes (Figure III.6G) [15]. This induction was completely abolished in adipocytes isolated from FGF21KO mice (Figures III.6H, III.10), suggesting that FGF21-dependent signaling is activated by CA. The FGF21 knockout did not affect the PKA-mediated acute response to CA treatment in inguinal adipocytes (Figure III.6I). However, metabolic reprogramming upon chronic CA treatment is blunted in the absence of FGF21, suggesting that FGF21 may contribute to certain aspects of the long-term effects of CA on adipocytes through autocrine or paracrine pathways (Figure III.6K).

Discussion

Thermogenic adipocytes in subcutaneous fat depots are highly recruitable under certain conditions such as cold exposure [1]. These cells play an important role in maintaining energy

homeostasis and improving overall metabolic health [16]. Herein, we show that CA treatment activates thermogenic and metabolic responses in human subcutaneous fat cells derived from multiple donors (Figures III.6, III.7). Recent studies demonstrate that lipolysis and lipogenesis are coupled in adipose tissue during chronic β3-adrenergic receptor stimulation [12]. In cold-exposed mice, genes involved in lipid catabolism and anabolism are both upregulated [11]. Cold-stimulated thermogenic fat activation in humans triggers triglyceride-free fatty acid cycling accompanied with altered metabolic gene profiles [17]. Consistent with these observations, we found that chronic CA treatment leads to a futile metabolic cycle in subcutaneous fat cells which may constitute the key mechanism through which CA consumption leads to metabolic protection. Notably, a recent clinical trial with healthy subjects suggests that acute CA ingestion increases energy expenditure and postprandial fat oxidation, in which the CA dose is judged as "sensorially acceptable" by participants [18]. A pharmacokinetic study revealed that circulating levels of CA were detectable 20 h after oral delivery, indicating that consumption of cinnamon may be a feasible way to activate thermogenesis in subcutaneous fat and ultimately protect against obesity and metabolic disorders [19].

This study investigated the thermogenic and metabolic actions of CA on adipocytes and the mechanisms by which they take place. We found that CA acts through a PKA/p38 MAPK-dependent pathway. Consistently, the phosphorylation of lipolysis- and thermogenesis- related proteins was diminished by treatment with the PKA inhibitor H-89, and thermogenic gene expression was attenuated by treatment with the p38 inhibitor SB203580. We also found that some of the chronic effects of CA are mediated by FGF21, an adipokine that is known to activate thermogenesis in adipocytes [14].

In summary, this study provides evidence that CA induces thermogenesis as well as chronic metabolic remodeling in a fat cell-autonomous manner. Particularly, the thermogenic and metabolic responses of human subcutaneous adipocytes to CA suggest that this may be a promising therapeutic target for obesity.

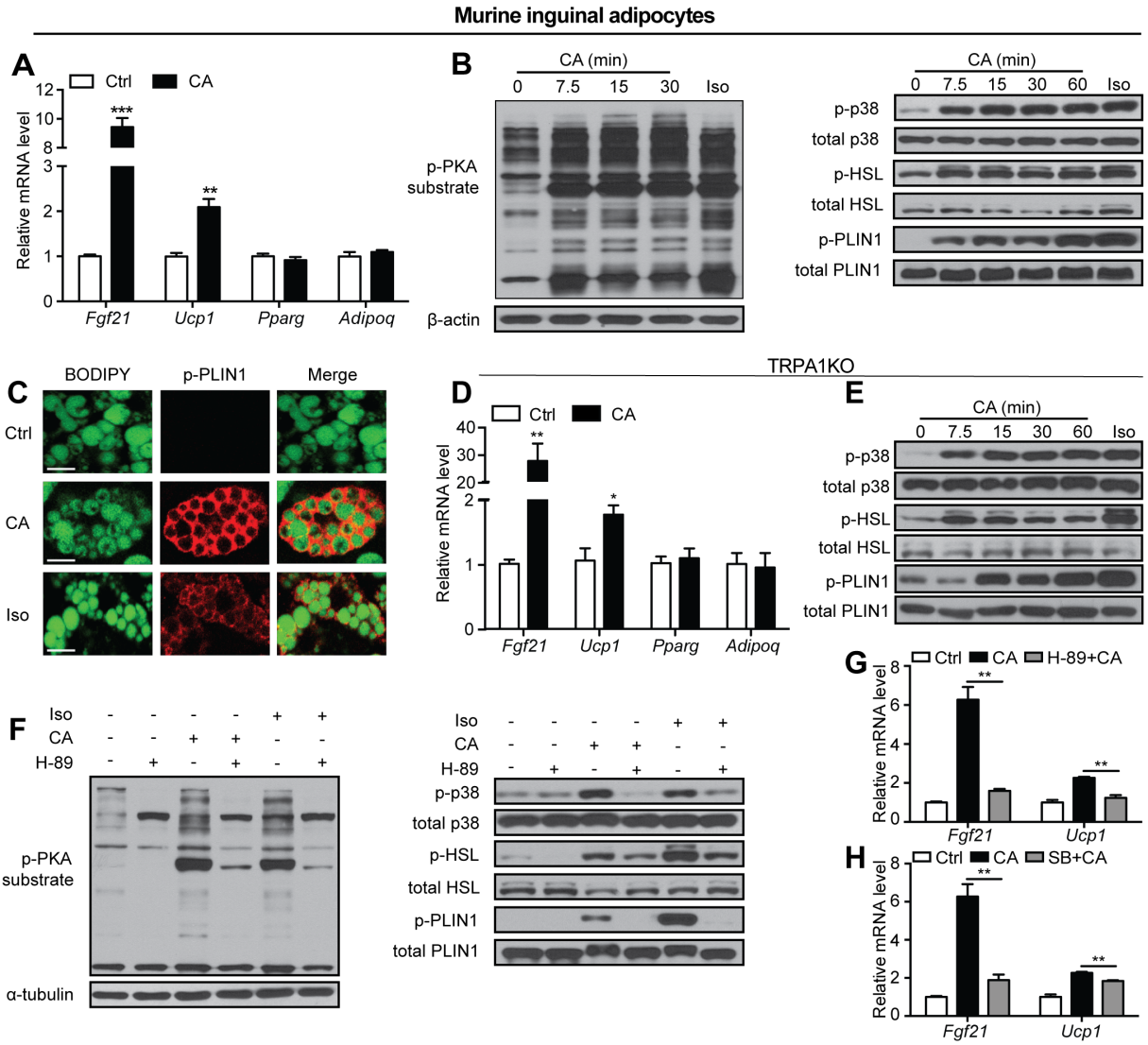

Figure III.1 *(legend on next page)*

Figure III.1 Acute CA treatment upregulates thermogenic gene expression and activates PKA signaling in murine subcutaneous fat cells.
A. Real-time qPCR analyses of thermogenic genes (*Fgf21* and *Ucp1)* and adipogenic markers (*Pparg* and *Adipoq*) in differentiated murine inguinal adipocytes (n=4) after 400 μM CA treatment for 4 h. It has been reported that CA treatment in 3T3-L1 preadipocytes negatively influences adipogenesis [6]. We observed similar levels of adipogenesis and equal pan-fat marker expression (*Pparg* and *Adipoq*) in control and CA treated groups. **B.** Representative immunoblots of PKA substrate phosphorylation, p38 MAPK phosphorylation, HSL phosphorylation (Ser660) and PLIN1 phosphorylation (Ser517) in differentiated inguinal adipocytes exposed to 400 μM CA for the indicated time or 10 μM Iso for 10 min as a positive control. **C.** Representative immunofluorescence staining of PLIN1 phosphorylation (red) in differentiated inguinal adipocytes treated with 400 μM CA for 1 h or 10 μM Iso for 1 h as a positive control. BODIPY was used to stain lipid droplets (green). Scale bar = 20 μm. **D.** Real-time qPCR analyses of thermogenic genes (*Fgf21* and *Ucp1)* and adipogenic markers (*Pparg* and *Adipoq*) in differentiated WT or TRPA1KO inguinal adipocytes following vehicle control or 400 μM CA treatment for 4 h (n=6). **E.** Representative immunoblots of p38 MAPK phosphorylation, HSL phosphorylation (Ser660) and PLIN1 phosphorylation (Ser517) in differentiated TRPA1KO inguinal adipocytes treated with 400 μM CA for the indicated time or 10 μM Iso for 10 min as a control. **F.** Representative immunoblots of phosphorylated PKA substrates, phosphorylated p38 MAPK, phosphorylated HSL (Ser660) and phosphorylated PLIN1 (Ser517) in differentiated inguinal adipocytes treated with 50 μM H-89 for 30 min and then 400 μM CA for 1 h or 10 μM Iso for 10 min as a positive control. **G** and **H.** Real-time qPCR analyses of thermogenic markers (*Fgf21, Ucp1*) in differentiated inguinal adipocytes treated with 50 μM H-89 (**G**, n=3) or 10 μM SB203580 (SB, **H**, n=3) for 1 h and then 400 μM CA for 4 h. All data in **A**, **D**, **G**, and **H** are presented as mean ± SEM. **p*<0.05, ***p*<0.01, ****p*<0.001.

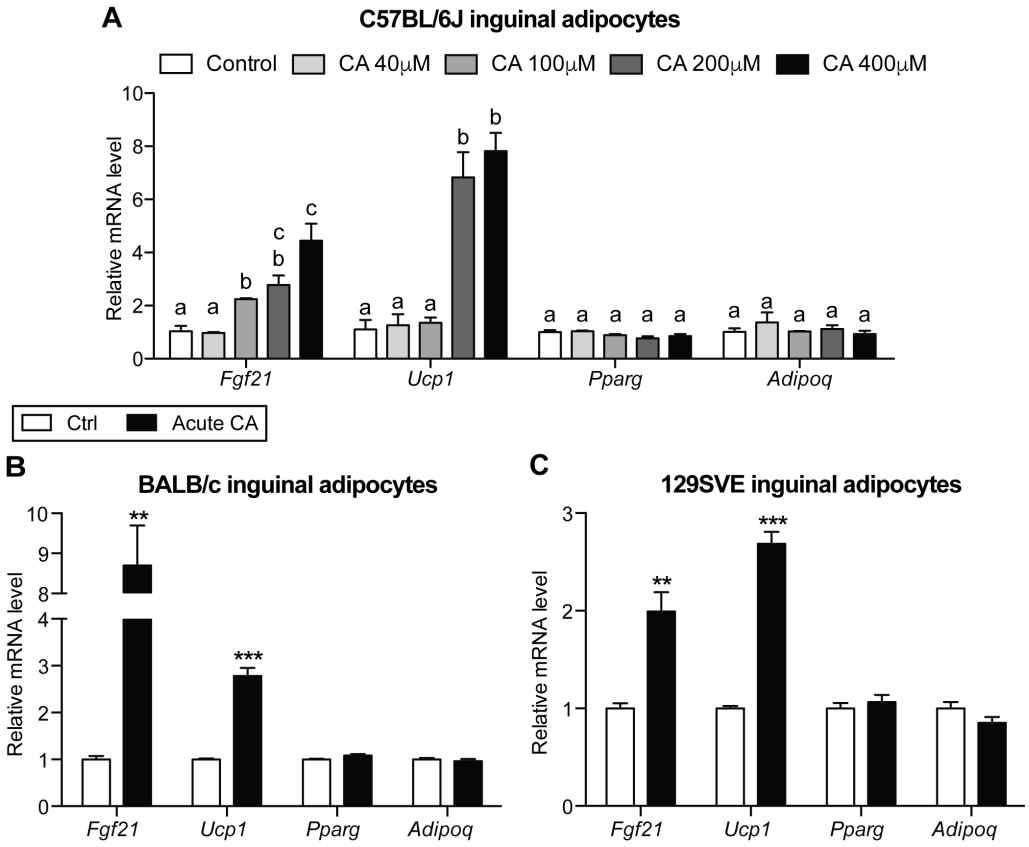

Figure III.2 CA upregulates thermogenic gene expression in primary inguinal adipocytes of multiple inbred WT mouse strains.

A. Real-time qPCR analyses of thermogenic (*Fgf21* and *Ucp1*) and adipogenic (*Pparg* and *Adipoq*) genes in C57BL/6J adipocytes treated with various doses of CA for 4 h (n=3). **B** and **C.** Real-time qPCR analyses of thermogenic genes (*Fgf21* and *Ucp1)* and adipogenic markers (*Pparg* and *Adipoq*) in differentiated inguinal adipocytes isolated from BALB/c (**B**, n=4) and 129SVE (**C**, n=3) mice treated with vehicle control or 400 μM CA for 4 h. All data are presented as mean ± SEM. A different letter denotes a significant difference between groups at $p<0.05$. $^{**}p<0.01$, $^{***}p<0.001$.

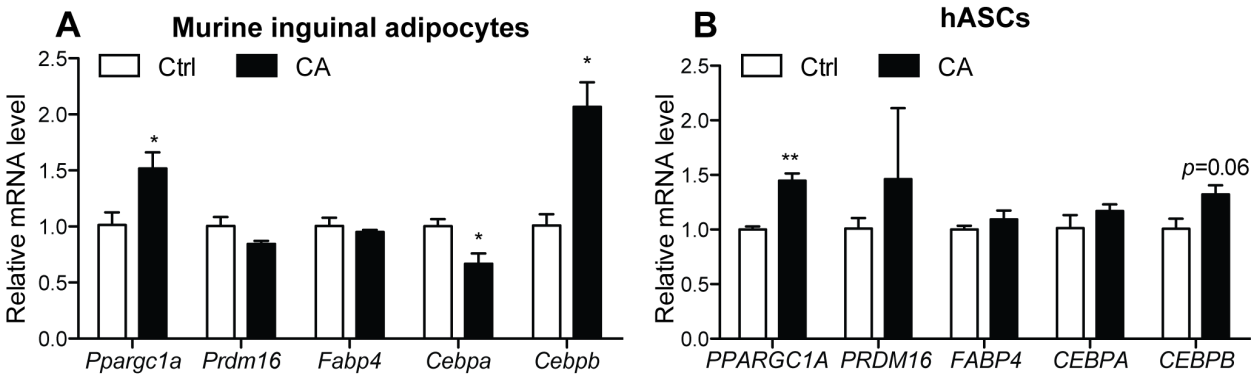

Figure III.3 Gene expression in CA-stimulated murine and human cells.
A. Real-time qPCR analyses of adipocyte marker genes in murine inguinal adipocytes treated with 400 μM CA for 4 h (n=3). **B.** Real-time qPCR analyses of thermogenic and adipogenic genes in differentiated hASCs treated with 200 μM CA for 4 h (n=3). All data are presented as mean ± SEM. *$p<0.05$, **$p<0.01$.

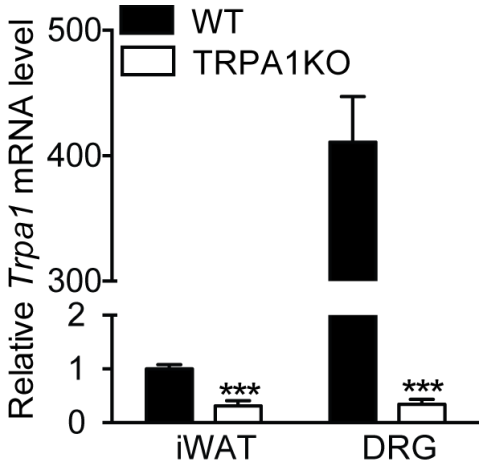

Figure III.4 Validation of TRPA1 knockout animals.
Real-time qPCR analyses of *Trpa1* expression level in inguinal white adipose tissue (iWAT) and dorsal root ganglia (DRG) of WT or TRPA1KO mice (n=6-10). Data are presented as mean ± SEM. DRG is included as a positive control, where abundant expression of *Trpa1* has been reported [20]. ***$p<0.001$.

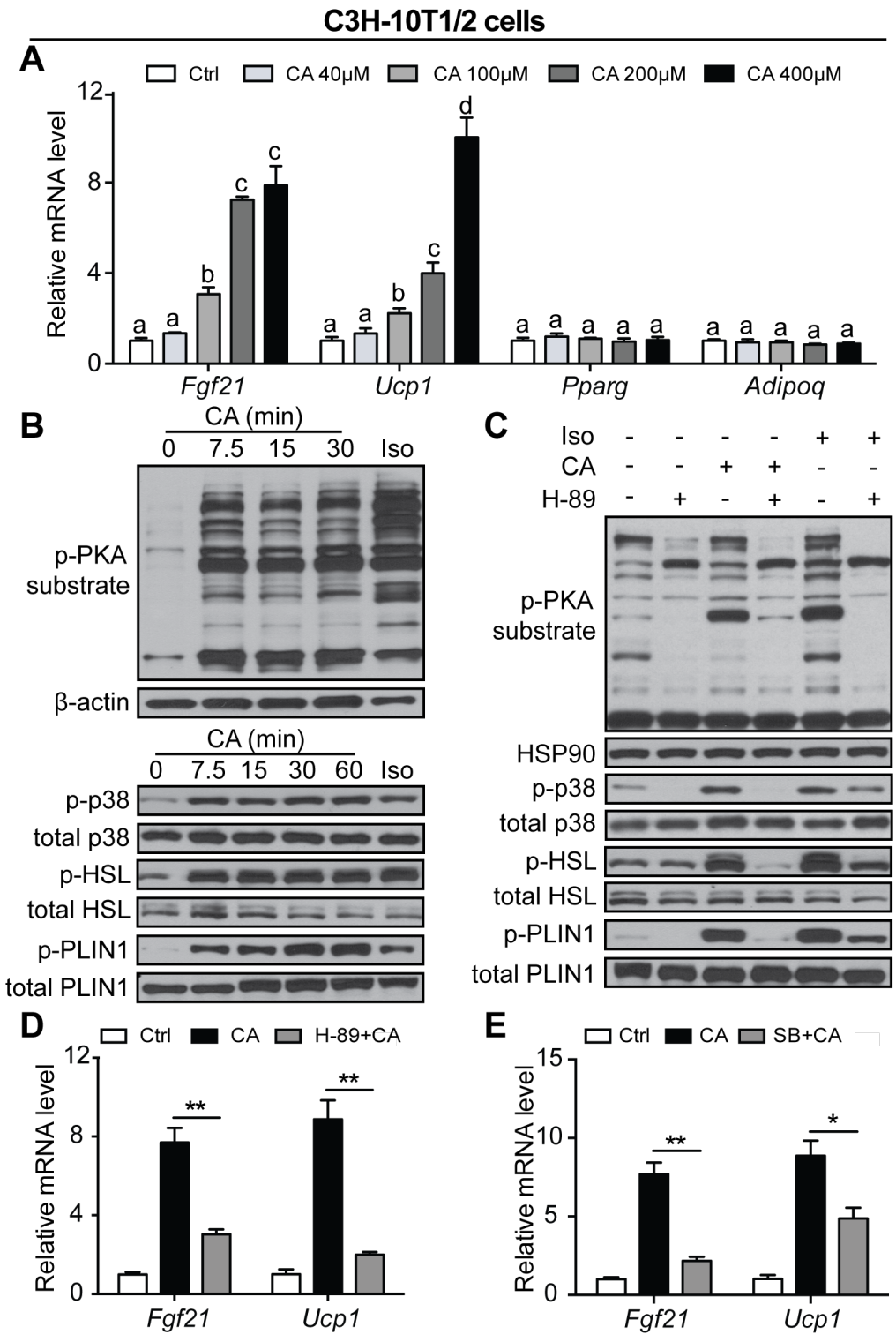

Figure III.5 *(legend on next page)*

Figure III.5 Acute CA treatment increases thermogenic marker expression and activates PKA signaling in immortalized C3H-10T1/2 cells, indicating this is a cell-autonomous adipocyte response and not due to the presence of other non-fat cell types that may be present in primary cultures.

A. Real-time qPCR analyses of thermogenic genes (*Fgf21* and *Ucp1)* and adipogenic markers (*Pparg* and *Adipoq*) in differentiated C3H-10T1/2 cells (n=3) treated with vehicle control, 40 μM , 100 μM, 200 μM or 400 μM CA for 4 h. **B** and **C.** Representative immunoblots of phosphorylated p38 MAPK, phosphorylated HSL (Ser660) and phosphorylated PLIN1 (Ser517) in differentiated C3H-10T1/2 cells treated with 400 μM CA for the indicated time (**B**) or 50 μM H-89 for 30 min and then 400 μM CA for 1 h (**C**). Iso treatment is included as a positive control. **D** and **E.** Real-time qPCR analyses of thermogenic markers in differentiated C3H-10T1/2 cells treated with 50 μM H-89 (**D**, n=3) or 10 μM SB203580 (SB, **E**, n=3) for 1 h and then 400 μM CA for 4 h. Dat in **A**, **D** and **E** are presented as mean ± SEM. A different letter denotes a significant difference between groups at $p<0.05$. *$p<0.05$, **$p<0.01$.

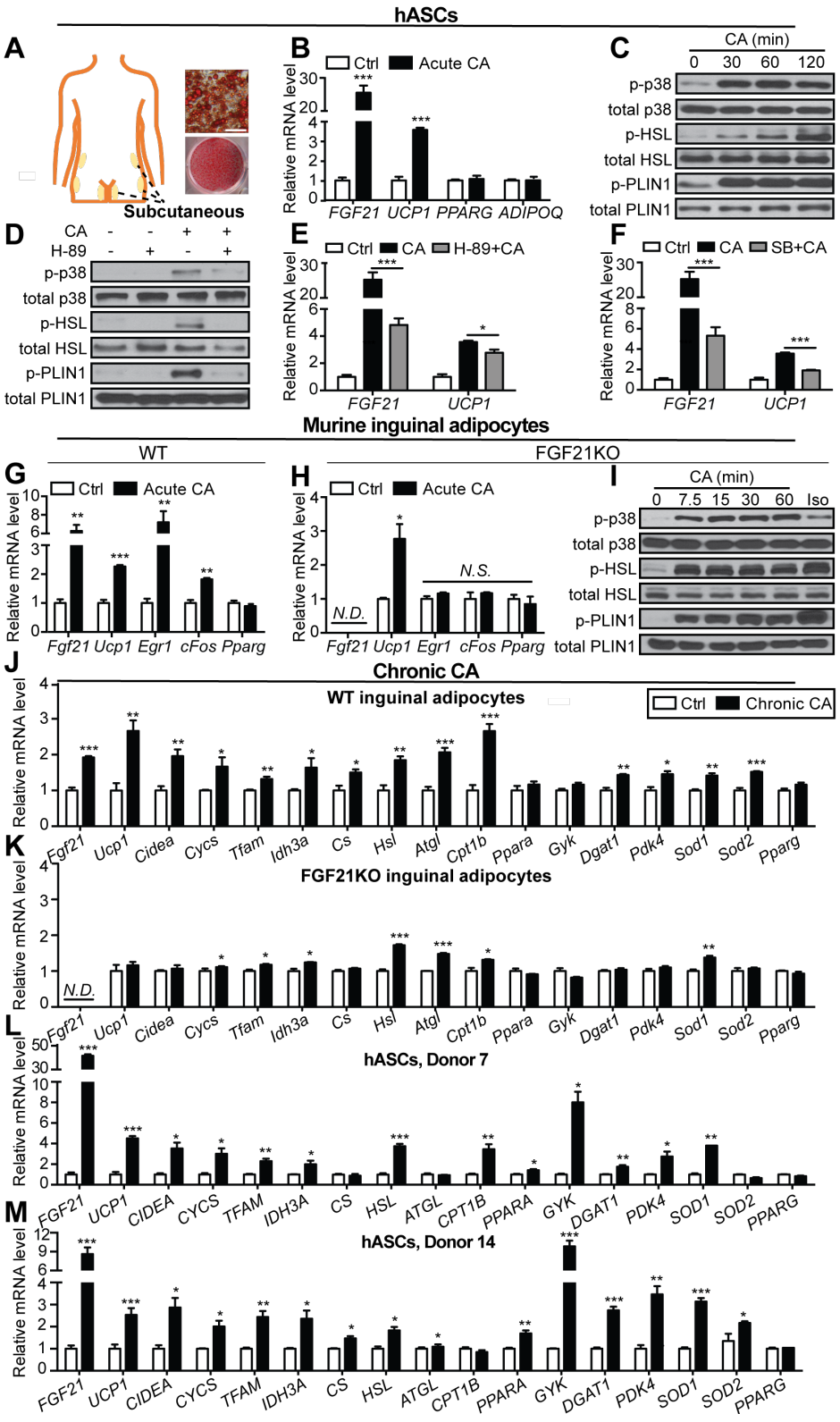

Figure III.6 *(legend on next page)*

Figure III.6 CA activates a thermogenic response and regulates lipid metabolic gene profiles in human subcutaneous fat cells.
A. Locations of the human subcutaneous fat biopsy sites used in this study and representative Oil Red O staining of differentiated hASCs. Scale bar = 50 μm. **B.** Real-time qPCR analyses of thermogenic genes (*FGF21* and *UCP1)* and adipogenic markers (*PPARG* and *ADIPOQ*) in differentiated hASCs after 200 μM CA treatment for 4 h (n=4). **C** and **D.** Representative immunoblots of phosphorylated p38 MAPK, phosphorylated HSL (Ser660) and phosphorylated PLIN1 (Ser522) in differentiated hASCs treated with 200 μM CA for the indicated time (**C**) or 50 μM H-89 for 30 min and then 200 μM CA for 2 h (**D**). **E** and **F.** Real-time qPCR analyses of thermogenic markers in differentiated hASCs treated with 50 μM H-89 (**E**, n=3) or 10 μM SB (**F**, n=3) for 1 h and then 200 μM CA for 4 h. **G** and **H.** Real-time qPCR analyses of thermogenic genes (*Fgf21* and *Ucp1*), FGF21-target genes (*Egr1, cFos*) and the adipogenic marker *Pparg* in differentiated inguinal adipocytes of WT mice (**G**, n=4) or FGF21KO mice (**H**, n=4) after 400 μM CA treatment for 4 h. **I.** Representative immunoblots of phosphorylated p38 MAPK, phosphorylated HSL (Ser660) and phosphorylated PLIN1 (Ser517) in differentiated inguinal adipocytes from FGF21KO mice treated with 400 μM CA for the indicated time. **J**-**M.** Real-time qPCR analyses of thermogenic and metabolic genes in differentiated WT (**J**, n=4) or FGF21KO (**K**, n=4) murine inguinal adipocytes after 200 μM CA treatment for 48 h, or differentiated hASCs stimulated with 200 μM CA for 24 h (**L** and **M**, n=4). All data in **B**, **E**-**H**, and **J**-**M** are presented as mean ± SEM. **p*<0.05, ***p*<0.01, ****p*<0.001.

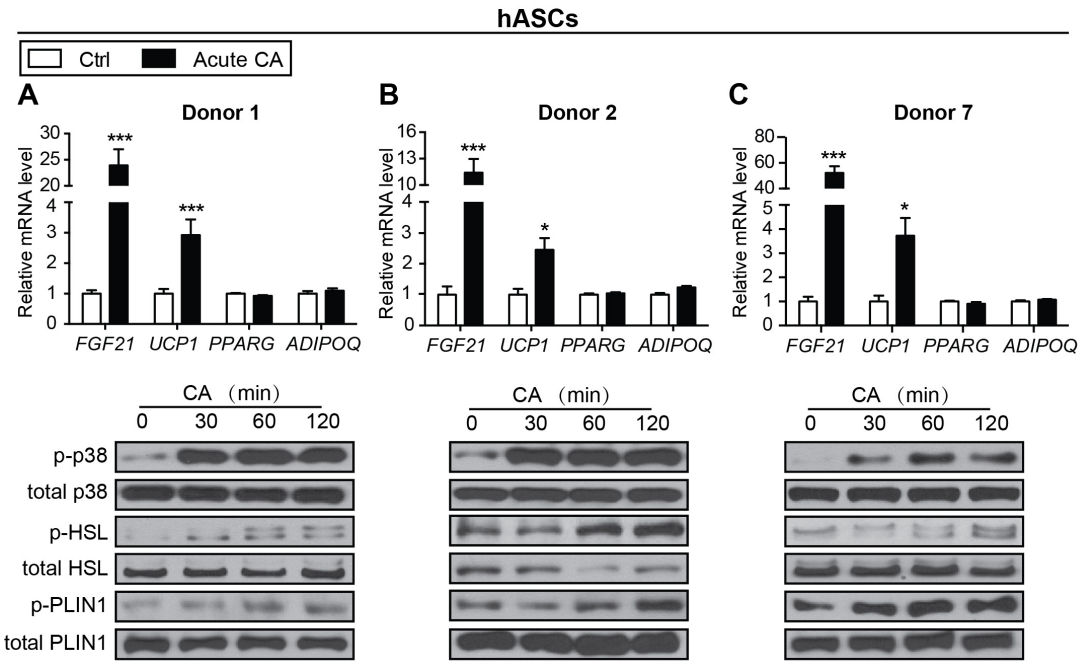

Figure III.7. Acute CA treatment increases thermogenic marker expression and activates PKA signaling in human subcutaneous adipocytes from multiple donors.

A-C. Real-time qPCR analyses of thermogenic genes (*FGF21* and *UCP1)* and adipogenic markers (*PPARG* and *ADIPOQ*) (n=3-4) and representative immunoblots of phosphorylated p38 MAPK, phosphorylated HSL (Ser660) and phosphorylated PLIN1 (Ser522) in differentiated hASCs from three donors treated with 200 μM CA for 4 h for qPCR or the indicated time for the western blots. Data are presented as mean ± SEM. **p*<0.05, ****p*<0.001.

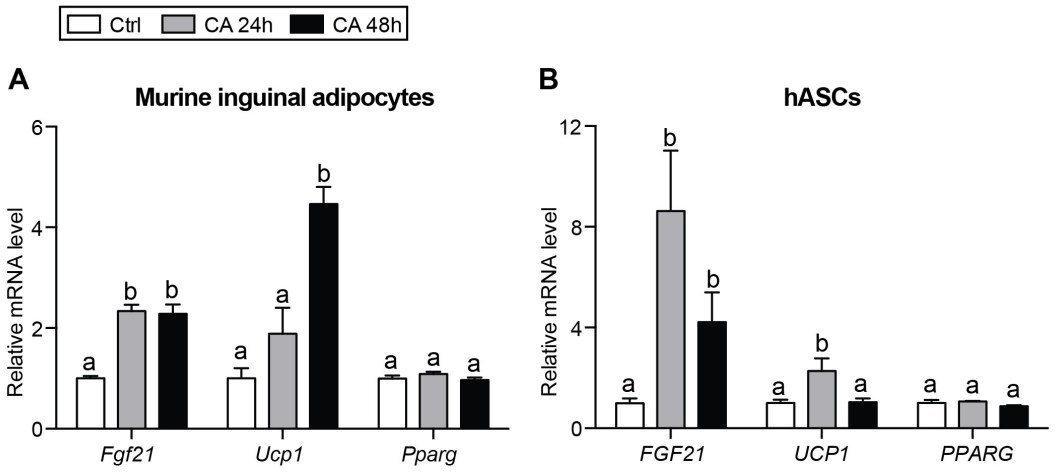

Figure III.8 Chronic CA treatment upregulates thermogenic gene expression in murine and human subcutaneous adipocytes.

A and **B.** Real-time qPCR analyses of thermogenic genes (*Fgf21* and *Ucp1)* and the adipogenic marker *Pparg* in differentiated inguinal adipocytes (**A**, n=3-4) or differentiated hASCs (**B**, n=3) exposed to vehicle control or 200 µM CA for 24 h or 48 h. 24 h CA treatment renders most robust thermogenic response in hASCs, whereas 48 h is the best condition in murine inguinal fat cells. Data are presented as mean ± SEM. A different letter denotes a significant difference between groups at $p<0.05$.

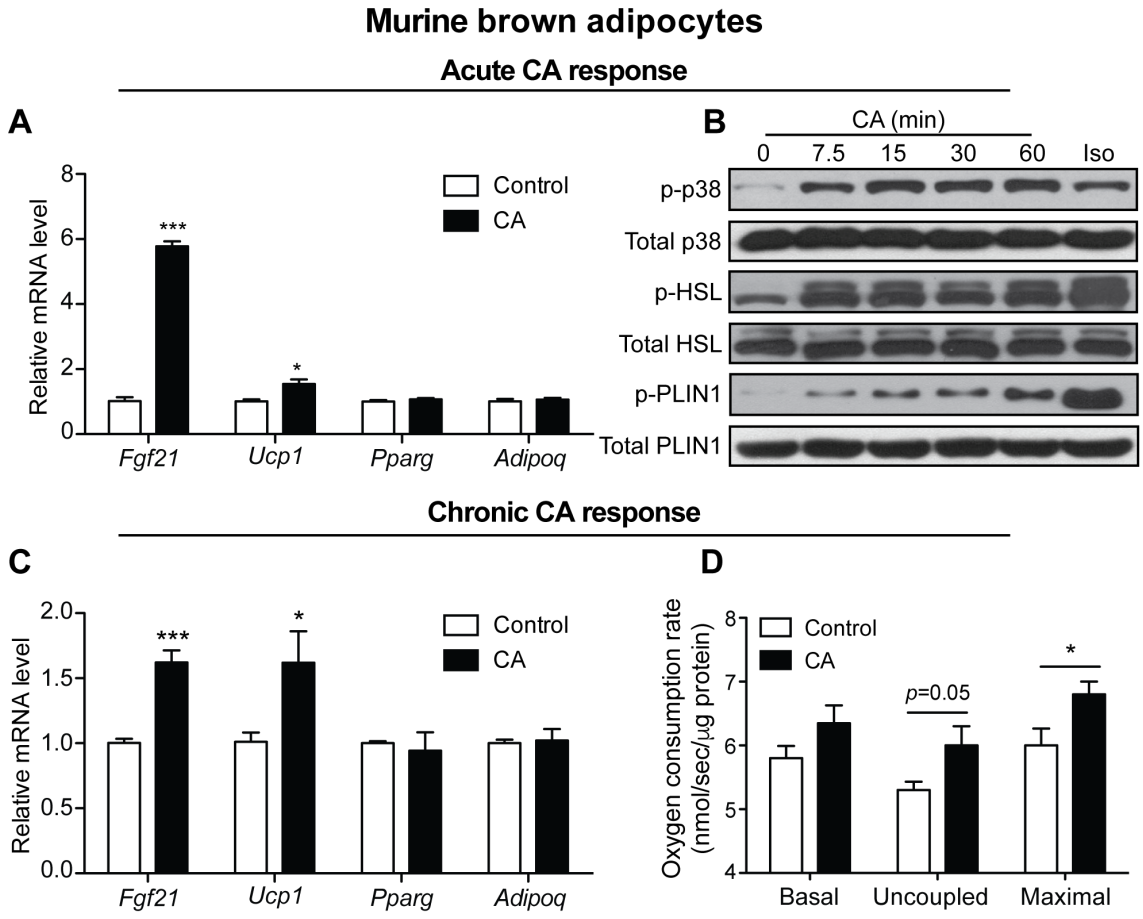

Figure III.9 CA upregulates thermogenesis in primary brown adipocytes.
A. Real-time qPCR analyses of thermogenic genes (*Fgf21* and *Ucp1)* and adipogenic markers (*Pparg* and *Adipoq*) in differentiated brown adipocytes treated with vehicle control or 200 μM CA for 4 h (n=4). **B.** Representative immunoblots of phosphorylated p38 MAPK, phosphorylated HSL (Ser660) and phosphorylated PLIN1 (Ser517) in differentiated brown adipocytes treated with 200 μM CA for the indicated time or 10 μM Iso for 10 min as a control. **C.** Real-time qPCR analyses of thermogenic (*Fgf21* and *Ucp1)* and adipogenic genes (*Pparg* and *Adipoq*) in differentiated brown adipocytes treated with vehicle control or 100 μM CA for 24 h (n=4-6). **D.** Basal, uncoupled, and maximal respiration of brown adipocytes treated wih 100 μM CA for 24 hours (n=6). Data in **A**, **C**, and **D** are presented as mean ± SEM. *p<0.05, **p<0.01, ***p<0.001.

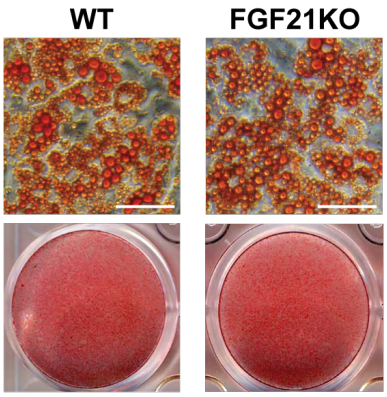

Figure III.10 FGF21KO cells differentiate to a similar extent as WT cells.
Representative Oil Red O staining of differentiated inguinal adipocytes isolated from WT or FGF21KO mice. It is worth noting that FGF21 deletion has been reported to impair differentiation of preadipocytes [21], but we observed robust and equal adipogenesis in either genotype under our experimental conditions.

Subject	Gender	Age	Ethnicity	BMI	Tissue location
1	F	44	Caucasian	21.32	Abdomen, inner thighs
2	F	24	Caucasian	24.0	Flanks, thighs
7	F	21	African American	25.0	Hips
14	F	30	Caucasian	37.15	Abdomen, hips

Table III.1 Characteristics of human donors used in this study.

Gene	Forward primers (5'- 3')	Reverse primers (5'- 3')
m36B4 (Rplp0)	GAGACTGAGTACACCTTCCCAC	ATGCAGATGGATCAGCCAGG
mAdipoq	GCACTGGCAAGTTCTACTGCAA	GTAGGTGAAGAGAACGGCCTTGT
mAtgl (Pnpla2)	AACACCAGCATCCAGTTCAA	GGTTCAGTAGGCCATTCCTC
mcFos	CGGGTTTCAACGCCGACTA	TTGGCACTAGAGACGGACAGA
mCebpa	TGGACAAGAACAGCAACGAG	TCACTGGTCAACTCCAGCAC
mCebpb	TCTACTACGAGCCCGACTGC	AGGTAGGGGCTGAAGTCGAT
mCidea	GCCGTGTTAAGGAATCTGCTG	TGCTCTTCTGTATCGCCCAGT
mCpt1b	ATCATGTATCGCCGCAAACT	CCATCTGGTAGGAGCACATGG
mCs	GGACAATTTTCCAACCAATCTGC	TCGGTTCATTCCCTCTGCATA
mCycs	GCAAGCATAAGACTGGACCAAA	TTGTTGGCATCTGTGTAAGAGAATC
mDgat1	TCCGTCCAGGGTGGTAGTG	TGAACAAAGAATCTTGCAGACGA
mEgr1	TCGGCTCCTTTCCTCACTCA	CTCATAGGGTTGTTCGCTCGG
mFabp4	ACACCGAGATTTCCTTCAAACTG	CCATCTAGGGTTATGATGCTCTTC
mFgf21	GTGTCAAAGCCTCTAGGTTTCTT	GGTACACATTGTAACCGTCCTC
mGyk	TGAACCTGAGGATTTGTCAGC	CCATGTGGAGTAACGGATTTCG
mHsl (Lipe)	TGAGATGCCACTCACCTCTG	GCCTAGTGCCTTCTGGTCTG
mIdh3a	TGGGTGTCCAAGGTCTCTC	CTCCCACTGAATAGGTGCTTTG
mPdk4	AGGGAGGTCGAGCTGTTCTC	GGAGTGTTCACTAAGCGGTCA
mPpara	AGAGCCCCATCTGTCCTCTC	ACTGGTAGTCTGCAAAACCAAA
mPparg	GCATGGTGCCTTCGCTGA	TGGCATCTCTGTGTCAACCATG
mPpargc1a	TATGGAGTGACATAGAGTGTGCT	CCACTTCAATCCACCCAGAAAG
mPrdm16	TGCTGACGGATACAGAGGTGT	CCACGCAGAACTTCTCGCTAC
mSod1	AACCAGTTGTGTTGTCAGGAC	CCACCATGTTTCTTAGAGTGAGG
mSod2	CAGACCTGCCTTACGACTATGG	CTCGGTGGCGTTGAGATTGTT
mTfam	ATTCCGAAGTGTTTTTCCAGCA	TCTGAAAGTTTTGCATCTGGGT
mUcp1	CTTTGCCTCACTCAGGATTGG	ACTGCCACACCTCCAGTCATT
hRPLP0	GCAGCATCTACAACCCTGAAG	CACTGGCAACATTGCGGAC
hADIPOQ	AACATGCCCATTCGCTTTACC	TAGGCAAAGTAGTACAGCCCA
hATGL (PNPLA2)	ATGGTGGCATTTCAGACAACC	CGGACAGATGTCACTCTCGC
hCEBPA	GTCGGTGGACAAGAACAGC	CAGCTGGCGGAAGATGC
hCEBPB	CTTCAGCCCGTACCTGGAG	GGAGAGGAAGTCGTGGTGC
hCIDEA	TTATGGGATCACAGACTAAGCGA	TGCTCCTGTCATGGTTGGAGA
hCPT1B	CATGTATCGCCGTAAACTGGAC	TGGTAGGAGCACATAGGCACT
hCS	AACTGCTACCCAAGGCTAAGG	CTTTTGAGAGCCAAGATACCTGT
hCYCS	CTTTGGGCGGAAGACAGGTC	TTATTGGCGGCTGTGTAAGAG

hDGAT1	GGTCCCCAATCACCTCATCTG	TGCACAGGGATGTTCCAGTTC
hFABP4	ACTGGGCCAGGAATTTGACG	CCCCATCTAAGGTTATGGTGCTC
hFGF21	ATGGATCGCTCCACTTTGACC	GGGCTTCGGACTGGTAAACAT
hGYK	CTGGGACAAGATAACTGGAGAGC	TCAACGGTAGACTGGGTTCTTA
hHSL (LIPE)	AGGAGCCAGCATTGAGACAAA	CGCAGGTGTTGATTCAGCTTC
hIDH3A	AGCCGGTCACCCATCTATGAA	TAGAGACACATGGTCGGACAT
hPDK4	GACCCAGTCACCAATCAAAATCT	GGTTCATCAGCATCCGAGTAGA
hPPARA	CGGTGACTTATCCTGTGGTCC	CCGCAGATTCTACATTCGATGTT
hPPARG	ACCAAAGTGCAATCAAAGTGGA	ATGAGGGAGTTGGAAGGCTCT
hPPARGC1A	TCTGAGTCTGTATGGAGTGACAT	CCAAGTCGTTCACATCTAGTTCA
hPRDM16	GTTCTGCGTGGATGCAAATCA	GGTGAGGTTCTGGTCATCGC
hSOD1	GGTGGGCCAAAGGATGAAGAG	CCACAAGCCAAACGACTTCC
hSOD2	GCTCCGGTTTTGGGGTATCTG	GCGTTGATGTGAGGTTCCAG
hTFAM	ATGGCGTTTCTCCGAAGCAT	TCCGCCCTATAAGCATCTTGA
hUCP1	AGGTCCAAGGTGAATGCCC	GCGGTGATTGTTCCCAGGA

Table III.2 Primer sequences for real-time qPCR analysis.

References

1. Rosen, E.D. and B.M. Spiegelman, *What we talk about when we talk about fat.* Cell, 2014. **156**(1-2): p. 20-44.

2. Cannon, B. and J. Nedergaard, *Brown adipose tissue: function and physiological significance.* Physiol Rev, 2004. **84**(1): p. 277-359.

3. Camacho, S., et al., *Anti-obesity and anti-hyperglycemic effects of cinnamaldehyde via altered ghrelin secretion and functional impact on food intake and gastric emptying.* Sci Rep, 2015. **5**: p. 7919.

4. Tamura, Y., et al., *Ingestion of cinnamaldehyde, a TRPA1 agonist, reduces visceral fats in mice fed a high-fat and high-sucrose diet.* J Nutr Sci Vitaminol (Tokyo), 2012. **58**(1): p. 9-13.

5. Allen, R.W., et al., *Cinnamon use in type 2 diabetes: an updated systematic review and meta-analysis.* Ann Fam Med, 2013. **11**(5): p. 452-9.

6. Khare, P., et al., *Cinnamaldehyde supplementation prevents fasting-induced hyperphagia, lipid accumulation, and inflammation in high-fat diet-fed mice.* Biofactors, 2016. **42**(2): p. 201-11.

7. Harms, M. and P. Seale, *Brown and beige fat: development, function and therapeutic potential.* Nat Med, 2013. **19**(10): p. 1252-63.

8. Ye, L., et al., *TRPV4 is a regulator of adipose oxidative metabolism, inflammation, and energy homeostasis.* Cell, 2012. **151**(1): p. 96-110.

9. Ma, S., et al., *Activation of the cold-sensing TRPM8 channel triggers UCP1-dependent thermogenesis and prevents obesity.* J Mol Cell Biol, 2012. **4**(2): p. 88-96.

10. Bartesaghi, S., et al., *Thermogenic Activity of UCP1 in Human White Fat-Derived Beige Adipocytes.* Molecular Endocrinology, 2015. **29**(1): p. 130-139.

11. Labbe, S.M., et al., *In vivo measurement of energy substrate contribution to cold-induced brown adipose tissue thermogenesis.* FASEB J, 2015. **29**(5): p. 2046-58.

12. Mottillo, E.P., et al., *Coupling of lipolysis and de novo lipogenesis in brown, beige, and white adipose tissues during chronic beta 3-adrenergic receptor activation.* Journal of Lipid Research, 2014. **55**(11): p. 2276-2286.

13. Barquissau, V., et al., *White-to-brite conversion in human adipocytes promotes metabolic reprogramming towards fatty acid anabolic and catabolic pathways.* Mol Metab, 2016. **5**(5): p. 352-65.

14. Fisher, F.M., et al., *FGF21 regulates PGC-1alpha and browning of white adipose tissues in adaptive thermogenesis.* Genes Dev, 2012. **26**(3): p. 271-81.

15. Fisher, F.M., et al., *Obesity Is a Fibroblast Growth Factor 21 (FGF21)-Resistant State.* Diabetes, 2010. **59**(11): p. 2781-2789.

16. Cohen, P., et al., *Ablation of PRDM16 and Beige Adipose Causes Metabolic Dysfunction and a Subcutaneous to Visceral Fat Switch.* Cell, 2014. **156**(1-2): p. 304-316.

17. Chondronikola, M., et al., *Brown Adipose Tissue Activation Is Linked to Distinct Systemic Effects on Lipid Metabolism in Humans.* Cell Metabolism, 2016. **23**(6): p. 1200-1206.

18. Michlig, S., et al., *Effects of TRP channel agonist ingestion on metabolism and autonomic nervous system in a randomized clinical trial of healthy subjects.* Sci Rep, 2016. **6**: p. 20795.

19. Zhao, H., et al., *Pharmacokinetic study of cinnamaldehyde in rats by GC-MS after oral and intravenous administration.* J Pharm Biomed Anal, 2014. **89**: p. 150-7.

20. Shang, S.J., et al., *Intracellular TRPA1 mediates Ca2+ release from lysosomes in dorsal root ganglion neurons.* Journal of Cell Biology, 2016. **215**(3): p. 369-381.

21. Dutchak, P.A., et al., *Fibroblast Growth Factor-21 Regulates PPAR gamma Activity and the Antidiabetic Actions of Thiazolidinediones.* Cell, 2012. **148**(3): p. 556-567.

Chapter IV

Development, Activation, and Therapeutic Potential of Thermogenic Adipocytes

Abstract

During the last decade, significant progress has been made in understanding adipocytes with a particular focus on thermogenic fat cells, which effectively convert chemical energy into heat in addition to their other metabolic functions. It has been increasingly recognized that different types and subtypes of adipocytes exist and the developmental origins of various types of fat cells are being intensively investigated. Previous work using immortalized fat cell lines has established an intricate transcriptional network that regulates adipocyte function. Recent work has illustrated how these key transcriptional components mediate thermogenic activation in fat cells. Last but not least, cumulative evidence supports an incontestable role of thermogenic fat in influencing systemic metabolism in humans. Here we summarize the exciting advancements in our understanding of thermogenic fat, discuss the advantages and limitations of the experimental tools currently available, and explore the future directions of this fast-evolving field.

Introduction

Portions of this chapter are from an article that is currently under review, it will be credited as: **Emont, M.P.***, Kim, D.*, Wu, J. Development, Activation, and Therapeutic Potential of Thermogenic Adipocytes. *Contributed equally.

The rediscovery of thermogenic adipocytes in human adults introduced a fresh target to investigate and modulate in hopes of leveraging the balance of energy homeostasis towards expenditure, therefore possibly presenting new opportunities counteract human obesity. While pursuing the potential metabolic benefits of these thermogenic fat cells, researchers in this area have investigated many aspects of the basic biology of adipocytes and the last ten years has witnessed a riveting renaissance of all things fat [1].

Broadly speaking, chemical energy storing, unilocular white adipocytes and heat producing, multilocular thermogenic fat cells constitute the majority of the fat in mammals. Emerging evidence additionally suggests that adipocytes in the bone marrow are distinctive in many aspects from fat found in the rest of the body and are often considered in a separate category of its own [2]. Among all the thermogenic fat cells, what we now call classical brown fat cells arise from a skeletal muscle like origin and localize within a number of specific anatomical locations [3]. In comparison, the exact definition of the inducible beige adipocyte is continuously evolving as investigation moves forward. In this mini review, what we refer to as beige adipocytes can be loosely defined as the thermogenic fat cells residing within white adipose tissue that do not share the same developmental origin as the classical brown adipocytes.

Thermogenesis, similar to any other energy consuming process, has evolved to be tightly controlled so that no unnecessary energy loss can occur. Signaling cascades that regulate thermogenic fat activation have recently been thoroughly reviewed elsewhere [4]. Here we will focus our discussion on the developmental origin, transcriptional control, and therapeutic potential of both brown and beige adipocytes.

Developmental Origins of Thermogenic Fat

It has been more than ten years since transcription co-component PR domain containing 16 (PRDM16) was identified as one of the key regulators for brown fat differentiation and a loss of function study revealed that instead of turning into white fat cells as expected, PRDM16 knockdown causes primary brown preadipocytes to differentiate into myocytes [3, 5]. Cell fate mapping experiments with skeletal muscle marker *Myf5* driven cre mediated reporter expression uncovered the surprising shared lineage between skeletal muscle and interscapular brown fat [3]. This skeletal muscle-like origin for brown adipocytes has been validated by subsequent studies using other skeletal muscle markers [6-8]. The finding that the adrenergic-induced thermogenic cells within the subcutaneous inguinal fat depot arise from a different developmental origin than brown fat led to the study of clonal cell lines derived from this depot, which found that beige fat arises from a subpopulation of distinct progenitor cells [3, 9].

Since then, further evidence has emerged showing that cold exposure induces *de novo* adipogenesis of beige adipocytes. The "Adipo-Chaser" mouse, which pulse labels mature adipocytes with lacZ, found that a large population of non-lacZ labeled multilocular adipocytes (newly differentiated beige fat cells) emerge in the white fat depots after cold exposure [10]. The developmental origin(s) of these inducible beige fat cells have been intensively investigated. Using a *Ucp1*-TRAP system to specifically analyze polysomes from the *Ucp1*-expressing cells in white fat depots showed that these cells had enriched expression of multiple genes associated with smooth muscle [11]. Further investigation using a myosin heavy chain 11 (*Myh11*)-cre driven GFP reporter found that many UCP1+ cells in the inguinal depot arose from *Myh11*+

progenitor cells [11]. This potential smooth muscle like origin of beige fat cells was also implicated by fate mapping studies using reporter mice that label cells from the SMA lineage (smooth muscle actin, also called ACTA2, actin alpha 2) [8, 12]. Vascular smooth muscle cells and pericytes, generally referred to as mural cells, derive from the mesenchyme and give rise to vessels. Mural cells expressing platelet derived growth factor receptor β (PDGFRβ) have been shown to differentiate into beige adipocytes in the inguinal depot in response to long-term cold exposure [13]. Interestingly, capillary cells from human adipose tissue explants have been shown to be able to differentiate into thermogenic adipocytes, further suggesting that vascular progenitors and beige adipocytes may share a common origin [14]. In addition to studies of what may lead to the formation and activation of inducible beige adipocytes, recent work has started to inspect how the deactivation of beige fat may be regulated. A swift decrease of thermogenic activity was observed upon stimuli withdrawal in beige fat, in contrast to classical brown fat [15]. This is consistent with the notion that beige adipocytes with "white-like" morphology exist in an inactivated state in the absence of thermogenic stimuli and could constitute at least one of the potential mechanisms for "interconversion" and "transdifferentiation" observed in previous investigations [16, 17].

Transcriptional Control of the Activation of Thermogenesis

A great deal of work has been done to characterize the transcriptional network responsible for thermogenic fat activation. Much of this regulation has emanated from interactions between peroxisome proliferator-activated receptor gamma (PPARγ) and two key transcriptional co-components: PRDM16, and peroxisome proliferator-activated receptor gamma coactivator 1 alpha (PGC1α) (Figure IV.1).

PPARγ is the master regulator of adipocyte differentiation and function [1] and chronic PPARγ agonism by drugs such as the thiazolidinedione rosiglitazone during adipocyte development results in an increased capacity for thermogenesis in these cells [18-20]. While the mechanisms by which PPARγ promotes thermogenic development are continuously being investigated, a number of posttranslational modifications of PPARγ have been suggested to play a role in the upregulation of the thermogenic program during adipocyte differentiation [20-22]. PPARγ both drives the transcription of and works alongside PRDM16, a transcriptional co-component that plays a pivotal role in regulating brown fat cell fate and beige fat function [3, 5, 23, 24]. Unlike the drastic cell type switch from brown adipocytes to myotubes seen when PRDM16 is knocked down in culture, deletion of PRDM16 in the brown fat lineage by *Myf5*-cre *in vivo* compromised brown fat function during aging but did not affect brown fat in early development, likely due to compensation from PRDM3 [25]. Despite arising from a separate lineage that PRDM16 may not affect, inducible beige adipocytes are functionally responsive to this transcriptional co-component. Beiging due to rosiglitazone treatment has been shown to be at least partially mediated through PRDM16 stabilization [20]. Gain and loss of function of PRDM16 in adipocytes increases and decreases the abundance of thermogenic beige adipocytes in subcutaneous adipose tissue, respectively [23, 24]. It was shown that PRDM16 transcriptional activity works in part by making a complex with CCAAT/enhancer binding protein β (C/EBPβ) [26]. Accordingly, thermogenic fat function can be affected by micro RNAs that regulate C/EBPβ, such as *mir-155* [27] or *miR-196a* [28].

The regulation of *Prdm16* transcription plays a substantial role in the maintenance of the

thermogenic program. Early b-cell factor 2 (EBF2) is a DNA binding protein that has been reported to direct PPARγ towards transcription of a brown adipocyte program, including upregulation of *Prdm16* transcription [29]. *Blnc1* is a long noncoding RNA that has been shown to interact with EBF2 to promote thermogenic adipocyte differentiation [30]. *Blnc1*, as well as the long noncoding RNA *lnc-BATE1*, were shown to upregulate thermogenesis via interactions with the structural protein heterogeneous nuclear ribonucleoprotein U (hnRNPU) [31, 32]. A screen to find transcription factors that induce thermogenic adipocyte differentiation identified ZBTB7B, which was shown to interact with *Blnc1* and hnRNPU to upregulate the expression of thermogenic genes [32]. ZFP423, in addition to its role in regulating adipocyte commitment [33], directly binds to EBF2 and inhibits browning through suppression of *Prdm16* transcription [34]. Other suppressors of *Prdm16* transcription also inhibit thermogenesis, including *miR-27b* and *miR-133* which both inhibit thermogenesis through targeting of the 3'- untranslated region (UTR) of *Prdm16* [35-38]. A number of proteins activate or inhibit thermogenesis through interaction with PRDM16. Activators include euchromatic histone-lysine N-methyltransferase 1 (EHMT1) [25, 39], ZFP516 [40], and lysine-specific demethylase 1 (LSD1) [41, 42], which also interacts with ZFP516 to promote thermogenic gene transcription [43]. Repressors include transducin like enhancer of split 3 (TLE3), a transcription factor that promotes white adipogenesis through competition with PRDM16 to bind promoters of genes associated with lipid storage and thermogenesis [44, 45].

PGC1α was initially identified as a transcriptional cofactor interacting with PPARγ with enriched expression in brown fat compared to white fat [46]. Further research has confirmed that it plays a pivotal role in mitochondrial biogenesis and oxidative metabolism through interactions with

various nuclear receptors [47]. PGC1α and related protein PGC1β have been shown to be crucial in the regulation of mitochondrial biogenesis in activated thermogenic fat [48-50]. *Pgc1a* transcription is induced by CREB and ATF2 [51, 52] and upregulation and stabilization of *Pgc1a* mRNA activates the thermogenic program. Interferon regulatory factor 4 (IRF4) regulates thermogenic gene transcription via direct interaction with PGC1α, and thermogenesis induced by PGC1α overexpression in fat is blunted in the absence of IRF4 [53]. Conversely, factors that inhibit PGC1α activity decrease thermogenesis. Twist Family BHLH Transcription Factor 1 (TWIST1) is a transcriptional regulator that interacts with PGC1α and suppresses the transcription of its target genes, possibly through a negative feedback mechanism [54]. Knockout of the related proteins RB and p107 were found to increase thermogenesis in adipocytes through alleviated repression of PGC1α [55, 56]. Similarly, RIP140 interacts with PGC1α, repressing transcription of thermogenic genes such as cell death-inducing DFFA-like effector A (*Cidea*) and *Ucp1* [57, 58]. Finally, inhibition of *miR-34a* robustly increases browning of white adipocytes by enhancing SIRT1-mediated PGC1α deacetylation, resulting in an increase of thermogenic gene transcription [59].

Therapeutic Potential of Thermogenic Fat

Better understanding of the development and activation of thermogenic adipocytes can help to build the foundation for potentially harnessing the metabolic benefits of these fat cells in humans. Since 2009, when multiple groups discovered activatable thermogenic fat in the supraclavicular and neck regions of humans [60-63], a great deal of research has been done to characterize human thermogenic fat. These initial ground-breaking discoveries were accompanied by both the excitement that these metabolically active cells may help to counteract

human obesity as well as caution concerning whether the amount and activity of these cells in an average human could constitute a palpable influence on systemic metabolism. Much of the hard work since then has addressed these concerns and evaluated the therapeutic potential of thermogenic fat in various human studies (Table IV.1). It has been shown that in healthy individuals acute cold exposure can improve glucose homeostasis and insulin sensitivity [64] and that varying lengths of chronic cold exposure can increase insulin sensitivity [65] and decrease obesity [66]. It has additionally been shown that a 10 day cold exposure protocol can increase insulin sensitivity in obese diabetic patients [67]. Cold activates thermogenic fat through the central nervous system, which signals to target tissues through the β-adrenergic pathway [1]. After early mixed results [68-71], recent work has shown that the β3-adrenergic receptor agonist mirabegron can stimulate human thermogenic fat [72]. Ongoing efforts have revealed that other pathways, such as stimulation with capsinoids [66, 73], chenodeoxycholic acid (CDCA) [74], or glucocorticoids [75], can all promote the activity of human thermogenic fat.

To further investigate the therapeutic potential of these cells, studies have sought to develop tools to more effectively study their activation and function. Clonal cell lines were derived from human neck fat and studied using RNA sequencing and using a *Ucp1* reporter system, identifying multiple novel markers for human thermogenic adipocytes [76, 77]. Murine systems that measure substrate uptake and thermogenic activity *in vivo* allow for investigation into fundamental questions regarding the physiological function of the activated thermogenic program. It has recently been reported that long chain fatty acids (LCFAs) are required for UCP1 function and can be used as a substrate for thermogenesis [78]. Injection of a luciferin-conjugate LCFA, which is cleaved by glutathione and activated upon uptake into cells, allows for real-time

detection of β-adrenergic agonist induced fatty acid uptake increase in the brown fat of mice expressing luciferase, presenting an imaging approach that allows investigation of metabolic regulation and pathological alterations of thermogenic fat [79]. This method was applied to *Ucp1*-cre driven luciferase-expressing mice and directly demonstrated that lipokine 12, 13-diHOME promotes fatty acid uptake in brown fat [80]. A number of mice have additionally been generated with reporter constructs for *Ucp1* expression, the 'ThermoMouse' which expresses luciferase under the control of the *Ucp1* promoter region [81] and the '*Ucp1*-2A luciferase knock-in mouse' which contains luciferase appended to the end of the *Ucp1* gene [82] can both faithfully recapitulate *Ucp1* regulation *in vivo* and can be used for future exploration to uncover regulatory signaling or drug compounds targeting thermogenic fat.

Investigation so far indicates that not only the activity level but also the actual amount of activatable thermogenic fat may vary from individual to individual [83], methods that can accurately measure activatable thermogenic fat can therefore be used to better personalize therapeutic strategies by identifying likely responders. Using radiolabeled substrates for thermogenesis as surrogates, studies have been carried out using positron emission tomography (PET) scans with either ^{18}F-FDG or the fatty acid tracer ^{18}F-FHTA, combined with computed tomography (CT) scanning to measure activated thermogenic fat [60-63, 84, 85]. Similarly, PET scans using ^{15}O to measure oxygen consumption have also been adapted to measure the activity of thermogenic fat [86, 87]. Nonionizing techniques have also been applied to evaluate thermogenic fat content and activity in humans. Contrast enhanced ultrasound can be used to measure the increased blood flow to thermogenic fat tissue following cold exposure [88]. Similar to infrared imaging of mice [89], measurements of surface temperature in the supraclavicular

region using infrared thermography can detect human thermogenic fat activity [90, 91]. Water-fat separated magnetic resonance imaging (MRI) was adapted to distinguish thermogenic and white fat based on contrasting tissue characteristics instead of measurement of thermogenic activity, by taking advantage of the fact that thermogenic fat is more densely vascularized than white fat [92, 93]. A recent study with a hybrid FDG-PET/MR scanner demonstrates that MRI when used in combination with PET may present a radiation-free alternative to CT [94]. Continuous efforts to develop accurate, non-invasive methods to detect and monitor thermogenic fat in humans are warranted to enable longitudinal studies in infants, children, and healthy adults in the future.

While thermogenic activity of supraclavicular and neck fat has been extensively studied in humans [75-77, 95-98], an increasing number of studies indicate that activatable thermogenic fat may very well exist elsewhere in the human body. Seasonal cold exposure has been shown to induce thermogenic gene expression in subcutaneous white adipose tissue [99] and long-term adrenergic stimulation as a result of burn injuries can thermogenically activate subcutaneous fat from multiple depots [100]. Studies of human subcutaneous adipocytes in culture have revealed that these cells respond to thermogenic stimuli, such as PPARγ agonist rosiglitazone [101], bone morphogenic proteins (BMP) 4 and 7 [102], natriuretic peptides [103], and the food compound cinnamaldehyde [104]. It is also worth noting that many human adipose cell lines have been used to investigate thermogenic regulation, including human multipotent adipose derived stem (hMADS) cells [103, 105-109], human induced pluripotent stem (iPS) cells [110-114], and a number of cell lines derived from fetal tissue [115-117]. It is unlikely that quantifiable changes in actual thermogenic capacity (e.g. respiration) can be measured in all of the above mentioned *in vitro* systems, given that the actual expression levels of thermogenic genes are fairly low in some

of these cell lines. However, it is tempting to speculate that gene expression based assays could potentially be carried out in many commonly available human fat cell systems, at least as an initial proof-of-principle investigation.

Future Directions

Most of the research done on both murine and human thermogenic fat thus far has focused on UCP1-mediated thermogenesis, however, recent work indicates that a deeper understanding of non-shivering thermogenesis and a broader definition of beige adipocytes are warranted. Creatine cycling, which enhances respiration in wild type mitochondria when there are limiting amounts of ADP, has been observed in adipocytes from UCP1 KO mice, suggesting that this constitutes a mechanism for UCP1 independent thermogenesis [118]. This creatine-dependent futile cycle was further confirmed using patch clamp analysis of mitochondria isolated from visceral adipocytes after thermogenic stimulation. This study found that the majority of epididymal mitochondria were UCP1 negative and that thermogenic capacity was achieved through creatine cycling in these abdominal UCP1-negative "beige" adipocytes [119]. Furthermore, mice with an adipocyte specific knockout of glycine amidinotransferase (GATM), the rate limiting enzyme in creatine synthesis, have an increased tendency towards obesity, demonstrating the systemic influence of adipose creatine-cycling [120]. UCP1-independent thermogenesis can also be mediated through N-acyl amino acids, endogenous uncouplers of mitochondrial respiration in brown and beige adipocytes [121].

In this thesis we have provided a method to further study the differences between subcutaneous and visceral fat as well as investigated the activation of thermogenesis and modulation of

metabolic programming in murine and human subcutaneous adipocytes. The development of a method with which we can study visceral and subcutaneous adipocytes side-by-side in culture not only provides a tool by which we can further explore the similarities and differences between these cell types but also raises questions about the factors that control the ability of subcutaneous and visceral cells to differentiate. Is it the support from the 3D structure of the hydrogel that allows the cells to differentiate more naturally or is it enhanced interactions with the collagen, which physiologically is a major component of the ECM? Similarly, the cinnamaldehyde project provides insight into the thermogenic and metabolic remodeling of adipocytes but raises further questions—what is CA signaling through if not TRPA1 and what is the pathway for the CA mediated activation of PKA? Despite these remaining questions, the work done here represents a step forward in our ability to study the similarities and differences between subcutaneous and visceral adipocytes as well as our understanding of the process of thermogenic fat activation in subcutaneous adipocytes. These findings can only help us in the quest to identify new targets that can help to materialize the potential of thermogenic adipocytes in influencing human physiology in health and disease.

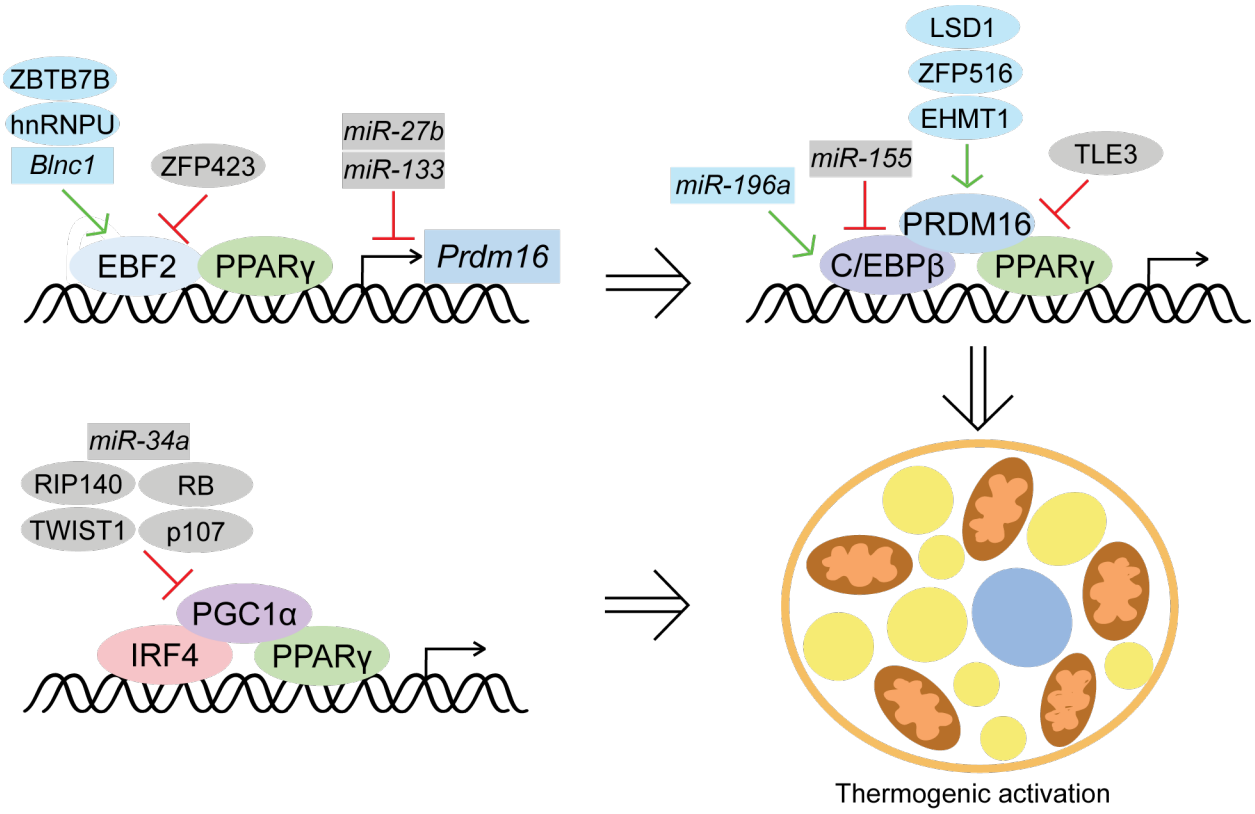

Figure IV.1 PRDM16 and PGC1α Interact with PPARγ to Activate the Thermogenic Program

Both the transcription of *Prdm16*, regulated by PPARγ and EBF2, as well as the function of PRDM16 as it forms transcriptional complexes with PPARγ and C/EBPβ, are responsible for driving thermogenic activation. Similarly, the transcriptional complexes that PGC1α forms with PPARγ and IRF4 mediate activation of the thermogenic program.

	in vivo	
Detection and measurement	PET/CT (^{18}F-FDG, ^{18}F-FTHA, ^{15}O)	[60-63, 84-87]
	Nonionizing (Contrast enhanced ultrasound, Infrared thermography, MRI, Near infrared spectroscopy)	[86, 88, 90-94]
Stimulation of thermogenic fat	Cold exposure (Improves glucose homeostasis, Decreases body fat)	[64-67]
	β-adrenergic stimulation (Mirabegron, Ephedrine)	[70, 72]
	Other drugs (Capsinoids, CDCA, Glucocorticoids)	[66, 73-75]
	in vitro	
Supraclavicular and Neck fat	(Forskolin, BMP7, Cortisol, db-cAMP, Norepinephrine, FGF21, Isoproterenol)	[75-77, 95-98]
Subcutaneous fat	(Rosiglitazone, Mirabegron, BMP4/BMP7, Natriuretic peptides, Cinnamaldehyde)	[14, 101-104]
Multipotent adipose derived stem (hMADS) cells	(Rosiglitazone, Natriuretic peptides, β-adrenergic receptor agonists, Arachidonic acid)	[103, 105-109]
iPS cells	(Lactate, Forskolin, cAMP, Isoproterenol, JAK inhibition)	[110-114]
Fetal stem cells	Fetal interscapular fat (Norepinephrine)	[116, 117]
	Fetal mesenchymal stem cells (Rosiglitazone)	[115]

Table IV.1 Recent Advancements in Human Thermogenic Fat Study

References

1. Rosen, E.D. and B.M. Spiegelman, *What we talk about when we talk about fat.* Cell, 2014. **156**(1-2): p. 20-44.

2. Scheller, E.L., et al., *Marrow Adipose Tissue: Trimming the Fat.* Trends Endocrinol Metab, 2016. **27**(6): p. 392-403.

3. Seale, P., et al., *PRDM16 controls a brown fat/skeletal muscle switch.* Nature, 2008. **454**(7207): p. 961-7.

4. Kajimura, S., B.M. Spiegelman, and P. Seale, *Brown and Beige Fat: Physiological Roles beyond Heat Generation.* Cell Metab, 2015. **22**(4): p. 546-59.

5. Seale, P., et al., *Transcriptional control of brown fat determination by PRDM16.* Cell Metab, 2007. **6**(1): p. 38-54.

6. Lepper, C. and C.M. Fan, *Inducible lineage tracing of Pax7-descendant cells reveals embryonic origin of adult satellite cells.* Genesis, 2010. **48**(7): p. 424-36.

7. Sanchez-Gurmaches, J., et al., *PTEN loss in the Myf5 lineage redistributes body fat and reveals subsets of white adipocytes that arise from Myf5 precursors.* Cell Metab, 2012. **16**(3): p. 348-62.

8. Berry, D.C., Y. Jiang, and J.M. Graff, *Mouse strains to study cold-inducible beige progenitors and beige adipocyte formation and function.* Nat Commun, 2016. **7**: p. 10184.

9. Wu, J., et al., *Beige adipocytes are a distinct type of thermogenic fat cell in mouse and human.* Cell, 2012. **150**(2): p. 366-76.

10. Wang, Q.A., et al., *Tracking adipogenesis during white adipose tissue development, expansion and regeneration.* Nat Med, 2013. **19**(10): p. 1338-44.

11. Long, J.Z., et al., *A smooth muscle-like origin for beige adipocytes.* Cell Metab, 2014. **19**(5): p. 810-20.

12. Jiang, Y., D.C. Berry, and J.M. Graff, *Distinct cellular and molecular mechanisms for beta3 adrenergic receptor-induced beige adipocyte formation.* Elife, 2017. **6**.

13. Vishvanath, L., et al., *Pdgfrbeta+ Mural Preadipocytes Contribute to Adipocyte Hyperplasia Induced by High-Fat-Diet Feeding and Prolonged Cold Exposure in Adult Mice.* Cell Metab, 2016. **23**(2): p. 350-9.

14. Min, S.Y., et al., *Human 'brite/beige' adipocytes develop from capillary networks, and their implantation improves metabolic homeostasis in mice.* Nature Medicine, 2016. **22**(3): p. 312-318.

15. Altshuler-Keylin, S., et al., *Beige Adipocyte Maintenance Is Regulated by Autophagy-Induced Mitochondrial Clearance.* Cell Metab, 2016. **24**(3): p. 402-419.

16. Cinti, S., *Transdifferentiation properties of adipocytes in the adipose organ.* Am J Physiol Endocrinol Metab, 2009. **297**(5): p. E977-86.

17. Rosenwald, M., et al., *Bi-directional interconversion of brite and white adipocytes.* Nat Cell Biol,

2013. **15**(6): p. 659-67.

18. Wilson-Fritch, L., et al., *Mitochondrial Biogenesis and Remodeling during Adipogenesis and in Response to the Insulin Sensitizer Rosiglitazone.* Molecular and Cellular Biology, 2003. **23**(3): p. 1085-1094.

19. Wilson-Fritch, L., et al., *Mitochondrial remodeling in adipose tissue associated with obesity and treatment with rosiglitazone.* J Clin Invest, 2004. **114**(9): p. 1281-9.

20. Ohno, H., et al., *PPARgamma agonists induce a white-to-brown fat conversion through stabilization of PRDM16 protein.* Cell Metab, 2012. **15**(3): p. 395-404.

21. Qiang, L., et al., *Brown remodeling of white adipose tissue by SirT1-dependent deacetylation of Ppargamma.* Cell, 2012. **150**(3): p. 620-32.

22. Wang, H., et al., *Browning of White Adipose Tissue with Roscovitine Induces a Distinct Population of UCP1+ Adipocytes.* Cell Metab, 2016. **24**(6): p. 835-847.

23. Seale, P., et al., *Prdm16 determines the thermogenic program of subcutaneous white adipose tissue in mice.* J Clin Invest, 2011. **121**(1): p. 96-105.

24. Cohen, P., et al., *Ablation of PRDM16 and beige adipose causes metabolic dysfunction and a subcutaneous to visceral fat switch.* Cell, 2014. **156**(1-2): p. 304-16.

25. Harms, M.J., et al., *Prdm16 is required for the maintenance of brown adipocyte identity and function in adult mice.* Cell Metab, 2014. **19**(4): p. 593-604.

26. Kajimura, S., et al., *Initiation of myoblast to brown fat switch by a PRDM16-C/EBP-beta transcriptional complex.* Nature, 2009. **460**(7259): p. 1154-8.

27. Chen, Y., et al., *miR-155 regulates differentiation of brown and beige adipocytes via a bistable circuit.* Nat Commun, 2013. **4**: p. 1769.

28. Mori, M., et al., *Essential role for miR-196a in brown adipogenesis of white fat progenitor cells.* PLoS Biol, 2012. **10**(4): p. e1001314.

29. Rajakumari, S., et al., *EBF2 determines and maintains brown adipocyte identity.* Cell Metab, 2013. **17**(4): p. 562-74.

30. Zhao, X.Y., et al., *A long noncoding RNA transcriptional regulatory circuit drives thermogenic adipocyte differentiation.* Mol Cell, 2014. **55**(3): p. 372-82.

31. Alvarez-Dominguez, J.R., et al., *De Novo Reconstruction of Adipose Tissue Transcriptomes Reveals Long Non-coding RNA Regulators of Brown Adipocyte Development.* Cell Metab, 2015. **21**(5): p. 764-776.

32. Li, S., et al., *Zbtb7b engages the long noncoding RNA Blnc1 to drive brown and beige fat development and thermogenesis.* Proc Natl Acad Sci U S A, 2017. **114**(34): p. E7111-E7120.

33. Gupta, R.K., et al., *Transcriptional control of preadipocyte determination by Zfp423.* Nature, 2010. **464**(7288): p. 619-23.

34. Shao, M., et al., *Zfp423 Maintains White Adipocyte Identity through Suppression of the Beige Cell Thermogenic Gene Program.* Cell Metab, 2016. **23**(6): p. 1167-1184.

35. Trajkovski, M., et al., *MyomiR-133 regulates brown fat differentiation through Prdm16.* Nat Cell Biol, 2012. **14**(12): p. 1330-5.

36. Liu, W., et al., *miR-133a regulates adipocyte browning in vivo.* PLoS Genet, 2013. **9**(7): p. e1003626.

37. Yin, H., et al., *MicroRNA-133 controls brown adipose determination in skeletal muscle satellite cells by targeting Prdm16.* Cell Metab, 2013. **17**(2): p. 210-24.

38. Kong, X., et al., *Glucocorticoids transcriptionally regulate miR-27b expression promoting body fat accumulation via suppressing the browning of white adipose tissue.* Diabetes, 2015. **64**(2): p. 393-404.

39. Ohno, H., et al., *EHMT1 controls brown adipose cell fate and thermogenesis through the PRDM16 complex.* Nature, 2013. **504**(7478): p. 163-7.

40. Dempersmier, J., et al., *Cold-inducible Zfp516 activates UCP1 transcription to promote browning of white fat and development of brown fat.* Mol Cell, 2015. **57**(2): p. 235-46.

41. Zeng, X., et al., *Lysine-specific demethylase 1 promotes brown adipose tissue thermogenesis via repressing glucocorticoid activation.* Genes Dev, 2016. **30**(16): p. 1822-36.

42. Duteil, D., et al., *Lsd1 prevents age-programed loss of beige adipocytes.* Proc Natl Acad Sci U S A, 2017. **114**(20): p. 5265-5270.

43. Sambeat, A., et al., *LSD1 Interacts with Zfp516 to Promote UCP1 Transcription and Brown Fat Program.* Cell Rep, 2016. **15**(11): p. 2536-49.

44. Villanueva, C.J., et al., *TLE3 is a dual-function transcriptional coregulator of adipogenesis.* Cell Metab, 2011. **13**(4): p. 413-427.

45. Villanueva, C.J., et al., *Adipose subtype-selective recruitment of TLE3 or Prdm16 by PPARgamma specifies lipid storage versus thermogenic gene programs.* Cell Metab, 2013. **17**(3): p. 423-35.

46. Puigserver, P., et al., *A Cold-Inducible Coactivator of Nuclear Receptors Linked to Adaptive Thermogenesis.* Cell, 1998. **92**(6): p. 829-839.

47. Handschin, C. and B.M. Spiegelman, *Peroxisome proliferator-activated receptor gamma coactivator 1 coactivators, energy homeostasis, and metabolism.* Endocr Rev, 2006. **27**(7): p. 728-35.

48. Lin, J., et al., *Peroxisome proliferator-activated receptor gamma coactivator 1beta (PGC-1beta), a novel PGC-1-related transcription coactivator associated with host cell factor.* J Biol Chem, 2002. **277**(3): p. 1645-8.

49. Uldry, M., et al., *Complementary action of the PGC-1 coactivators in mitochondrial biogenesis and brown fat differentiation.* Cell Metab, 2006. **3**(5): p. 333-41.

50. Lai, L., et al., *Transcriptional coactivators PGC-1alpha and PGC-lbeta control overlapping programs required for perinatal maturation of the heart.* Genes Dev, 2008. **22**(14): p. 1948-61.

51. Herzig, S., et al., *CREB regulates hepatic gluconeogenesis through the coactivator PGC-1.* Nature, 2001. **413**(6852): p. 179-83.

52. Cao, W., et al., *p38 Mitogen-Activated Protein Kinase Is the Central Regulator of Cyclic AMP-Dependent Transcription of the Brown Fat Uncoupling Protein 1 Gene.* Molecular and Cellular Biology, 2004. **24**(7): p. 3057-3067.

53. Kong, X., et al., *IRF4 is a key thermogenic transcriptional partner of PGC-1alpha.* Cell, 2014. **158**(1): p. 69-83.

54. Pan, D., et al., *Twist-1 is a PPARdelta-inducible, negative-feedback regulator of PGC-1alpha in brown fat metabolism.* Cell, 2009. **137**(1): p. 73-86.

55. Hansen, J.B., et al., *Retinoblastoma protein functions as a molecular switch determining white versus brown adipocyte differentiation.* Proceedings of the National Academy of Sciences, 2004. **101**(12): p. 4112-4117.

56. Scime, A., et al., *Rb and p107 regulate preadipocyte differentiation into white versus brown fat through repression of PGC-1alpha.* Cell Metab, 2005. **2**(5): p. 283-95.

57. Hallberg, M., et al., *A functional interaction between RIP140 and PGC-1alpha regulates the expression of the lipid droplet protein CIDEA.* Mol Cell Biol, 2008. **28**(22): p. 6785-95.

58. Powelka, A.M., et al., *Suppression of oxidative metabolism and mitochondrial biogenesis by the transcriptional corepressor RIP140 in mouse adipocytes.* J Clin Invest, 2006. **116**(1): p. 125-36.

59. Fu, T., et al., *MicroRNA 34a inhibits beige and brown fat formation in obesity in part by suppressing adipocyte fibroblast growth factor 21 signaling and SIRT1 function.* Mol Cell Biol, 2014. **34**(22): p. 4130-42.

60. van Marken Lichtenbelt, W.D., et al., *Cold-activated brown adipose tissue in healthy men.* N Engl J Med, 2009. **360**(15): p. 1500-8.

61. Virtanen, K.A., et al., *Functional brown adipose tissue in healthy adults.* N Engl J Med, 2009. **360**(15): p. 1518-25.

62. Cypess, A.M., et al., *Identification and importance of brown adipose tissue in adult humans.* N Engl J Med, 2009. **360**(15): p. 1509-17.

63. Saito, M., et al., *High incidence of metabolically active brown adipose tissue in healthy adult humans: effects of cold exposure and adiposity.* Diabetes, 2009. **58**(7): p. 1526-31.

64. Chondronikola, M., et al., *Brown adipose tissue improves whole-body glucose homeostasis and insulin sensitivity in humans.* Diabetes, 2014. **63**(12): p. 4089-99.

65. Lee, P., et al., *Temperature-acclimated brown adipose tissue modulates insulin sensitivity in humans.* Diabetes, 2014. **63**(11): p. 3686-98.

66. Yoneshiro, T., et al., *Recruited brown adipose tissue as an antiobesity agent in humans.* J Clin

Invest, 2013. **123**(8): p. 3404-8.

67. Hanssen, M.J., et al., *Short-term cold acclimation improves insulin sensitivity in patients with type 2 diabetes mellitus.* Nat Med, 2015. **21**(8): p. 863-5.

68. Cypess, A.M., et al., *Cold but not sympathomimetics activates human brown adipose tissue in vivo.* Proc Natl Acad Sci U S A, 2012. **109**(25): p. 10001-5.

69. Vosselman, M.J., et al., *Systemic beta-adrenergic stimulation of thermogenesis is not accompanied by brown adipose tissue activity in humans.* Diabetes, 2012. **61**(12): p. 3106-13.

70. Carey, A.L., et al., *Ephedrine activates brown adipose tissue in lean but not obese humans.* Diabetologia, 2013. **56**(1): p. 147-55.

71. Carey, A.L., et al., *Chronic ephedrine administration decreases brown adipose tissue activity in a randomised controlled human trial: implications for obesity.* Diabetologia, 2015. **58**(5): p. 1045-54.

72. Cypess, A.M., et al., *Activation of human brown adipose tissue by a beta3-adrenergic receptor agonist.* Cell Metab, 2015. **21**(1): p. 33-8.

73. Yoneshiro, T., et al., *Nonpungent capsaicin analogs (capsinoids) increase energy expenditure through the activation of brown adipose tissue in humans.* Am J Clin Nutr, 2012. **95**(4): p. 845-50.

74. Broeders, E.P., et al., *The Bile Acid Chenodeoxycholic Acid Increases Human Brown Adipose Tissue Activity.* Cell Metab, 2015. **22**(3): p. 418-26.

75. Ramage, L.E., et al., *Glucocorticoids Acutely Increase Brown Adipose Tissue Activity in Humans, Revealing Species-Specific Differences in UCP-1 Regulation.* Cell Metab, 2016. **24**(1): p. 130-41.

76. Shinoda, K., et al., *Genetic and functional characterization of clonally derived adult human brown adipocytes.* Nat Med, 2015. **21**(4): p. 389-94.

77. Xue, R., et al., *Clonal analyses and gene profiling identify genetic biomarkers of the thermogenic potential of human brown and white preadipocytes.* Nat Med, 2015. **21**(7): p. 760-8.

78. Fedorenko, A., P.V. Lishko, and Y. Kirichok, *Mechanism of fatty-acid-dependent UCP1 uncoupling in brown fat mitochondria.* Cell, 2012. **151**(2): p. 400-13.

79. Henkin, A.H., et al., *Real-time noninvasive imaging of fatty acid uptake in vivo.* ACS Chem Biol, 2012. **7**(11): p. 1884-91.

80. Lynes, M.D., et al., *The cold-induced lipokine 12,13-diHOME promotes fatty acid transport into brown adipose tissue.* Nat Med, 2017. **23**(5): p. 631-637.

81. Galmozzi, A., et al., *ThermoMouse: an in vivo model to identify modulators of UCP1 expression in brown adipose tissue.* Cell Rep, 2014. **9**(5): p. 1584-93.

82. Mao, L., et al., *Visualization and Quantification of Browning Using a Ucp1-2A-Luciferase Knock-in Mouse Model.* Diabetes, 2017. **66**(2): p. 407-417.

83. Betz, M.J. and S. Enerback, *Targeting thermogenesis in brown fat and muscle to treat obesity and metabolic disease.* Nat Rev Endocrinol, 2017.

84. Ouellet, V., et al., *Brown adipose tissue oxidative metabolism contributes to energy expenditure during acute cold exposure in humans.* J Clin Invest, 2012. **122**(2): p. 545-52.

85. Blondin, D.P., et al., *Dietary fatty acid metabolism of brown adipose tissue in cold-acclimated men.* Nat Commun, 2017. **8**: p. 14146.

86. Muzik, O., et al., *15O PET measurement of blood flow and oxygen consumption in cold-activated human brown fat.* J Nucl Med, 2013. **54**(4): p. 523-31.

87. M, U.D., et al., *Human brown adipose tissue [(15)O]O2 PET imaging in the presence and absence of cold stimulus.* Eur J Nucl Med Mol Imaging, 2016. **43**(10): p. 1878-86.

88. Flynn, A., et al., *Contrast-Enhanced Ultrasound: A Novel Noninvasive, Nonionizing Method for the Detection of Brown Adipose Tissue in Humans.* J Am Soc Echocardiogr, 2015. **28**(10): p. 1247-54.

89. Crane, J.D., et al., *A standardized infrared imaging technique that specifically detects UCP1-mediated thermogenesis in vivo.* Mol Metab, 2014. **3**(4): p. 490-4.

90. Symonds, M.E., et al., *Thermal imaging to assess age-related changes of skin temperature within the supraclavicular region co-locating with brown adipose tissue in healthy children.* J Pediatr, 2012. **161**(5): p. 892-8.

91. Haq, T., et al., *Optimizing the methodology for measuring supraclavicular skin temperature using infrared thermography; implications for measuring brown adipose tissue activity in humans.* Sci Rep, 2017. **7**(1): p. 11934.

92. Hu, H.H., et al., *Characterization of human brown adipose tissue by chemical-shift water-fat MRI.* AJR Am J Roentgenol, 2013. **200**(1): p. 177-83.

93. Romu, T., et al., *Characterization of brown adipose tissue by water-fat separated magnetic resonance imaging.* J Magn Reson Imaging, 2015. **42**(6): p. 1639-45.

94. McCallister, A., et al., *A pilot study on the correlation between fat fraction values and glucose uptake values in supraclavicular fat by simultaneous PET/MRI.* Magn Reson Med, 2017. **78**(5): p. 1922-1932.

95. Jespersen, N.Z., et al., *A classical brown adipose tissue mRNA signature partly overlaps with brite in the supraclavicular region of adult humans.* Cell Metab, 2013. **17**(5): p. 798-805.

96. Lee, P., et al., *Functional thermogenic beige adipogenesis is inducible in human neck fat.* Int J Obes (Lond), 2014. **38**(2): p. 170-6.

97. Markussen, L.K., et al., *Characterization of immortalized human brown and white pre-adipocyte cell models from a single donor.* PLoS One, 2017. **12**(9): p. e0185624.

98. Pino, M.F., et al., *Investigating the effects of Orexin-A on thermogenesis in human deep neck brown adipose tissue.* Int J Obes (Lond), 2017.

99. Kern, P.A., et al., *The effects of temperature and seasons on subcutaneous white adipose tissue in humans: evidence for thermogenic gene induction.* J Clin Endocrinol Metab, 2014. **99**(12): p. E2772-9.

100. Sidossis, L.S., et al., *Browning of Subcutaneous White Adipose Tissue in Humans after Severe Adrenergic Stress.* Cell Metab, 2015. **22**(2): p. 219-27.

101. Bartesaghi, S., et al., *Thermogenic activity of UCP1 in human white fat-derived beige adipocytes.* Mol Endocrinol, 2015. **29**(1): p. 130-9.

102. Elsen, M., et al., *BMP4 and BMP7 induce the white-to-brown transition of primary human adipose stem cells.* Am J Physiol Cell Physiol, 2014. **306**(5): p. C431-40.

103. Bordicchia, M., et al., *Cardiac natriuretic peptides act via p38 MAPK to induce the brown fat thermogenic program in mouse and human adipocytes.* J Clin Invest, 2012. **122**(3): p. 1022-36.

104. Jiang, J., et al., *Cinnamaldehyde induces fat cell-autonomous thermogenesis and metabolic reprogramming.* Metabolism, 2017.

105. Elabd, C., et al., *Human multipotent adipose-derived stem cells differentiate into functional brown adipocytes.* Stem Cells, 2009. **27**(11): p. 2753-60.

106. Mattsson, C.L., et al., *beta(1)-Adrenergic receptors increase UCP1 in human MADS brown adipocytes and rescue cold-acclimated beta(3)-adrenergic receptor-knockout mice via nonshivering thermogenesis.* Am J Physiol Endocrinol Metab, 2011. **301**(6): p. E1108-18.

107. Pisani, D.F., et al., *The omega6-fatty acid, arachidonic acid, regulates the conversion of white to brite adipocyte through a prostaglandin/calcium mediated pathway.* Mol Metab, 2014. **3**(9): p. 834-47.

108. Loft, A., et al., *Browning of human adipocytes requires KLF11 and reprogramming of PPARgamma superenhancers.* Genes Dev, 2015. **29**(1): p. 7-22.

109. Barquissau, V., et al., *White-to-brite conversion in human adipocytes promotes metabolic reprogramming towards fatty acid anabolic and catabolic pathways.* Mol Metab, 2016. **5**(5): p. 352-65.

110. Ahfeldt, T., et al., *Programming human pluripotent stem cells into white and brown adipocytes.* Nat Cell Biol, 2012. **14**(2): p. 209-19.

111. Carriere, A., et al., *Browning of white adipose cells by intermediate metabolites: an adaptive mechanism to alleviate redox pressure.* Diabetes, 2014. **63**(10): p. 3253-65.

112. Mohsen-Kanson, T., et al., *Differentiation of human induced pluripotent stem cells into brown and white adipocytes: role of Pax3.* Stem Cells, 2014. **32**(6): p. 1459-67.

113. Moisan, A., et al., *White-to-brown metabolic conversion of human adipocytes by JAK inhibition.* Nat Cell Biol, 2015. **17**(1): p. 57-67.

114. Guenantin, A.C., et al., *Functional Human Beige Adipocytes From Induced Pluripotent Stem Cells.* Diabetes, 2017. **66**(6): p. 1470-1478.

115. Morganstein, D.L., et al., *Human fetal mesenchymal stem cells differentiate into brown and white adipocytes: a role for ERRalpha in human UCP1 expression.* Cell Res, 2010. **20**(4): p. 434-44.

116. Seiler, S.E., et al., *Characterization of a primary brown adipocyte culture system derived from human fetal interscapular fat.* Adipocyte, 2015. **4**(4): p. 303-10.

117. Di Franco, A., et al., *Searching for Classical Brown Fat in Humans: Development of a Novel Human Fetal Brown Stem Cell Model.* Stem Cells, 2016. **34**(6): p. 1679-91.

118. Kazak, L., et al., *A creatine-driven substrate cycle enhances energy expenditure and thermogenesis in beige fat.* Cell, 2015. **163**(3): p. 643-55.

119. Bertholet, A.M., et al., *Mitochondrial Patch Clamp of Beige Adipocytes Reveals UCP1-Positive and UCP1-Negative Cells Both Exhibiting Futile Creatine Cycling.* Cell Metab, 2017. **25**(4): p. 811-822.e4.

120. Kazak, L., et al., *Genetic Depletion of Adipocyte Creatine Metabolism Inhibits Diet-Induced Thermogenesis and Drives Obesity.* Cell Metab, 2017.

121. Long, J.Z., et al., *The Secreted Enzyme PM20D1 Regulates Lipidated Amino Acid Uncouplers of Mitochondria.* Cell, 2016. **166**(2): p. 424-435.